MAGNETIC INTERACTIONS IN 3-DIMENSIONAL HEISENBERG FERROMAGNETS

A NUCLEAR RESONANCE STUDY OF SIX ISOMORPHOUS COMPOUNDS WITH THE $K_2CuCl_4 \cdot 2H_2O$ STRUCTURE

T. O. KLAASSEN

MAGNETIC INTERACTIONS IN 3-DIMENSIONAL HEISENBERG FERROMAGNETS

A nuclear resonance study of six isomorphous compounds with the $K_2CuCl_4 \cdot 2H_2O$ structure

PROEFSCHRIFT

ter verkrijging van de graad van Doctor in de Wiskunde en Natuurwetenschappen aan de Rijksuniversiteit te Leiden, op gezag van de Rector Magnificus Dr. A.E. Cohen, Hoogleraar in de Faculteit der Letteren, volgens besluit van het college van Dekanen te verdedigen op woensdag 27 juni 1973 te klokke 15.15 uur

door

TJEERD ONNO KLAASSEN
geboren te Vlaardingen in 1943

Krips Repro - Meppel

PROMOTOR: Prof. Dr. N.J. Poulis

This investigation is part of the research program of the "Stichting voor Fundamenteel Onderzoek der Materie (FOM)", which is financially supported by the "Nederlandse Organisatie voor Zuiver-Wetenschappelijk Onderzoek (ZWO)".

Aan Gerrie en Nanna

CONTENTS

Chapter I

INTRODUCTION AND SUMMARY

For more than ten years it has been known that the isomorphous compounds $K_2CuCl_4 \cdot 2H_2O$, $(NH_4)_2CuCl_4 \cdot 2H_2O$, $Rb_2CuCl_4 \cdot 2H_2O$ and $(NH_4)_2CuBr_4 \cdot 2H_2O$ order ferromagnetically at a temperature of about 1 K. The specific heat, susceptibility and magnetization measurements of Miedema et al.[1,2] and Wielinga et al.[3] indicate that the magnetic behaviour of these four salts is equivalent. All the specific heat curves could be brought to coincide using a reduced temperature scale. The thermodynamic and critical behaviour of these compounds has been explained using various theoretical models for the 3-dimensional b.c.c. Heisenberg ferromagnet with $S = \frac{1}{2}$ [4,5]. The nearest neighbour and next-nearest neighbour superexchange interaction constants J_1 and J_2 could be calculated from the experimental values for the Curie-Weiss temperature θ, the ordering temperature T_c, and the temperature dependence of the specific heat. The main purpose of the work presented in this thesis is to extend the knowledge concerning this series of isomorphous Heisenberg ferromagnets, including $Cs_2CuCl_4 \cdot 2H_2O$ and $Rb_2CuBr_4 \cdot 2H_2O$, by providing insight in the magnetic properties from a microscopic point of view. To that aim the magnetic and electric hyperfine interactions of all nuclei (except those of the oxygen ions) have been determined using nuclear resonance techniques. From the nuclear interactions, information is obtained concerning the covalent bond formation of the outer valence electrons of both the diamagnetic and magnetic ions. The transfer of unpaired spin from the magnetic copper ions towards the various diamagnetic ligands can then be calculated using a molecular orbital approach. The change of the unpaired spin density distribution on substitution of the diamagnetic halide and alkali ions provides information about the various spin transfer mechanisms.

The spin transfer coefficients can be related to the magnitude of the super exchange interactions between the copper ions. Therefore the mentioned experiments also yield a qualitative estimate of the magnitude of the various super exchange couplings in the six different compounds. This is the more interesting as no simple relation between the unit cell dimensions and the exchange constants, as determined from the macroscopic quantities, is found to exist.

The nuclear resonance experiments also allow to determine the direction of the spontaneous magnetization in the ferromagnetic state in zero field, which is found to be different for the chlorine and the bromine compounds. From the extremely large difference between the values for the nuclear interaction parameters of one of the chlorine ions in the paramagnetic state and those in the ferromagnetic state, a possible origin of this different preferred direction of magnetization is suggested.
The temperature dependence of the spontaneous magnetization very near T_c has been measured. Because of very favourable conditions, especially in the bromine compounds, the value of the critical exponent β, which describes the exponential behaviour of the spontaneous magnetization just below the Curie temperature, has been determined much more accurately than is possible with macroscopic methods.

In chapter 2 a short review of the macroscopic magnetic properties of the 3-dimensional Heisenberg ferromagnet is presented. Especially the relations between nearest and next-nearest neighbour super exchange interactions and macroscopically observable quantities are given. Also the influence of anisotropy on the magnetic properties is discussed.
The theoretical concept of covalent bond formation of a 3d-metal ion in an octahedral environment is outlined extensively in chapter 3. A simplified molecular orbital approach is employed to obtain expressions for the electron orbitals involved. The influence of the unpaired spin transfer from the magnetic ion towards the ligands on the crystal field splitting and the spin-orbit coupling of the magnetic ion is discussed. Expressions for the ligand hyperfine interactions due to the spin transfer are given. Also an approximate relation between the magnitude of the super exchange interaction and spin transfer coefficients for a very simple case is derived.
In chapter 4 the properties of the Cu^{2+} ion in the considered compounds are treated. The electric crystal field at the copper ion has tetragonal symmetry with important rhombic distortions. First of all the expressions for the electronic g tensor, the hyperfine interaction tensor and the electric field gradient tensor, all correct to second order in the spin-orbit coupling, are derived for the situation of purely ionic bonding. These expressions are then modified according to the molecular orbital approach outlines in the preceding chapter to account for a partly covalent bonding of the copperion.
In chapter 5 the nuclear spin Hamiltonian will be discussed. The various contributions to the total magnetic interaction of the nucleus are given. We will enter into the analysis of nuclear resonance spectra for a value of the nuclear

spin I = 3/2, which is appropriate for most of the nuclei in these compounds. Apart from perturbation theory expressions for the resonance frequencies, which cannot be applied in all occurrent situations, also the generally valid analysis following the method of Brown and Parker will be outlined. The experimental set-up is described shortly, the crystal structure of these compounds is presented. From the point symmetry of the various nuclear sites in the unit cell the number of expected resonance spectra is obtained. The local directions within a copper octahedron are defined and a notation for the zero field spectra in the ferromagnetic state is given. This chapter ends by some comments with respect to specific aspects of nuclear resonance in ferromagnetic substances.

The results of the experiments in the paramagnetic state are treated in chapter 6. Successively we deal with the determination of the crystal field splittings, the electronic g-tensor and the values of the Curie-Weiss temperatures θ for all compounds. Thereafter the determination of the directions of the principal axes of the frequency shift and electric field gradient tensors of all nuclei, and the values of their components are described.

The nuclear resonance spectra observed in the ferromagnetic state in zero field, and the information which can be obtained from them, will be reported in chapter 7. Also the results on the temperature dependence of the spontaneous magnetization just below T_c will be given here.

Ultimately, in chapter 8, the results on the nuclear interaction tensors will be analyzed to yield the spin transfer coefficients for the various diamagnetic ions. From the variation of these coefficients on substitution of the halide and alkali ions, information about the spin transfer mechanisms is obtained. A qualitative discussion of the exchange interaction in relation to the spin transfer coefficients will be presented.

The major part of the experimental work discussed in the chapters 6 and 7 of this thesis has already been published in Physica [6,7,8]. Moreover two short notes have been published in the proceedings of international conferences [9,10]

References.

1) Miedema, A.R., Van Kempen, H. and Huiskamp, W.J., Physica 29 (1963) 1266 (Commun. Kamerlingh Onnes Lab., Leiden, No. 336a).

2) Miedema, A.R., Wielinga, R.F. and Huiskamp, W.J., Physica 31 (1965) 1585 (Commun. Kamerlingh Onnes Lab., Leiden, No. 345a).

3) Wielinga, R.F., Thesis, Leiden (1968).

4) Dalton, N.W. and Wood, D.W., Phys. Rev. 138 (1965) 779.
5) Wood, D.W. and Dalton, N.W., Proc. Phys. Soc. 87 (1966) 755.
6) Klaassen, T.O., Gevers, A. and Poulis, N.J., Physica 61 (1972) 95 (Commun. Kamerlingh Onnes Lab., Leiden, No. 393a).
7) Klaassen, T.O., Gevers, A, Looyestijn, W.J. and Poulis, N.J., Physica 64 (1973) 149 (Commun. Kamerlingh Onnes Lab., Leiden, No. 398c).
8) Klaassen, T.O., Looyestijn, W.J. and Poulis, N.J., to be published in Physica.
9) Klaassen, T.O. and Poulis, N.J., Proc. 7th Intern. Conf. Magnetism, Grenoble (1970) 1157.
10) Klaassen, T.O. and Poulis, N.J., Proc. 17th Congress Ampere, Turku (1972), to be published.

Chapter 2

EXCHANGE INTERACTION IN A 3-DIMENSIONAL b.c.c. HEISENBERG FERROMAGNET

It is well known that the magnetic properties, especially those of insulating substances, can be described theoretically very well by introducing an interaction between the unpaired electron spins of the form

$$H_{ex} = - \sum_{ij} J_{ij} \vec{S}_i \cdot \vec{S}_j \qquad (2.1)$$

J_{ij} is called the exchange interaction between the spins $\vec{S}_i$ and $\vec{S}_j$. This interaction, as introduced originally by Heisenberg[1,2] and discussed by Dirac[3], contains only the ordinary Coulomb interaction. This "direct" exchange interaction is very strongly dependent on the distance between the magnetic ions, and so the exchange constant J_{ij} has only an appreciable value if i and j are direct neighbours. This direct exchange interaction leads to a ferromagnetic interaction between the spins as the exchange constant J_{ij} is always positive. Kramers has introduced the concept of super exchange interaction, i.e. exchange interaction between two magnetic ions via one or more diamagnetic ions[4]. The sign of the exchange integral J_{ij} can be positive or negative, depending on the detailed electronic structure of the intermediate ions.

In this chapter we will give a short review concerning some important thermodynamic and magnetic properties of a magnetic insulator in relation to the super exchange interaction. Especially the methods to obtain the exchange constants from experiments will be discussed. Moreover, attention will be paid to the theoretical relations between exchange interactions and magnetic properties as have been derived by several authors, using exact series expansion calculations. The microscopic aspects of the super exchange and its relation to spin transfer effects will be dealed with in chapter 3.

As it has been found from the experiments by Miedema et al.[5,6] that the magnetic properties of the series of compounds with the $K_2CuCl_4 \cdot 2H_2O$ structure can be explained fairly well by the theoretical models for the 3-dimensional body centered cubic Heisenberg ferromagnet, we will deal with this model only. The influence of weak anisotropy will be discussed.

2.1. b.c.c. Heisenberg ferromagnet with nearest neighbour interaction. The appropriate exchange hamiltonian for this ferromagnet is

$$H_{ex} = - \sum_{ij}^{N} J_{ij} \vec{S}_i \cdot \vec{S}_j \tag{2.2}$$

where $J_{ij} = J$ if i and j are nearest neighbours, otherwise $J_{ij} = 0$. The summation runs of all N electron spins. The exchange constant J can be obtained from the following four experimental quantities.

a) The Curie-Weiss constant θ, which determines the high temperature zero field susceptibility $\chi = C/(T - \theta)$, where C is the Curie constant $C = Ng^2S(S + 1)\mu_B^2/3k$.

b) The quantity $C_m(T)T^2/R$ which can be determined from the magnetic specific heat at high temperatures.

c) The total energy E gained by magnetic ordering, which can be obtained from the specific heat results: $E = \int_0^\infty C_m(T)dT$.

d) The experimental value of $C_m(T)T^{-3/2}$ which describes the specific heat in the low temperature (spin wave) region.

The expressions relating J to these parameters are

$$\theta = 2zS(S + 1)J/3k \tag{2.3}$$

$$E/R = zS^2|J|/k \tag{2.4}$$

$$C_m(T)T^2/R = 2zS^2(S + 1)^2J^2/3k^2 \tag{2.5}$$

$$C_m(T)T^{-3/2} = 5.68 \times 10^{-2}(J/k)^{-3/2} \tag{2.6}$$

z is the number of nearest neighbours; z = 8 for a b.c.c. structure. The numerical constant in eq. (2.6) is the first coefficient in the Dyson expansion for the heat capacity, appropriate for a b.c.c. structure[7]. Moreover, experimental quantities can be obtained for the critical energy and the critical entropy defined by

$$\frac{E_\infty - E_c}{kT_c} = \frac{1}{k}\int_1^\infty C_m(t)dt \tag{2.7}$$

$$\frac{S_\infty - S_c}{k} = \frac{1}{k}\int_1^\infty \frac{C_m(t)}{t}dt \tag{2.8}$$

where $t = T/T_c$, the reduced temperature. Because both quantities do not depend on J, they have to be the same for all 3-dimensional b.c.c. nearest neighbour Heisenberg ferromagnets.

The experimental value of J calculated from eq. (2.3) - (2.6) and the value for the critical energy and critical entropy can be compared with the theoretical values as calculated by Domb et al.[8] for the quantities (2.7) and (2.8) and the critical parameter kT_c/J. These theoretical values are given in table 1. The experimental results of Miedema et al.[5,6] on four of the six copper compounds have been interpreted originally on the basis of this model. A rather good agreement between Domb's theoretical values and the values derived experimentally has been found. Afterwards Wood and Dalton[9] obtained a much better agreement by introducing also next-nearest neighbour interactions between the magnetic ions.

2.2. b.c.c. Heisenberg ferromagnet with nearest and next-nearest neighbour interaction. The exchange hamiltonian for this case is equivalent to that given in eq. (2.2) but now: $J_{ij} = J_1$ if i and j are nearest neighbours and $J_{ij} = J_2$ if i and j are next-nearest neighbours, otherwise $J_{ij} = 0$. The number of nearest and next-nearest neighbours for a b.c.c. crystal is $z_1 = 8$ and $z_2 = 6$ respectively. The equation (2.3) - (2.5) can easily be modified, according to Wood and Dalton[9], to

$$\theta = (4J_1 + 3J_2)/k \tag{2.9}$$

$$E/R = (4J_1 + 3J_2)/2k \tag{2.10}$$

$$C_{mag}T^2/R = 3(4J_1^2 + 3J_2^2)/4k^2 \tag{2.11}$$

The values for z_1, z_2 and $\underline{S} = \frac{1}{2}$ are already substituted. The theoretical values for the critical energy, critical entropy and kT_c/J_1 as a function of the parameter $\alpha = J_2/J_1$ for $0 \leq \alpha \leq 1$ as obtained by Wood et al.[9] are given in table 1. Other calculations concerning the dependence of kT_c/J_1 on α have been performed by Wood et al[10] and Cooke[11]. Their results agree rather well and can be described approximately by

$$\frac{kT_c(\alpha)}{J_1} = \frac{kT_c(0)}{J_1}(1 + b\alpha) \tag{2.12}$$

Table 1

Theoretical estimates of the critical parameters for a b.c.c. Heisenberg ferromagnet

$\alpha = J_2/J_1$	0	0.1	0.2	0.3	0.4	0.5	0.6	0.7	0.8	0.9	1.0
$(E_\infty - E_c)/kT_c$	0.460	0.438	0.419	0.404	0.393	0.385	0.378	0.372	0.367	0.363	0.357
$(S_\infty - S_c)/k$	0.235	0.234	0.229	0.225	0.223	0.219	0.218	0.216	0.213	0.211	0.210
kT_c/J_1	2.55	2.86	3.05	3.28	3.46	3.81	4.03	4.25	4.48	4.71	4.94

η	0	0.1	0.2	0.3	0.4	0.5	0.6	0.7	0.8	0.9	1.0
$E_\infty - E_c/kT_c$	0.169	0.169	0.170	0.175	0.184	0.201	0.222	0.252	0.295	0.335	0.460
kT_c/J	3.18	3.17	3.16	3.14	3.11	3.06	3.01	2.94	2.85	2.74	2.55

The values for b and $kT_c(0)/J_1$ vary for the different authors between b = 0.94 - 1.00 and $kT_c(0)/J_1$ = 2.55 - 2.64. Swendsen[12] has recently calculated the analytical expression

$$kT_c/J_1 = b_0 + b_1\alpha + b_2\alpha^2$$

where b_0 = 2.603; b_1 = 2.445 and b_2 = -0.107 for a b.c.c. structure with $0 \leq \alpha \leq 1$.

All calculations on the low temperature behaviour agree insofar, that it is found that the specific heat as well as the spontaneous magnetization, on a reduced temperature scale T/T_c, are independent of α.

2.3. Simple anisotropic b.c.c. Heisenberg ferromagnet with nearest neighbours interaction only. Although the properties of the copper compounds can be explained very well on the basis of the models for an isotropic Heisenberg ferromagnet, it is known from E.S.R. and magnetization measurements on $(NH_4)_2CuBr_4 \cdot 2H_2O$ by Suzuki et al.[13,14] that a small anisotropic interaction is present in this compound. The anisotropy field is determined to be about 270 Oe at T = 0 K, which is of the order of 1% of the (isotropic) exchange field. Another indication of the presence of anisotropy is found by Velu et al.[15] from the measured low temperature spontaneous magnetization of the two bromine compounds. They find that the experimental curves agree much better with theoretical calculations if an anisotropy field of about 300 Oe is supposed.

Dalton and Wood[16] have calculated the influence of a uniaxial anisotropy on the properties of a b.c.c. ferromagnet by considering a hamiltonian of the form

$$H_{ex} = - \sum_{ij} J_{ij} [S_i^z S_j^z + \eta (S_i^x S_j^x + S_i^y S_j^y)] \qquad (2.14)$$

where $J_{ij} = J$ if i and j are nearest neighbours and $J_{ij} = 0$ otherwise. The anisotropy parameter η can have the values $0 \leq \eta \leq 1$. For the extreme values $\eta = 0$ and 1 eq. (2.14) reduces to the familiar Ising and Heisenberg hamiltonian respectively. The values for $(E_\infty - E_c)/kT_c$ and kT_c/J as a function of η as obtained from high temperature series expansion are given in table 1.
The calculated critical exponent γ for the zero field susceptibility just above T_c seems to exhibit an anomalous behaviour at $\eta \approx 1$. That may explain perhaps the experimental value $\gamma = 1.31$ found by de Jongh et al.[17] for $(NH_4)_2CuBr_4 \cdot 2H_2O$ which is surprisingly small compared to the theoretical estimate $\gamma = 1.43$[18] for an isotropic Heisenberg ferromagnet. Further Dalton and Wood show that the spontaneous magnetization in the spin wave region depends on η, while the critical exponent β for the magnetization near T_c probably is independent of weak anisotropy.

2.4. Possible origins of anisotropic interaction. Because most expressions for the here mentioned anisotropic interactions are very complicated, and so a quantitative calculation of their magnitude is out of order, only a very short review of the type of interaction will be given.

a) Anisotropy of the dipolar interaction. The dipolar field at the copper site due to all surrounding magnetic moments can be calculated straight forwardly. Suzuki et al.[13] and Wielinga[19] have found that the anisotropy field originating from this mechanism is less than 1 Oe at T = 0 K and can therefore be neglected.

b) Single ion anisotropy need not be considered as it is zero for the case $S = \frac{1}{2}$.

c) Dzyaloshinski-Moriya anisotropic exchange interaction[20,21]. The ground state of the magnetic ion is perturbed in second order by the combined effect of the spin-orbit coupling and the exchange interaction. This yields an anisotropic interaction of the form $D(\vec{S}_1 \times \vec{S}_2)$ where D is of the order of $\Delta g \cdot J$ (Δg is the departure of the electronic g value from the free spin value and J is the isotropic exchange interaction). As there is no centre of symmetry between neighbouring copper ions in the $K_2CuCl_4 \cdot 2H_2O$ structure, there may exist such an interaction.

d) Biquadratic exchange[22] of the form $j(\vec{S}_1 \cdot S_2)^2$, which is a second order perturbation term including only the exchange interaction, vanishes identically for $S = \frac{1}{2}$.

e) Pseudo-dipolar exchange interaction[23]. A third order perturbation involving again the spin-orbit coupling and the exchange interaction. The interaction is approximately of the form $\sum_{ij} C_{ij}(S_{1i}S_{2j})$ $(i,j = x,y,z)$, where C is of the order of $(\Delta g)^2 J$. This mechanism can be approximated to give an anisotropy field which agrees in order of magnitude with the value observed experimentally[19].

References.

1) Heisenberg, W., Z. Phys. 38 (1926) 411.
2) Heisenberg, W., Z. Phys. 49 (1928) 619.
3) Dirac, P.A.M., Proc. Roy. Soc. A 123 (1929) 714.
4) Kramers, H.A., Physica 1 (1934) 182.
5) Miedema, A.R., van Kempen, H. and Huiskamp, W.J., Physica 29 (1963) 1266.
6) Miedema, A.R., Wielinga, R.F. and Huiskamp, W.J., Phys. Lett. 17 (1965) 87.
7) Dyson, F.J., Phys. Rev. 102 (1956) 1217 and 1230.
8) Domb, C. and Wood, D.W., Proc. Phys. Soc. 86 (1965) 1.
9) Wood, D.W. and Dalton, N.W., Proc. Phys. Soc. 87 (1966) 755.
10) Wood, D.W. and Dalton, N.W., Phys. Rev. 159 (1967) 384.
11) Cooke, J.F., Phys. Rev. B2-1 (1970) 220.
12) Swendsen, R.H., Phys. Rev. B5-1 (1972) 116.
13) Suzuki, H. and Watanabe, T., Phys. Lett. 26A (1967) 103.
14) Suzuki, H. and Watanabe, T., J. Phys. Soc. Japan 30 (1971) 367.
15) Velu, E., Renard, J-P. and Dupas, C., Solid State Commun. 11 (1972) 1.
16) Dalton, N.W. and Wood, D.W., Proc. Phys. Soc. 90 (1967) 459.
17) De Jongh, L.J., Miedema, A.R. and Wielinga, R.F., Physica 46 (1970) 44.
18) Baker, G.A., Gilbert, H.E., Eve, J. and Rushbrooke, G.S., Phys. Rev. 164 (1967) 800.
19) Wielinga, R.F., Thesis, Leiden 1968.
20) Dzyaloshinski, I., J. Phys. Chem. Solids 4 (1958) 241.
21) Moriya, T., Phys. Rev. 120 (1960) 91.
22) Yosida, K.J., J. Appl. Phys. 39-2 (1968) 511.
23) Van Vleck, J.H., Phys. Rev. 52 (1937) 1178.

Chapter 3

MOLECULAR ORBITAL APPROACH OF COVALENT BONDING

3.1. Introduction. To calculate the properties of a magnetic ion from a microscopic point of view, it is necessary to find the appropriate wave functions describing the unpaired electrons of the magnetic ion. The crystal structure of the here considered compounds shows that the magnetic ion (Cu^{2+}) is surrounded by a distorted octahedron of negatively charged ligands. Therefore we start with a general description of the wave functions of the unpaired electrons of a positively charged magnetic ion M in a perfectly octahedral surrounding of six equivalent negatively charged ligands X. It will be supposed that the unpaired electrons of the magnetic ion are in 3d orbits, and that the ligands have closed outer s and p shells. All properties of the magnetic ion and the ligands will be derived for this ideal situation. Afterwards the proper modifications will be made to account for the distortion of the octahedron and the inequivalency of the six ligands. The adaptation of the derived formulae to the actual situation will be described, as far as the ligand hyperfine interaction is concerned, in chapter 7 in connection with the analysis of the experimental data. Above all the experimental data will provide the directives for the necessary modifications to be made.

There are three main approaches to the calculations of the microscopic properties of a magnetic ion.

a) Crystal field method: the properties of the d electrons on M in the electrostatic field of the ligands X_6 are calculated. As no electrontransfer from X to M is included, this method cannot be expected to account adequately for most of the experimental results.

b) Configuration interaction method[1,2,3]: In this method electrontransfer is allowed for by adding to the normal ionic configuration an admixture of configurations in which an electron has been transferred.

c) Molecular orbital method[4,5]: electrontransfer is taken into account by letting the wave function of each electron be a linear combination of atomic orbitals (LCAO) belonging to M and X.

The last two methods yield to equivalent results if no approximations are made.

We will use here a simplified molecular orbital method[6], in the sense that we will give a description in terms of one-electron orbitals. On deriving the expression for the molecular orbitals we will only use the outer pure s and p orbits of the ligands and the 3d orbitals of the metal ion. It must however be mentioned that this model does not exclude the existence of hybridized orbitals. Their existence simply can be incorporated in the admixture coefficients. The influence of the unfilled 4s and 4p orbitals of the metal ion and the filled inner s and p orbitals of the ligand will be neglected.

The set of molecular orbitals will be derived by considering first the appropriate wave functions for a two-atom system M-X which possesses only one bond. Next, if we can neglect any correlation effects between the six bonds in the octahedral complex, the "independent bonding model"[1] can be applied to develop the wave functions for the complete system.

3.2. Molecular orbitals in the M-X system. The electron orbitals of interest are for the metal ion

$M(3d^n)$:	filled or	$3z^2 - r^2$; $x^2 - y^2$	(e_g)	(σ)
	partly filled	xy; yz; xz	(t_{2g})	(π)

and for the ligand

$X(s^2p^6)$;filled	p_x, p_y, p_z	(σ or π)
	s	(σ)

the type of orbit is σ or π, where these symbols designate zero or unit angular momentum about the M-X bonding axis respectively. In fig. 1 some of these orbits are shown. The p orbit of the ligand contains two electrons with opposite spin direction ($\uparrow\downarrow$) and is in a typical case about 10 eV lower in energy than the 3d orbit of the M ion which contains one unpaired electron with spin up ($\uparrow$). The covalent bond formation involves transfer of the p electron with spin down ($\downarrow$) to the 3d orbit.

We now consider the appropriate linear combinations of the atomic orbitals p and d (for s and d analogous expressions can be derived) which yield the new molecular orbitals Φ_A and Φ_B for the two ions respectively.

$$\Phi_A = N_A(d - Ap) \quad \text{antibonding}$$
$$\Phi_B = N_B(p + Bd) \quad \text{bonding} \qquad (3.1)$$

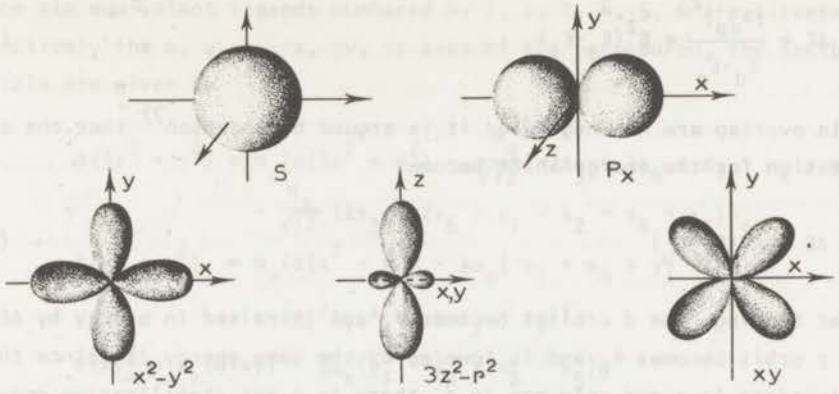

Fig. 1. Angular dependence of some of the M and X electron orbitals.

A and B are small admixture coefficients, and N_A and N_B are normalizing constants which can be deduced from the orthonormality relations for Φ_A and Φ_B.

$$\langle\Phi_A|\Phi_A\rangle = \langle\Phi_B|\Phi_B\rangle = 1 \qquad \text{so that}$$

$$N_A^{-2} = 1 - 2AS + A^2 \tag{3.2}$$

$$N_B^{-2} = 1 - 2BS + B^2$$

$$\langle\Phi_A|\Phi_B\rangle = 0 = B - A + S - ABS$$

where $S = \langle d|p\rangle$ is the overlap integral. When the small term ABS is neglected we find the relation between the admixture coefficients

$$A = B + S \tag{3.3}$$

The admixtures occur because the one-electron Hamiltonian h for the system has a matrix element between p and d, $\langle p|h|d\rangle = a_{dp}$. If we neglect the terms in overlap, the perturbation theory expression for the admixture is

$$A \approx B \approx \frac{a_{dp}}{E_d - E_p} \tag{3.4}$$

where E_d and E_p are the energies of the pure d and p orbit respectively, and it is assumed that $a_{dp} \ll E_d - E_p$.
With the same approximations the shift in energy of the molecular orbitals with respect to the pure p and d orbits is

$$\Delta E = \frac{|a_{dp}|^2}{E_d - E_p} = B^2(E_d - E_p) \qquad (3.5)$$

If terms in overlap are not neglected it is argued by Anderson[7] that the correct expression for the energy shift becomes

$$\Delta E = A^2(E_d - E_p) \qquad (3.6)$$

Thus, after bonding, the d orbital becomes Φ_A and is raised in energy by ΔE, while the p orbit becomes Φ_B and is lowered by the same energy ΔE. Since there are two electrons in p and only one in d, there is a net stabilization energy of the bond of ΔE.

As far as the magnetic properties are concerned the covalent effects of the bonding-antibonding pair of electrons with spin ↑ cancel, since equal amounts of electron ($N_B^2 B^2$) are transferred in both directions; only overlap effects are observable. The only measurable electrontransfer effect is that associated with the bonding electron with spin ↓, or alternatively, with the antibonding hole in Φ_A with spin ↑. The sum of this transfer admixture B and the overlap admixture S gives a total admixture B + S ≡ A, and hence an unpaired spin density on the ligand of

$$f = N_A^2 A^2 \qquad (3.7)$$

This value of f equals the amount of p electron $N_A^2 A^2$ transferred from the p into the d orbit. So the distribution of unpaired spin density can be described by the admixture coefficients of the antibonding orbital Φ_A.

3.3. Molecular orbitals in an octahedral complex. By virtue of the "independent-bonding model" the bonding in an octahedral complex can be treated analogous to a single bond in the M-X system. However it is more convenient to consider the molecular orbitals for the complete complex MX_6. To set up the appropriate molecular orbitals one has to take linear combinations of the s and p orbitals belonging to the six ligands, which transform as the various irreducible representations of the octahedral group. These can then be admixed to the central ion orbitals which transform as the same irreducible representation. As the magnetic properties are described by the anti-bonding orbitals analogous to eq. (3.1) which specify the distribution of the unpaired spin, only these orbitals will be discussed.

If the six equivalent ligands numbered by 1, 2, 3, 4, 5, 6 are situated at respectively the x, y, z, -x, -y, -z axes of the octahedron, the antibonding orbitals are given by

$$\begin{aligned}
\Phi(3z^2 - r^2) &= N_\sigma\{d(3z^2 - r^2) - \frac{\alpha_\sigma}{\sqrt{12}}(-2z_3 + 2z_6 + x_1 - x_4 + y_2 - y_5) \\
&\quad - \frac{\alpha_s}{\sqrt{12}}(2s_3 + 2s_6 - s_1 - s_2 - s_4 - s_5)\} \\
\Phi(x^2 - y^2) &= N_\sigma\{d(x^2 - y^2) - \tfrac{1}{2}\alpha_\sigma(-x_1 + x_4 + y_2 - y_5) \\
&\quad - \tfrac{1}{2}\alpha_s(s_1 + s_4 - s_2 - s_5)\} \\
\Phi(xy) &= N_\pi\{d(xy) - \tfrac{1}{2}\alpha_\pi(y_1 - y_4 + x_2 - x_5)\} \qquad (3.8) \\
\Phi(yz) &= N_\pi\{d(yz) - \tfrac{1}{2}\alpha_\pi(z_2 - z_5 + y_3 - y_6)\} \\
\Phi(zx) &= N_\pi\{d(zx) - \tfrac{1}{2}\alpha_\pi(x_3 - x_6 + z_1 - z_4)\}
\end{aligned}$$

The normalization constants are given by

$$N_\sigma^{-2} = 1 - 4\alpha_\sigma S_\sigma - 4\alpha_s S_s + \alpha_\sigma^2 + \alpha_s^2$$

$$N_\pi^{-2} = 1 - 4\alpha_\pi S_\pi + \alpha_\pi^2$$

Where the overlap integrals are defined as

$$S_\sigma = -\langle d(x^2 - y^2)|x_1\rangle,\ S_s = \langle d(x^2 - y^2)|s_1\rangle,\ S_\pi = \langle d(xy)|y_1\rangle$$

The experimental results are most times expressed in terms of the fraction f of unpaired electron transferred to a ligand orbit. For singly occupied d orbits these fractions are from eq. (3.8)

$$f_\sigma = \frac{1}{3}N_\sigma^2\alpha_\sigma^2 \ ;\ f_\pi = \frac{1}{4}N_\pi^2\alpha_\pi^2 \ ;\ f_s = \frac{1}{3}N_\sigma^2\alpha_s^2$$

These are exactly the same quantities as defined in eq. (3.7).

It must be noted however that in the copper compounds under consideration the copper ion is surrounded by six not equivalent ligands in a distorted octahedral arrangement. For an adequate description of the molecular orbitals of this complex, to each of the three pairs of equivalent ligands a different set of parameters (α_σ, α_π, α_s, S_σ, S_π, S_s) has to be ascribed. Furthermore, in first order, only the x^2-y^2 orbital is singly occupied for the copper ion. The other (filled) 3d orbitals admix in the x^2-y^2 orbital only in second order via the spin-orbit coupling and the rhombic distortion of the octahedron. As has

already been mentioned, the necessary modifications to account for these deviations will be made in connection with the experimental results.

3.4. Influence of covalency effects on some properties of the magnetic ion.

3.4.1. Crystal field splitting. The crystal field splitting Δ denotes the energy difference between the two e_g orbitals and the three t_{2g} orbitals. According to the simple ionic model, this energy difference occurs because the $3z^2-r^2$ and the x^2-y^2 orbits have lobes pointing towards the ligands and are therefore less stable than the xy, yz and xz orbits which avoid the ligands. Apart from this ionic part of the crystal field splitting E_{ion}, which can be calculated[8], also covalent admixture gives a contribution to the total energy splitting E_{tot}.

We saw that the effect of covalent bonding in the simple two-atom system was to raise the energy of the antibonding d orbit by an amount $\Delta E \simeq A^2(E_d-E_p)$. There is therefore also a contribution E_{cov} to the total crystal field splitting, corresponding to the difference between the antibonding energy shifts for the σ and π orbitals[9].

In terms of the admixture coefficients of eq. (3.8) for an octahedral complex, we then deduce

$$E_{cov} = \Delta E_\sigma - \Delta E_\pi \simeq (\alpha_\sigma^2 - \alpha_\pi^2)(E_d - E_p) + \alpha_s^2(E_d - E_s) \qquad (3.9)$$

Although this expression can only be regarded as very approximate, it illustrates some of the factors affecting E_{cov}.

The total crystal field splitting, as measured by optical absorption, can thus be given by

$$E_{tot} = E_{ion} + E_{cov}$$

3.4.2. Orbital magnetic moment and spin-orbit coupling. The introduction of covalent bonding into an ionic complex leads to a reduction of the orbital magnetic moment[10,11] of the magnetic ion. On a very simple picture this reduction arises because of the transfer of a fraction f of unpaired spin to the ligands, leaving a fraction (1-f) in the central d orbit. Roughly there is a reduction k = (1-f) in the orbital magnetic moment of M.

Formally the reduction factor k_{ij} is defined by

$$k_{ij} = \frac{\langle \phi_i | \vec{\ell} | \phi_j \rangle}{\langle d_i | \vec{\ell} | d_j \rangle}$$

where $\vec{\ell}$ is the orbital angular momentum operator, the ϕ's the molecular orbitals of eq. (3.8) and the d's the corresponding pure d orbitals. There are two reduction factors, $k_{\pi\pi}$ (within the t_{2g} orbits) and $k_{\sigma\pi}$ (between the e_g and t_{2g} orbits). These can be calculated from the above given matrix elements to be approximately

$$k_{\pi\pi} = N_\pi^2(1 - 4\alpha_\pi S_\pi + \tfrac{1}{2}\alpha_\pi^2)$$
$$k_{\sigma\pi} = N_\sigma N_\pi(1 - 2\alpha_\sigma S_\sigma - 2\alpha_\pi S_\pi - \tfrac{1}{2}\alpha_\pi\alpha_\sigma) \qquad (3.10)$$

where in $k_{\sigma\pi}$ the s contribution has been neglected.

Apart from a reduction of the orbital momentum, also a reduction of the spin-orbit coupling parameter λ will occur[12].
The one-electron spin-orbit Hamiltonian for the octahedral complex can be written as[13]

$$H_{s.o.} = \lambda_d \vec{\ell}\cdot\vec{s} + \lambda_p \sum_i \vec{\ell}_i\cdot\vec{s}$$

where λ_d and λ_p are the spin-orbit coupling constants for respectively the central d and the ligand p orbits; $\vec{\ell}$ and $\vec{\ell}_i$ are the angular momentum operators centered about the central nucleus and the ligand nuclei respectively. The summation runs over all ligands.
The effective spin-orbit coupling constants λ_{ij} for the central ion can be calculated analogous to the calculation of the reduction factors $k_{\pi\pi}$ and $k_{\sigma\pi}$, leading to

$$\lambda_{\pi\pi} = N_\pi^2(\lambda_d + \tfrac{1}{2}\alpha_\pi^2\lambda_p)$$
$$\lambda_{\sigma\pi} = N_\sigma N_\pi(\lambda_d - \tfrac{1}{2}\alpha_\sigma\alpha_\pi\lambda_p) \qquad (3.11)$$

3.5. Ligand transferred hyperfine interaction. As a result of the spin transfer from the magnetic ion to the ligands, there will be an interaction between the ligand nuclei and the unpaired spin of the magnetic ion; the so-called transferred hyperfine interaction[10,14]. In sofar as the magnetic part of this interaction is concerned, the interaction can be written as

$$\sum_i f_i \vec{S}\cdot\vec{\vec{A}}_i^o\cdot\vec{I} \qquad (3.12)$$

where f_i is the fraction of unpaired spin in the ligand i th orbital, A_i^o is the hyperfine structure constant of that ligand. I is the ligand nuclear spin and $s = \frac{1}{2}$ is the unpaired electron spin. The sum is taken over all orbitals of

the ligand which possess a fraction of unpaired spin.
If the ligand nuclear spin $I > \frac{1}{2}$ the spin transfer to the ligand p orbits will also contribute to the nuclear electric quadrupole interaction.
In the regular octahedron the transferred hyperfine interaction is equivalent for all six ligand nuclei. We choose ligand number 3 on the positive z axis (see section 3.3) of the octahedron to calculate this interaction. The ligand nuclear transferred hyperfine interaction Hamiltonian, containing only the terms due to the spin transfer effects with the central ion, must have axial symmetry about the z axis, and can be written as

$$H_{\text{ligand}} = AS_zI_z + B(S_xI_x + S_yI_y) + P_q\{3I_z^2 - I(I+1)\} \qquad (3.13)$$

A and B represent the sum of the spin transfer contributions, as given in eq. (3.12), and the dipolar interaction. The last term in eq. (3.13) represents the ligand nuclear quadrupole interaction.
We will now calculate the contribution from each of the ligand orbitals to A, B and P_q.

3.5.1. Magnetic contribution of the s orbits. There can be a fractional occupation f_s of unpaired spin in the ligand s orbit if unpaired electrons in e_g orbits of the magnetic ion are present. The hyperfine interaction due to a singly occupied ligand s orbit is given by the usual isotropic Fermi-Dirac contact term

$$A_s^o \vec{S}\cdot\vec{I} \qquad (3.14)$$

where

$$A_s^o = \frac{16}{3}\pi g_n\beta\beta_n|\phi(0)|^2$$

is the hyperfine structure constant for an s electron. Here g_n is the nuclear Landé factor, β and β_n are the Bohr and nuclear magnetons respectively and $\phi(0)$ is the value of the considered s wave function at the nucleus. In the simple case, where for the metal ion an orbital singlet lies lowest and $s = \frac{1}{2}$ (which exactly fits for Cu^{2+}) the contribution to A and B in eq. (3.13) is equal, and given by

$$A_s = f_sA_s^o \qquad (3.15)$$

3.5.2. Magnetic contribution of the p orbits. The ligand P_σ orbit, in this case p_z, which has lobes pointing along the bond axis, will contain a fraction

f_σ of unpaired spin if unpaired e_g electrons are present at the magnetic ion. Similarly the p_π orbits p_x and p_y will each contain a fraction f_π if unpaired t_{2g} electrons are present. The transferred hyperfine interaction, corresponding for instance to the p_z orbital is, according to Abragam and Pryce[15] given by

$$2A_\sigma S_z I_z - A_\sigma (S_x I_x + S_y I_y) - k' \vec{S} \cdot \vec{I} \tag{3.16}$$

where $A_\sigma = f_\sigma A_p^o$ and A_p^o is the hyperfine structure constant of the p orbit, given by $A_p^o = \frac{4}{5} g_n \beta \beta_n \langle r^{-3} \rangle_p$. $\langle r^{-3} \rangle_p$ is an average over the ligand p orbit. The isotropic term in k' is due to the polarization of the core s electrons by the fraction of unpaired spin in the p orbits, and can formally be given by

$$k' = f_\sigma k = 2 g_n \beta \beta_n \langle r^{-3} \rangle_p K \cdot f_\sigma$$

K is an empirical constant which is presumably much smaller than unity. So the contribution to A and B of eq. (3.13) of p_σ is respectively

$$2A_\sigma = 2 f_\sigma A_p^o \qquad \text{and} \qquad -A_\sigma = -f_\sigma A_p^o \tag{3.17}$$

while the corresponding contributions from the combined effect of p_x and p_y are respectively

$$-2A_\pi = -2 f_\pi A_p^o \qquad \text{and} \qquad A_\pi = f_\pi A_p^o \tag{3.18}$$

In addition there is an isotropic term

$$-(f_\sigma + 2 f_\pi) k \tag{3.19}$$

which is usually much smaller than A_s of eq. (3.15) and in general cannot be distinguished from the total isotropic term.

3.5.3. The magnetic dipolar interaction. This is the classical interaction between the magnetic dipole moment μ_1 of the unpaired electron at the magnetic ion with the nuclear magnetic moment μ_2 of the ligand. For point dipoles lying on the z axis and separated by a distance R, the interaction is

$$R^{-3} (\vec{\mu}_1 \cdot \vec{\mu}_2 - 3 \mu_{1z} \mu_{2z})$$

With $\vec{\mu}_1 = - g \beta \vec{s}$ and $\vec{\mu}_2 = g_n \beta_n \vec{I}$ this reduces to

$$2A_d S_z I_z - A_d (S_x I_x + S_y I_y) \tag{3.20}$$

where $A_d = gg_n\beta\beta_n R^{-3}$.
The contributions of this dipolar interaction to A and B are then $2A_d$ and $-A_d$ respectively.

Summarizing, it is seen that A and B of eq. (3.13) are given by

$$A = A_s + 2(A_d + A_\sigma - A_\pi)$$
$$B = A_s - (A_d + A_\sigma - A_\pi) \qquad (3.21)$$

where we have omitted the small isotropic term as given in eq. (3.19).

3.5.4. Ligand nuclear quadrupole interaction. This interaction is proportional to the electric quadrupole moment Q of the nucleus and to the electric field gradient at the nucleus. The latter depends on the electron charge distribution, and in that respect differs from the magnetic hyperfine interaction which only depends on the distribution of unpaired spin. There will therefore be contributions to the electric field gradient from the partly filled antibonding orbitals as well as from the filled bonding orbitals. The s orbits of the ligands will not contribute to P_q of eq. (3.13) since these orbits are spherical symmetric and therefore give no electric field gradient. Following Abragam and Pryce[15], a single hole in the p_z orbit contributes to P_q as

$$\frac{\frac{4}{5} e^2 Q \langle r^{-3} \rangle_p}{4I(2I-1)} \qquad (3.22)$$

Q is the nuclear electric quadrupole moment and e the charge on the electron. A single hole in the p_x or p_y orbit contributes $-\frac{1}{2}$ times this quantity. Thus a fully filled p shell gives a vanishing contribution to the quadrupole interaction, as would be expected.

If we assume that admixture of the central ion 4s and 4p orbitals into the ligand p orbitals can be neglected and that the admixture coefficients in the bonding and antibonding orbitals are equal (A = B in eq. (3.1); so a neglect of the overlap S), it follows from eq. (3.22) that for a $3d^9$ configuration of the central ion (Cu^{2+}) P_q is given by

$$P_q = \frac{\frac{4}{5} e^2 Q \langle r^{-3} \rangle_p}{4I(2I-1)} (f_\sigma - f_\pi) \qquad (3.23)$$

By analysing the experimental results on the ligand transferred hyperfine

interaction in terms of the expressions given above, it must be noted that these expressions only hold for a single metal-ligand bond. Modifications, apart from those concerning the already mentioned distortion of the octahedral surrounding of the metal ion and the inequivalency of the ligands, are needed to account for:

a) magnetic hyperfine interactions with other nearby magnetic ions.
b) dipolar interactions with more magnetic ions and with ligands which also possess an amount of unpaired spin.
c) the electric field gradient at the nucleus caused by all other ionic charges in the crystal and any other covalent bonds of the ligand.

3.6. Relation between covalency and super exchange interaction. Most of the proposed super exchange mechanisms in insulators agree in being strongly related to covalency effects. Although there does not exist at the moment a rigorous theory which, in a general case, enables to calculate quantitatively the magnitude of super exchange interactions, there are enough similarities between the various approaches to this problem to formulate some semi-empirical rules. These are the so-called Goodenough-Kanamori rules[16-19], which also have been discussed by Anderson[7].

I. If two magnetic ions can transfer unpaired spin into the same ligand orbit, these spins will try to couple antiparallel by Pauli's principle, so there is an antiferromagnetic contribution to the exchange interaction. The magnitude is proportional to the probability of finding these spins simultaneously in the ligand orbit, i.e. proportional to the product of the relevant spin transfer coefficients.

II. If two magnetic ions can transfer unpaired spin into different orbits on the same ligand, the spins will try to couple parallel by Hund's rule and so there is a ferromagnetic contribution to the exchange interaction. As before, the magnitude is proportional to the probability of finding these spins simultaneously on the ligand, i.e. proportional to the product of the relevant spin transfer coeffiecients.

To illustrate the dependence of the super exchange interaction on the spin transfer coefficients, we will derive for the antiferromagnetic case the approximate expression for the super exchange interaction.

We consider two metal ions M^{2+} separated by a ligand X^-: $M_1^{2+} - X^- - M_2^{2+}$, with each one unpaired spin in the antibonding orbitals Φ_1 and Φ_2. In the configuration interaction approach (see section 3.1) spin transfer in such a complex is described by the admixture into the groundstate of excited configurations,

in which one electron is hopped from one ion to another. As pointed out by Anderson[20] the excited configuration $M_1^+ - X^- - M_2^{3+}$, in which an electron is hopped from M_2 to M_1, gives the largest contribution to the exchange interaction. Only this configuration will be considered.

It can be seen that in this excited state the two "unpaired" electrons on M_1 have to be antiparallel according to Pauli's principle. There are two, energetically equivalent, groundstates; one with the unpaired spins at M_1 and M_2 parallel, and one with the spins antiparallel. The one-electron Hamiltonian h is spin-independent, and thus can mix the excited state only into the "spins antiparallel" groundstate. The relevant matrix element for this mixing being of the form

$$b = \langle \Phi_1 | h | \Phi_2 \rangle$$

b is called the transfer integral.

In second order perturbation theory this "antiparallel" groundstate is therefore depressed relative to the "parallel" groundstate by an energy of approximately b^2/U, where U is the energy difference between groundstate and excited state. U can be estimated from ionization potentials. A more rigorous calculation leads to an energy shift of $4b^2/U$. This lowering in energy of the antiparallel groundstate means that there is an antiferromagnetic interaction

$$J\vec{S}_1 \cdot \vec{S}_2 = \frac{4b^2}{U} \vec{S}_1 \cdot \vec{S}_2$$

To derive the relation between J and the spin transfer coefficients we have to realize that the transfer integral b is essentially the matrix element of h connecting the orbits d_1 and d_2 via the ligand p_σ orbit, so that

$$b = \langle \Phi_1 | h | \Phi_2 \rangle \simeq \frac{\langle d_1 | h | p \rangle \langle p | h | d_2 \rangle}{E_d - E_p}$$

Using the expression $\langle d|h|p\rangle \simeq A(E_d - E_p)$ as given in eq. (3.4) we get $b \simeq A^2(E_d - E_p) \simeq f_\sigma(E_d - E_p)$, where f_σ is the unpaired spin density in the ligand p_σ orbit due to one metal ion.

The super exchange interaction can thus be approximated by

$$J \simeq f_\sigma^2 \frac{4(E_d - E_p)^2}{U} \tag{3.24}$$

So far we have only considered "delocalization" super exchange; there are

three other contributions to the total exchange interaction.

a) Correlation super exchange, which involves the simultaneous transfer of two electrons from the ligand to the two magnetic ions. This interaction shows a similar dependence on the spin transfer coefficients of the ligand orbit as does the delocalization super exchange, although the magnitude in certain cases can be of the order of b^2/U^2.

b) Exchange polarization; also proportional to the product of the spin transfer coefficients, but most times much smaller than delocalization super exchange.

c) True Heisenberg exchange, i.e. the sum of ordinary electrostatic exchange integrals between the two magnetic ions. This contribution is always ferromagnetic, but in our case probably very small because of the large distance between the magnetic ions. According to Nesbet[21] the total exchange interaction is the sum of the individual contributions of the various mechanisms.

References.

1) Keffer, F., Oguchi, T., O'Sullivan, W. and Yamashita, J., Phys. Rev. 115, (1959) 1553.
2) Rimmer, D.E., Proc. Int. Conf. on Magnetism, Nottingham, 1964 (London, Institute of Physics and Physical Society) p. 337.
3) Hubbard, J., Rimmer, D.E. and Hopgood, F.R.A., Proc. Phys. Soc. 88 (1966) 13.
4) Mulliken, R.S., Phys. Rev. 43 (1933) 279.
5) Van Vleck, J.H., J. Chem. Phys 3 (1935) 807.
6) Owen, J. and Thornley, J.M.H., Rep. Prog. Phys. 29 (1966) 675.
7) Anderson, P.W., Magnetism Vol. 1., Eds. G.T. Rado and H. Suhl (Academic Press, New York - London 1963) p. 58.
8) Sugano, S. and Shulman, R.G., Phys. Rev. 130 (1963) 517.
9) Anderson, P.W., Solid State Phys. Vol. 13 - 1963, Eds. F. Seitz and D. Turnbull (Academic Press, New York - London) p. 99.
10) Owen, J. and Stevens, K.W.H., Nature, Lond. 171 (1953) 836.
11) Stevens, K.W.H., Proc. Roy. Soc. A219 (1953) 542.
12) Owen, J., Proc. Roy. Soc. A227 (1955) 183.
13) Misetich, A.A. and Buch, T., J. Chem. Phys. 41 (1964) 2524.
14) Shulman, R.G. and Jaccarino, V., Phys. Rev. 103 (1956) 1126.
15) Abragam, A. and Pryce, M.H.L., Proc. Roy. Soc. A205 (1951) 135.
16) Goodenough, J.B., Phys. Rev. 100 (1955) 564.
17) Goodenough, J.B., J. Phys. Chem. Solids 6 (1958) 287.

18) Goodenough, J.B., Magnetism and the Chemical Bond, (Interscience Publishers, New York - London, 1963) chapter III.

19) Kanamori, J., J. Phys. Chem. Solids 10 (1959) 87.

20) Anderson, P.W., Phys. Rev. 115 (1959) 2.

21) Nesbet, R.K., Phys. Rev. 119 (1960) 658.

Chapter 4

THE PROPERTIES OF THE Cu^{2+} ION IN A CRYSTALLINE ELECTRIC FIELD OF CUBIC SYMMETRY WITH TETRAGONAL AND RHOMBIC COMPONENTS

In this chapter the specific properties of the Cu^{2+} ion in the presence of spin transfer effects will be presented. The expressions for the relevant parameters of a 3d - metal ion - the electronic $\overset{\leftrightarrow}{g}$ tensor, the magnetic hyperfine interaction tensor $\overset{\leftrightarrow}{A}$ and the electric field gradient tensor at the nucleus - strongly depend on the electron configuration in its 3d shell. Therefore it has no sense to derive expressions in a generalized form for all iron group ions.
From the known crystal structure of $K_2CuCl_4 \cdot 2H_2O$ and the isomorphous compounds (see section 5.5) it can be concluded that the crystal field at the copper site will have cubic symmetry with tetragonal and rhombic distortions.

4.1. Ionic model.

The groundstate of the free Cu^{2+} ion (electron configuration $3d^9$) is to a good approximation ^2D. In the solid state the crystalline field arising from the surrounding ions causes an energy splitting of the orbital levels (see fig. 2).
A crystal field of cubic symmetry splits the orbital levels in a lower degenerate e_g doublet and a higher degenerate t_{2g} triplet[1]. The e_g doublet lies lowest because we deal with a hole in the closed 3d shell rather than with an unpaired electron. The tetragonal component of the crystal field splits the e_g doublet into two orbital singlets and the t_{2g} triplet into one doublet and a singlet. The orbital degeneracy in the upper t_{2g} doublet is removed by the presence of a rhombic distortion of the crystal field and/or by the spin-orbit coupling. In the case of the compounds considered here, the tetragonal distortion of the octahedral surrounding of the copper ion is due to the elongation of the octahedron along one axis. (This axis is therefore the z axis of the coordinate system which will be used to describe the various interaction tensors.) That means that the (x^2-y^2) orbit will have the lowest energy of the two e_g orbits.
The cubic crystal field causes a complete quenching of the orbital magnetic

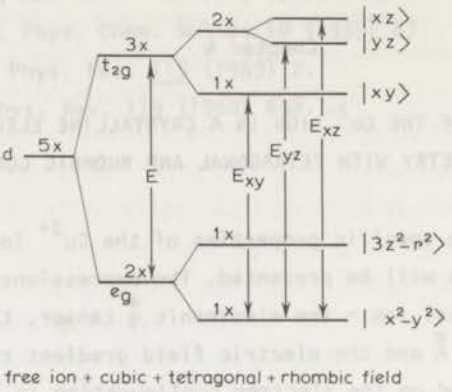

Fig. 2. Orbital energy levels for a Cu^{2+} ion in a crystal field of cubic symmetry with tetragonal and rhombic distortions.

moment associated with the (x^2-y^2) orbit, so that the magnetic properties of the copper ion are entirely due to the spin degeneracy (Kramers doublet) remaining in this groundstate[2]. The effect of the tetragonal component of the crystal field is to admix, via the spin-orbit coupling, the excited t_{2g} orbitals into the groundstate. Because of the unquenched orbital magnetic moments associated with the t_{2g} orbitals, this yields contributions of these orbitals to the electronic $\overset{\rightarrow}{\vec{g}}$ tensor and the copper nuclear hyperfine interaction tensor $\overset{\rightarrow}{\vec{A}}$. These contributions will have axial symmetry about the tetragonal axis of the octahedron. Moreover the rhombic component of the crystal field gives rise to an admixture of the $(3z^2-r^2)$ orbit into the groundstate, leading to extra contributions to $\overset{\rightarrow}{\vec{g}}$ and $\overset{\rightarrow}{\vec{A}}$ which do not have axial symmetry about the tetragonal axis. The departure of axial symmetry of the $\overset{\rightarrow}{\vec{g}}$ and $\overset{\rightarrow}{\vec{A}}$ can thus be considered as a measure for the rhombic distortion of the octahedron.

Following the work of Bleany et al.[1], the wave functions of the two components of the groundstate Kramers doublet are given by

$$|\tilde{+}\rangle = \tfrac{1}{2}\sqrt{5}\, Nf(r)\{(ax^2+by^2+cz^2+i\gamma xy)|+\rangle+(i\alpha yz-\beta zx)|-\rangle\} \qquad (4.1)$$

$$|\tilde{-}\rangle = \tfrac{1}{2}\sqrt{5}\, Nf(r)\{(i\alpha yz+\beta zx)|+\rangle+(ax^2+by^2+cz^2-i\gamma xy)|-\rangle\}$$

$|+\rangle$ and $|-\rangle$ are the two spin functions for the spin-up and spin-down states;

f(r) is the radial part of the wave functions. N is a normalizing factor given by

$$N^{-2} = 1 + (\alpha^2 + \beta^2 + \gamma^2)/12$$

The values of a, b and c are restricted by the conditions

$$\begin{aligned} a + b + c &= 0 \\ a^2 + b^2 + c^2 &= 6 \end{aligned} \tag{4.2}$$

If we denote the energy differences between the t_{2g} levels and the (x^2-y^2) level by E_{xy}, E_{xz} and E_{yz} (see fig. 2) the admixture coefficients α, β and γ can be expressed in a, b, c, the spin-orbit coupling constant λ and these energy differences.

$$\alpha = -\frac{\lambda}{E_{yz}}(b - c) + \tfrac{1}{2}\lambda^2\left(\frac{c-a}{E_{yz}E_{xz}} + \frac{a-b}{E_{yz}E_{xy}}\right) \tag{4.3}$$

β and γ are obtained from α by cyclic permutation of (a,b,c) and (E_{yz},E_{xz}, E_{xy}).

It can be shown that for rhombic symmetry the $\overset{\rightarrow\rightarrow}{g}$ and $\overset{\rightarrow\rightarrow}{A}$ tensors are symmetric tensors and that the directions of their respective principal axes coincide with the x, y and z axes to which the angular dependence of the 3d orbits is related[3]. The same holds for the electric field gradient tensor at the nucleus. The tensors are thus fully described by their components along the x, y and z axes. As we deal essentially with tensor components, they will be labelled by a double index.

From the wave functions given in eq. (4.1) the components of the tensors $\overset{\rightarrow\rightarrow}{g}$ and $\overset{\rightarrow\rightarrow}{A}$ can be calculated to be

$$g_{xx} = 2.0023 + \frac{2}{3}\alpha(b - c) - \frac{1}{3}(\beta^2 + \beta\gamma + \gamma^2) \tag{4.4}$$

$$A_{xx} = 2g_n\beta\beta_n\langle r^{-3}\rangle_{3d}[-\{1 - \tfrac{1}{6}(\beta^2 + \gamma^2)\}\kappa + \tfrac{2}{3}\alpha(b - c) - \tfrac{1}{3}\beta\gamma +$$

$$+\tfrac{1}{7}\{2a^2 - 4 + \gamma c - \beta b + \tfrac{1}{6}(\beta^2 + \gamma^2) + \tfrac{1}{2}\alpha(\beta + \gamma) - \tfrac{1}{6}a^2(\alpha^2 + \beta^2 + \gamma^2)\}] \tag{4.5}$$

The y and z components can be obtained by cyclic permutation. The numerical factor κ in eq. (4.5) represents the effect of the polarization of the copper core s electrons. The expressions for g_{ii} and A_{ii} are correct to second order in the coefficients α, β, γ and thus also correct to second order in λ/E.

The components of the nuclear electric quadruple interaction tensor, due to the unpaired hole in the 3d shell, are given by

$$P_{xx} = \frac{e^2 Q \langle r^{-3} \rangle_{3d}}{7I(2I - 1)} (a^2 - 2), \text{ etc.} \tag{4.6}$$

From the experimental values of the components of the $\overset{\ddagger}{g}$ tensor the values of a, b, c, α, β, γ, λ/E_{xy}, λ/E_{yz} and λ/E_{xz} can be calculated by successive approximations. This can be done unambiguously because the parameters involved are related to each other in such a manner as to leave only three independent parameters.

4.2. Covalent model. To account for spin transfer effects in the copper complex we have to use instead of the pure 3d orbitals, the appropriate molecular orbitals as given in eq. (3.6), to form the wave functions of the two components of the groundstate. We will not give here the correct wave functions but only the correct expressions for the components of the interaction tensors.

As outlined in section 3.4.2, covalent bond formation causes a reduction of the values of the spin-orbit coupling constant λ and the orbital magnetic moments associated with the t_{2g} orbits. Therefore in the calculation of the contribution of the admixed t_{2g} states to the $\overset{\ddagger}{g}$ tensor, a reduced value for has to be used. If also the effect of the reduction in orbital magnetic moment is included in the reduced value for λ, we obtain, using eq. (3.8) and (3.9)

$$\lambda_{cov} = N_\sigma^2 N_\pi^2 (\lambda_d - \tfrac{1}{2}\alpha_\sigma \alpha_\pi \lambda_p)(1 - 2\alpha_\pi S_\pi - 2\alpha_\sigma S_\sigma - \tfrac{1}{2}\alpha_\sigma \alpha_\pi) \tag{4.7}$$

where

$$N_\sigma^{-2} = (1 - 4\alpha_\sigma S_\sigma - 4\alpha_s S_s + \alpha_\sigma^2 + \alpha_s^2)$$

$$N_\pi^{-2} = (1 - 4\alpha_\pi S_\pi + \alpha_\pi^2)$$

as given in eq. (3.8). λ_p is the spin-orbit coupling constant of the ligand p orbitals.

To derive this expression for λ_{cov} we have made two assumptions. First it is supposed that the σ spin transfer coefficients and overlap integrals of the four ligands which interact with the copper (x^2-y^2) orbital (i.e. oxygen and halide ions) are equal. We feel this is not too bad an approximation. Secondly the difference between the π spin transfer coefficients and overlap integrals for the six ligands is neglected. As will be seen experimentally the π covalency effects are relatively small and thus the neglect of any differences in the

coefficients does not affect the value of λ_{cov} seriously.
It must be mentioned that possibly a further reduction of the value of the spin-orbit coupling constant may occur because of the virtual expansion of the copper 3d orbitals as proposed by Marshall et al.[4]. Therefore we cannot expect the value of λ_{cov} which can be calculated from eq. (4.7) to be the same as that determined from the experimental data on the $\overset{\ddagger}{g}$ tensor. λ_{cov} has thus to be treated as an adjustable parameter.

As is common use in MO-LCAO calculations, the coefficients a, b and c from eq. (4.1) will be described by one parametric angle ϕ, which is a measure for the rhombic distortion of the octahedron[5,6,7]. From the conditions of eq. (4.2) it is easily seen that a, b and c can be written as

$$\begin{aligned} a &= \sqrt{3}\cos\phi - \sin\phi \\ b &= -\sqrt{3}\cos\phi - \sin\phi \\ c &= 2\sin\phi \end{aligned} \tag{4.8}$$

$\phi = 0$ if no rhombic distortion is present.
If we express the coefficients α, β and γ also in the same parameter ϕ, we obtain the more convenient expressions for g_{ii}, correct to second order in λ/E:

$$\begin{aligned} g_{xx} &= 2.0023 - \frac{2\lambda_{cov}}{E_{yz}}(\cos\phi + \sqrt{3}\sin\phi)^2 - (\frac{\lambda_{cov}}{E})^2[(\cos\phi + \sqrt{3}\sin\phi)^2 + 3] \\ g_{yy} &= 2.0023 - \frac{2\lambda_{cov}}{E_{xz}}(\cos\phi - \sqrt{3}\sin\phi)^2 - (\frac{\lambda_{cov}}{E})^2[(\cos\phi - \sqrt{3}\sin\phi)^2 + 3] \\ g_{zz} &= 2.0023 - \frac{8\lambda_{cov}}{E_{xy}}\cos^2\phi - (\frac{\lambda_{cov}}{E})^2(4\cos^2\phi + 3) \end{aligned} \tag{4.9}$$

where E is the average value of E_{yz}, E_{xz} and E_{xy}.
In the same way we can now also derive the components of the copper hyperfine interaction tensor, correct to second order in λ/E, to be

$$\begin{aligned} A_{xx} &= 2g_n\beta\beta_n\langle r^{-3}\rangle_{3d}[-(1-\delta_x)\kappa + \frac{8}{7}\Delta g_{xx}W - \frac{1}{14}(\Delta g_{yy}+\Delta g_{zz})W - \\ &\quad - \frac{4}{7}N_\sigma^2 + \frac{2}{7}(\sqrt{3}\cos\phi - \sin\phi)^2 N_\sigma^2 + \varepsilon_x] \\ A_{yy} &= 2g_n\beta\beta_n\langle r^{-3}\rangle_{3d}[-(1-\delta_y)\kappa + \frac{8}{7}\Delta g_{yy}W - \frac{1}{14}(\Delta g_{xx}+\Delta g_{zz})W - \\ &\quad - \frac{4}{7}N_\sigma^2 + \frac{2}{7}(\sqrt{3}\cos\phi + \sin\phi)^2 N_\sigma^2 + \varepsilon_y] \end{aligned} \tag{4.10}$$

$$A_{zz} = 2g_n\beta\beta_n\langle r^{-3}\rangle_{3d}[-(1-\delta_z)\kappa + \frac{8}{7}\Delta g_{zz}W - \frac{1}{14}(\Delta g_{xx}+\Delta g_{yy})W -$$

$$-\frac{4}{7}N_\sigma^2 + \frac{8}{7}N_\sigma^2\sin^2\phi$$

Here K is the core polarization factor

$W^{-1} = (1 - 2\alpha_\pi S_\pi - 2\alpha_\sigma S_\sigma - \frac{1}{2}\alpha_\sigma\alpha_\pi)$

$\Delta g_{ii} = g_{ii}(\text{exp}) - 2.0023$

N_σ^2 is given in eq. (4.7)

δ_i and ε_i are small terms of second order in λ/E given by

$$\delta_x = (\frac{\lambda}{E})^2\{1 + \frac{1}{2}(\sqrt{3}\cos\phi - \sin\phi)^2\}$$

$$\delta_y = (\frac{\lambda}{E})^2\{1 + \frac{1}{2}(\sqrt{3}\cos\phi + \sin\phi)^2\}$$

$$\delta_z = (\frac{\lambda}{E})^2\{2 - \cos2\phi\}$$

$$\varepsilon_x = (\frac{\lambda}{E})^2\{\frac{6}{7}(\cos2\phi - \sqrt{3}\sin2\phi) + 3\}$$

$$\varepsilon_y = (\frac{\lambda}{E})^2\{\frac{6}{7}(\cos2\phi + \sqrt{3}\sin2\phi) + 3\}$$

$$\varepsilon_z = (\frac{\lambda}{E})^2\{-\frac{12}{7}\cos2\phi + 3\}$$

The components of the quadrupole interaction tensor are also modified: the two parameters describing the nuclear quadrupole interaction are, according to eq. (4.6).

$$\nu_q = P_{zz} = \frac{e^2Q\langle r^{-3}\rangle_{3d}}{7I(2I-1)} \cdot 2N_\sigma^2\cos2\phi \qquad (4.11)$$

$$\eta = \left|\frac{P_{yy} - P_{xx}}{P_{zz}}\right| = \sqrt{3}|\text{tg } 2\phi|$$

where η is the so-called asymmetry parameter.

References.

1) Bleany, B., Bowers, K.D. and Pryce, M.H.L., Proc. Roy. Soc. A228 (1955) 166.

2) Abragam, A. and Bleany, B., Electron paramagnetic resonance of transition metal ions (Clarendon Press, Oxford, 1970) p. 51.

3) Abragam, A. and Bleany, B., Electron paramagnetic resonance of transition metal ions (Clarendon Press, Oxford, 1970) p. 654.

4) Marshall, W. and Stuart, R., Phys. Rev. 123 (1961) 2048.

5) O'Brien, C.M., Proc. Roy. Soc. (London) A281 (1964) 323.

6) Kuska, H.A., Rogers, M.T. and Drullinger, R.E., J. Phys. Chem. 71 (1967) 109.

7) Ammeter, J., Rist, G. and Günthard, Hs.H., J. Chem. Phys. 57 (1972) 3852.

Chapter 5

NUCLEAR RESONANCE IN CRYSTALS WITH THE $K_2CuCl_4 \cdot 2H_2O$ STRUCTURE

Introduction. In the preceding chapters the relation between spin transfer, electronic $\overleftrightarrow{g}$ tensor, crystal field splitting, (transferred) hyperfine interaction and super exchange interaction has been discussed. This chapter will deal with the methods to determine the (transferred) hyperfine and electric quadrupole interaction parameters of the nuclei of both the magnetic and non-magnetic ions, using nuclear resonance techniques. First the nuclear spin Hamiltonian will be discussed; attention will be paid to the analysis of the experimentally observed nuclear resonance spectra. Next the experimental equipment and some special features concerning nuclear resonance experiments in ferromagnetic substances will be treated successively. We will conclude this chapter with the discussion of the crystal structure of the copper compounds and the site symmetry of the various nuclear positions.

5.1. Nuclear spin Hamiltonian. In a nuclear resonance experiment in crystals containing paramagnetic ions only those nuclear interactions are relevant, which are related to the magnetic dipole and the electric quadrupole moment of the nucleus. The nuclear spin Hamiltonian can therefore be divided into two parts:

$$H_n = H_Q + H_m \tag{5.1}$$

H_Q describes the interaction of the nuclear electric quadrupole tensor $\overleftrightarrow{Q}$ with the electric field gradient tensor $\overleftrightarrow{\nabla E}$ at the nucleus which has the form

$$H_Q = \overleftrightarrow{Q} : \overleftrightarrow{\nabla E} \tag{5.2}$$

Both $\overleftrightarrow{Q}$ and $\overleftrightarrow{\nabla E}$ are symmetric second rank tensors.
It can be shown[1] that the electric quadrupole tensor can simply be described by the scalar nuclear electric quadrupole moment eQ.
The Cartesian elements of the electric field gradient tensor (EFG) are

$$V_{ij} = \frac{\delta^2 V}{\delta x_i \delta x_j} \quad (x_i, x_j = x,y,z) \tag{5.3}$$

where V denotes the electrostatic potential at the nucleus due to all surrounding charges. The EFG tensor is a symmetric one, so we can choose the cartesian coordinate system (X,Y,Z) so as to have all non-diagonal elements in eq. (5.3) equal to zero. X,Y,Z are then the principal axes of the EFG tensor, where the usual convention $|V_{zz}| \geq |V_{yy}| \geq |V_{xx}|$ is followed. As all charges are situated outside the nucleus $\sum_i V_{ii} = 0$, so the EFG tensor can be represented by only two parameters:

$$eq = V_{zz} \quad \text{and} \quad \eta = \frac{V_{xx} - V_{yy}}{V_{zz}} \quad (0 \leq \eta \leq 1)$$

The electric quadrupole interaction Hamiltonian can now be written as

$$H_Q = \frac{e^2qQ}{4I(2I-1)} \{3I_z^2 - I(I+1) + \tfrac{1}{2}\eta(I_+^2 + I_-^2)\} \qquad (5.4)$$

I is the nuclear spin and I_+ and I_- are the usual step-operators $I_\pm = I_x \pm iI_y$.

H_m describes the interaction of the nuclear magnetic dipole moment with the total local magnetic field $\vec{H}_t$ at the nucleus.

$$H_m = -\gamma\hbar\vec{I}\cdot\vec{H}_t \qquad (5.5)$$

γ is the gyromagnetic ratio of the nucleus. $\vec{H}_t$ is given by the vector sum of the various magnetic fields

$$\vec{H}_t = \vec{H}_0 + \frac{\overleftrightarrow{A}\langle S\rangle}{\gamma} + \vec{H}_{dip} + \vec{H}_L + \vec{H}_{dem} + \vec{H}_{nn} \qquad (5.6)$$

$\vec{H}_0$ is the external applied magnetic field.

$\frac{\overleftrightarrow{A}\langle S\rangle}{\gamma}$ is the (transferred) hyperfine field as discussed in section 3.5. Here the time averaged value of the electron spin $\vec{S}$ is used, as the electron spins very rapidly reorientate due to the exchange interaction. The nuclear spins see therefore only the time averaged value $\langle\vec{S}\rangle$.

$\vec{H}_{dip}$ is the classical dipolar field die to all surrounding magnetic moments (including the transferred magnetic moment at the ligands).

$\vec{H}_L$ is the Lorentz field $+\frac{4\pi}{3}\vec{M}$, where $\vec{M}$ is the magnetization per unit volume of the crystal.

$\vec{H}_{dem}$ is the shape dependent demagnetizing field $-\overleftrightarrow{N}\cdot\vec{M}$, where $\overleftrightarrow{N}$ is the demagnetizing factor.

$\vec{H}_{nn}$ stands for the direct or indirect interactions between the nuclear

moments (nuclear dipole-dipole interaction, indirect nuclear exchange interaction[2,3]).

Concluding, the appropriate Hamiltonian to describe the nuclear spin interaction is

$$H_n = -\gamma\hbar\vec{I}\cdot\vec{H}_t + \frac{e^2qQ}{4I(2I-1)}\{3I_z^2 - I(I+1) + \tfrac{1}{2}\eta(I_+^2 + I_-^2)\} \qquad (5.7)$$

In general the eigenvalue problem for this Hamiltonian can not be solved analytically; only if one of the interactions vanishes it is soluble in certain cases. If one of the two interactions is much smaller than the other one, first and second order perturbation theory can be applied to obtain analytical expressions for the nuclear spin energy levels.

5.2. Analysis of experimentally observed nuclear resonance spectra. In the series of isomorphous copper compounds all atomic nuclei, except the nucleus of the only abundant oxygen isotope ^{16}O, possess a nuclear magnetic moment. The nuclear spin has the value $I = 3/2$ for most nuclei. The only exceptions are: $^{1}H(I = 1/2)$, $^{14}N(I = 1)$, $^{85}Rb(I = 5/2)$ and $^{133}Cs(I = 7/2)$. Therefore especially the shape of the resonance spectra of nuclei with $I = 3/2$ will be considered.

Although from Hamiltonian (5.7) no analytical expressions for the nuclear spin energy levels can be derived, Brown and Parker[4] obtained analytical relations between the experimental resonance frequencies and the parameters involved in (5.7). These relations do not give information about the form of the resonance spectrum, but only enable to calculate from the $(2I + 1)$ independent resonance frequencies, after the construction of the energy level scheme, the values for the parameters

$$\nu_q = \frac{3e^2qQ}{2I(2I-1)h}\ , \quad \eta \text{ and } \nu_L = \frac{\gamma}{2\pi}|\vec{H}_t| \ .$$

In short these Brown and Parker relations can be derived as follows.
From the experimentally determined resonance frequencies the appropriate energy level diagram is constructed. A reference level is fixed, such as to have the sum of the frequency differences between the levels and the reference level equal to zero, i.e.

$$\sum_i \nu_i = 0 \qquad i = 1,2,\ldots\ldots,(2I+1) \qquad (5.8)$$

(see fig. 3c for the case I = 3/2). With the ν_i, now known from the experiment, the "experimental" secular equation can be formed

$$(\nu - \nu_1)(\nu - \nu_2) \ldots\ldots\ldots (\nu - \nu_n) = 0 \qquad (5.9)$$

$$n = 2I + 1$$

(The roots of this equation evidently are the experimentally determined energy levels). Eq. (5.9) can be written as a polynomial

$$\nu^n + a_1\nu^{n-1} + \ldots\ldots\ldots + a_n = 0 \qquad (5.10)$$

with

$$\begin{aligned} a_1 &= -\sum_i \nu_i = 0 \\ a_2 &= \sum_{ij} \nu_i\nu_j \quad (i < j) \\ a_3 &= -\sum_{ijk} \nu_i\nu_j\nu_k \quad (i < j < k) \\ &\text{etc.} \end{aligned} \qquad (5.11)$$

If we work with the sums of powers of the roots of eq. (5.9) we obtain

$$\begin{aligned} S_1 &= \sum_i \nu_i = a_1 = 0 \\ S_2 &= \sum_i \nu_i^2 = -2a_2 \\ S_3 &= \sum_i \nu_i^3 = -3a_3 \\ &\text{etc.} \end{aligned} \qquad (5.12)$$

By constructing the theoretical secular equation for Hamiltonian (5.7) in an I_z representation, we obtain a similar polynomial as that of eq. (5.9). The coefficients of this polynomial can be expressed in the parameters of Hamiltonian (5.7). As the roots of both polynomials are identical, also the coefficients have to be identical. By equating the coefficients of both polynomials, we obtain the following expressions for S_i

$$\begin{aligned} S_1 &= \sum_i \nu_i = 0 \\ S_2 &= \sum_i \nu_i^2 = p_1\nu_L^2 + p_2\nu_q^2\left(1 + \frac{\eta^2}{3}\right) \\ S_3 &= \sum_i \nu_i^3 = p_3\nu_q\nu_L^2(3\cos^2\theta - 1 + \eta\sin^2\theta\cos 2\phi) + p_4\nu_q^3(1 - \eta^2) \\ &\text{etc.} \end{aligned} \qquad (5.13)$$

θ and ϕ are the polar coordinates which describe the direction of $\vec{H}_t$ in the coordinate system of the principal axes of the EFG tensor. The values for the coefficients p_i for different values of I are given in table 2.

Table 2

Values for the coefficients p_i in form. (5.13)

I	1	3/2	5/2	7/2
p_1	2	5	$\frac{35}{2}$	42
p_2	1/6	1	$\frac{28}{3}$	$\frac{35}{2}$
p_3	1/2	3	28	$\frac{105}{2}$
p_4	1/36	0	$\frac{40}{9}$	48

The expressions (5.13) can always be applied if the necessary (2I + 1) independent nuclear resonance transitions are observed.

In this analyzing method the only problem consists in the construction of the proper level scheme from the experimentally determined resonance transitions. In the crystals investigated often a large number of resonance transitions, belonging to different nuclei, appears in the same frequency range. In such a situation the study of the variation of the resonance frequencies when magnitude and direction of the applied magnetic field and temperature are altered, can be very helpful to accomplish the identification of the observed transitions. Moreover the knowledge of the approximate energy level schemes can be necessary. Therefore we will present a short review concerning the shape of the resonance spectra in those situations in which analytical expressions for the resonance frequencies can be obtained from Hamiltonian (5.7) using perturbation theory. We will restrict ourselves to resonance spectra of nuclei with I = 3/2.

a) $H_Q = 0$. This situation is met for nuclei with a cubic surrounding, as in that case the electric field gradient at the nucleus vanishes. Also for nuclei with I = 1/2 the quadrupole interaction equals zero, because the scalar quadrupole moment eQ ≡ 0. The resonance frequency is simply given by

$$\nu = \nu_L = \frac{\gamma}{2\pi} |\vec{H}_t| \qquad (5.14)$$

b) $H_m = 0$, $H_Q \neq 0$. These are the circumstances in a pure quadrupole resonance experiment in a paramagnetic substance where the external magnetic field is zero. According to Das and Hahn[5] the energy levels for I = 3/2 are doubly degenerate (see fig. 3a) with a frequency splitting given exactly by

$$\nu = \nu_q (1 + \frac{\eta^2}{3})^{\frac{1}{2}} \quad ; \quad \nu_q = \frac{e^2 qQ}{2h} \tag{5.15}$$

From this pure quadrupole resonance frequency (PQR) evidently it is not possible to get separate information about ν_q and η. When both values are required, experiments in small applied magnetic fields are necessary.

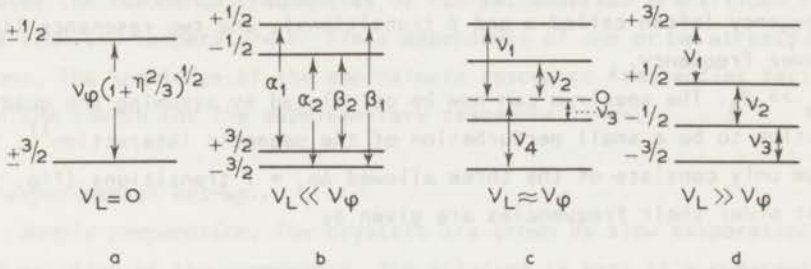

Fig. 3. Nuclear energy level schemes for I = 3/2 for different ratios of the magnetic and electric quadrupole interaction.

c) $H_m \ll H_Q$. The twofold degeneracy of the energy levels is removed by the small Zeeman interaction (see fig. 3b). For I = 3/2 exact first-order perturbation theory expressions can be obtained for the level splittings[5]. Depending on the direction of the total magnetic field and the radio frequency field, in principle all six possible transitions can be observed. In this situation the m_I = + 1/2 and - 1/2 levels mix, as do also the m_I = + 3/2 and - 3/2 levels, which makes the Δm_I = 2,3 transitions not strictly forbidden. If the direction of $\vec{H}_t$ with respect to the principal axes system of the EFG tensor is defined by the polar coordinates θ and ϕ, as has been done already in eq. (5.13), the six resonance frequencies are given by

$$\begin{aligned}
\nu_{\alpha_1,\alpha_2} &= \nu_q (1 + \frac{\eta^2}{3})^{\frac{1}{2}} \pm (\nu_1 - \nu_2) && : m_I = \pm\tfrac{1}{2} \rightarrow \pm\tfrac{3}{2} \\
\nu_{\beta_1,\beta_2} &= \nu_q (1 + \frac{\eta^2}{3})^{\frac{1}{2}} \pm (\nu_1 + \nu_2) && : m_I = \pm\tfrac{1}{2} \rightarrow \mp\tfrac{3}{2} \\
\nu_{1/2} &= \nu_1 && : m_I = -\tfrac{1}{2} \rightarrow +\tfrac{1}{2} \\
\nu_{3/2} &= \nu_2 && : m_I = -\tfrac{3}{2} \rightarrow +\tfrac{3}{2}
\end{aligned} \tag{5.16}$$

where

$$\nu_{(1)}^{(2)} = \nu_L [(\frac{2}{\rho} \pm 1)^2 \cos^2\theta +$$

$$+ \{(1 \mp \frac{1}{\rho})^2 + \frac{\eta^2}{\rho^2} \pm (1 \mp \frac{1}{\rho}) \frac{\eta}{\rho} \cos 2\phi\} \sin^2\theta]^{\frac{1}{2}}$$

$$\rho = (1 + \frac{\eta^2}{3})^{\frac{1}{2}} \quad , \quad \nu_L = \frac{\gamma}{2\pi} |\vec{H}_t|$$

This spectrum consists of 4 resonance lines symmetrically situated about the PQR frequency (often called α and β transitions), and two resonance lines at much lower frequency.

d) $H_m >> H_Q$. The spectrum can now be calculated by assuming the quadrupole interaction to be a small perturbation of the magnetic interaction[1]. The spectrum only consists of the three allowed $\Delta m_I = 1$ transitions (fig. 3d). In first order their frequencies are given by

$$\begin{aligned} \nu_2 &= \nu_L = \frac{\gamma}{2\pi} |\vec{H}_t| \\ \nu_{1,3} &= \nu_L \pm \frac{1}{2} \nu_q (3\cos^2\theta - 1 + \eta \sin^2\theta \cos 2\phi) \end{aligned} \tag{5.17}$$

e) $H_m \approx H_Q$. For this situation the energy level scheme generally can only be derived by very high order perturbation theory calculations which tend to become very complicated. However for the case $\theta = \phi = 0$, that means for $\vec{H}_t // Z$, the secular equation can be solved exactly[6], leading to the energy levels (given in frequency units)

$$\begin{aligned} E(+\tfrac{3}{2}) &= -\frac{1}{2} \nu_q \{P(1 - 2R^-) - R^-\} \\ E(+\tfrac{1}{2}) &= +\frac{1}{2} \nu_q \{P(1 - 2R^+) - R^+\} \\ E(-\tfrac{1}{2}) &= -\frac{1}{2} \nu_q \{P(1 - 2R^-) + R^-\} \\ E(-\tfrac{3}{2}) &= +\frac{1}{2} \nu_q \{P(1 + 2R^+) + R^+\} \end{aligned} \tag{5.18}$$

where $P = \dfrac{\gamma\hbar|\vec{H}_t|}{\nu_q}$ and $R^{\pm} = \{1 + \frac{1}{3}\eta^2(2P \pm 1)^{-2}\}^{\frac{1}{2}}$

For all other situations we have obtained the information about the shape of the resonance spectrum by numerical calculation on an IBM 360 computer of the eigenvalue of the Hamiltonian. In tabulated form the resonance frequencies of all six possible transitions have been calculated as a function of the para-

meters ν_L/ν_q and η for the magnetic field parallel to the X and Y axes of the EFG tensor. Using these tables complicated experimental resonance pattern can be recognized. After the so performed identification of the resonance lines the method of Brown and Parker can be applied to calculate the interaction parameters accurately.
The tables prove also to be very useful in the case that not the necessary three transitions to apply the Brown and Parker method are observed. Using these tables the resonance frequencies of not yet observed transitions can be predicted from the temperature or field dependence of one or two already detected transitions. The knowledge of the approximate resonance frequencies facilitates very much the search for the supplementary resonance lines.

5.3. The experimental set-up.

5.3.1. Sample preparation. The crystals are grown by slow evaporation of a saturated solution of the components. The solution is kept at a constant temperature of approximately 0 °C to avoid the formation of crystals with a different structure. This is found to be especially important in growing the compounds $Cs_2CuCl_4 \cdot 2H_2O$ and $Rb_2CuBr_4 \cdot 2H_2O$. In this way single crystals of about $\frac{1}{2}$ - 1 cm^3 are obtained with nicely developed crystal faces. The crystals are polished in a cylindrical or ellipsoidal shape with approximate dimensions of 5 x 5 x 10 mm. In most cases a crystallographic [110] axis is chosen as the long axis of the sample.

5.3.2. Mounting of the sample. For the experiments in the temperature range between 300 K and 1.2 K the crystal is placed in a sample holder inside the cryostat. This sample holder can be rotated from outside the cryostat over 40° about two mutual perpendicular axes, as to be able to orientate the crystal perfectly in the desired direction with respect to the external magnetic field. The electromagnet can be rotated over 180° in the horizontal plane. Before the experiment starts the crystal is always orientated at ^{4}He temperatures by observing the nuclear resonance spectrum of the protons of the waters of hydration. With the magnetic field rotating in the [110] plane of the crystal, two of the four proton resonance lines coincide for all directions of the magnetic field in that plane (see fig. 7). If the plane of rotation of the magnetic field is not perfectly parallel to the [110] plane, these two proton lines split up because of the difference in dipolar interaction with the copper ions. By orientating the crystal so as to observe for each direction of the magnetic field only one resonance line for these two protons, the [110] plane of the

crystal can be made parallel to the plane of rotation of the magnetic field to within less than 1°.
For the experiments at ^{3}He temperatures the crystal is placed inside a small glass dewar, connected to the closed ^{3}He system. The crystal is orientated visually by observing the direction of one or more crystal faces, which are left intact for this purpose, and fixed by a small amount of Apiezon-N grease. The accuracy of this method of orientation is approximated to be not better than within ± 4°. All determinations of the hyperfine interaction tensors have therefore been carried out at ^{4}He temperatures.

5.3.3. Measurement and control of the temperature. Temperatures between 13 K and 20 K are obtained by using liquid hydrogen; the temperature is determined from the vapour pressure and controlled by stabilizing the vapour pressure mechanically.
In the ^{4}He temperature range the temperature is measured using a Speer resistor (10Ω nominally, 1/4W) which is part of an a.c. Wheatstone bridge. The resistor is emerged in the helium fluid. The value of the resistance is calibrated very accurately versus the temperature (for 1.7 K < T < 1.9 K in intervals of 5 mK), which is determined from the vapour pressure. For temperatures below 2 K (superfluid state of helium) differences in temperature can be measured with an accuracy better than 10^{-4}K. The exactness of the temperature determination at the absolute temperature scale is about ± 0.01 K. The unbalance of the a.c. Wheatstone bridge, operating at 30 Hz, is used to drive a d.c. current through a heater resistor (50Ω) in the ^{4}He bath, to stabilize the temperature. Using the strong temperature dependence of the resonance frequency of a bromine resonance line in one of the bromine compounds at T ≈ 1.7 K it has been found experimentally that the short-term temperature stability at that temperature range is better than 10^{-5}K. In the ^{3}He cryostat the temperatures are derived directly from the vapour pressure reading of an oil manometer for T ≥ 0.7 K. Below this temperature the pressure indication of a NRC Alphatron, calibrated against the susceptibility of Cerium Magnesiumnitrate, is used to determine the temperature. Besides the temperature measurements are performed using the Wheatstone bridge. A 10Ω nominally $\frac{1}{10}$ W Allen and Bradley resistor and a 300Ω heater resistor are tightly bound to the crystal. The heat contact is ensured by the Apiezon-N grease between crystal and resistors. The whole is emerged in the ^{3}He fluid. Near the Curie temperatures of the various chlorine compounds (0.7 K - 1.0 K) the temperature stability is found to be 10^{-4}K, while the accuracy of the determination of temperature differences is about 2.10^{-4}K.

The lowest obtainable temperature in this ^{3}He system is 0.26 K without, and 0.32 K with the resistors bound to the crystal.

5.3.4. Electronic equipment. The resonance experiments are performed using a set of modified Pound-Watkins oscillators, which can be frequency modulated, for frequencies from 0.1 MHz up to 40 MHz. For the frequency range 40 MHz - 150 MHz a transistorized Collpits-type oscillator is used, while the experiments at still higher frequencies, up to 300 MHz, are carried out with a hybrid-T bridge spectrometer.

The resonance signals in the paramagnetic state in external magnetic field are detected using 300 Hz field modulation and first or second harmonic phase sensitive detection which yield the first and second derivative of the absorption signal respectively. The measurements in zero external field in the paramagnetic state (pure quadrupole resonance) as well as in the ferromagnetic state are performed with frequency modulation for frequencies below 40 MHz. Second harmonic detection is then always necessary as to get rid of the spurious amplitude modulation of the high frequency oscillator voltage which always accompanies the frequency modulation. For frequencies above 40 MHz the use of frequency modulation is not possible as it causes too large spurious signals to be able to detect the resonance lines. Therefore 300 Hz field modulation and second harmonic detection has been applied for the experiments above 40 MHz. All measurements have been performed by sweeping the frequency of the oscillator at fixed magnetic field.

The external magnetic field is produced by a Varian 9 inch rotating base magnet with a 5 cm pole gap. The maximum obtainable field is about 11 kOe. The field-strength is measured with a Collpits type oscillator acting as a proton magnetic resonance magnetometer. With the aid of a set of radiofrequency coils containing water probes, magnetic fields from 0.1 kOe up to 11 kOe can be measured. The determination of fields smaller than 100 Oe, and especially the compensation of the remanent field of the magnet to obtain exactly zero field, has been performed by observing the electron resonance line of the free radical compound D.P.P.H..

5.4 Nuclear resonance absorption in a ferromagnetic material. Nuclear resonance excitation in ferromagnetic materials takes place indirectly through the response of the sample magnetization rather than by the radio frequency field acting directly on the nuclear moments. For this reason the character of the resonant response depends on the magnetization process in the material. In multi domain ferromagnetic insulators (zero field) and in saturated ferromag-

netic insulators (external field) the principal magnetization process at radio frequencies is by magnetization rotation. In a very simple picture it can be understood that this yields an enhancement of the effective r.f. field acting on the nuclei. In the limit that the electron and nuclear spins are decoupled the effect of a transverse radiofrequency field $\vec{H}_1$ on a homogeneously saturated ferromagnet is to turn the electron magnetization $\vec{M}$ through an angle $H_1/H_0 + H_A$ (see fig. 4), thus establishing a transverse electron magnetization $\vec{M}_t$

$$\vec{M}_t = M \frac{\vec{H}_1}{H_0 + H_A} \tag{5.19}$$

where H_A is the static anisotropy field, which is chosen for simplicity parallel to the external static magnetic field H_0. If we suppose the nuclear transferred

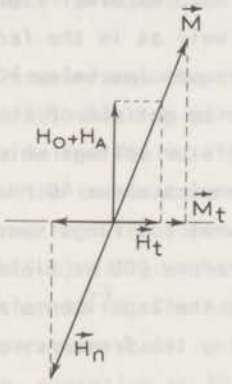

Fig. 4. NMR enhancement in a ferromagnet.

hyperfine field H_n to be isotropic, the nuclei see the total transverse field

$$\vec{H}_1 + \frac{\vec{M}_t}{M} H_n = (1 + \frac{H_n}{H_0 + H_A}) \vec{H}_1 \tag{5.20}$$

The transition probability, and thus the absorption rate, will then be enhanced by the factor $(1 + H_n/H_0 + H_A)^2$. Especially for the zero field experiments in the ferromagnetic state the enhancement of the absorption rate will be very large, as the anisotropy field in these compounds is of the order of only 200 Oe[7,8], while the hyperfine fields can be of the order of 10 - 100 kOe.

To obtain information about the shape of the nuclear resonance lines we cannot use this simple picture. We have to realize that the nuclear and electronic spins are coupled by the hyperfine interaction. We can describe the

sample response in terms of a uniform magnetization $\vec{M}$ and regard the nuclear magnetization as uniform too and represent it by $\vec{m}$. The transverse parts of the nuclear and electronic magnetization are given by[9]

$$\begin{aligned} \vec{m}_t &= \overleftrightarrow{\chi}_n \ (\vec{H}_1 + H_n \vec{M}_t/M) \\ \vec{M}_t &= \overleftrightarrow{\chi}_e \ (H_1 + H_n \vec{m}_t/M) \end{aligned} \tag{5.21}$$

where $\overleftrightarrow{\chi}_n$ and $\overleftrightarrow{\chi}_e$ are the nuclear and electronic susceptibility tensor respectively. The rate of energy absorption is given by

$$P = \frac{1}{2} \, \mathrm{Re}\{i\omega \vec{H}_1 \cdot (\vec{M}_t + \vec{m}_t)\} \tag{5.22}$$

where ω is a frequency close to the resonance frequency of the nuclei. By separating the electron and nuclear magnetizations and retaining only the leading terms, we obtain for the absorption rate

$$\begin{aligned} P = \frac{1}{2} \omega \chi_e'' \{1 + 2\chi_e' (H_n/M)^2 \chi_n'\} H_1^2 + \\ + \frac{1}{2} \omega \chi_n'' (\chi_e' H_n/M)^2 H_1^2 \end{aligned} \tag{5.23}$$

From this expression it can be concluded that the resonance losses not only involve the imaginary part of the nuclear susceptibility χ_n'', but also the real part χ_n' through a modulation of the electronic losses χ_e''. Because of the enhancement of the driving r.f. field, it is possible to saturate the nuclear absorption χ_n'', so that only the term in χ_n' remains. In that case a nuclear resonance line with a dispersion shape will be observed. In general most resonance lines observed in the ferromagnetic state in zero field in these compounds are found to have a shape which is a mixture of an absorption and a dispersion shape.

5.5. Crystallographic structure. The crystal structure of nearly all compounds which are isomorphous to $K_2CuCl_4 \cdot 2H_2O$ has been studied by various authors, using X-ray diffraction techniques[10,11,12]; only for $Rb_2CuBr_4 \cdot 2H_2O$ no crystallographic data are known. In our attempt to extend the series of isomorphous compounds, we have been successful in growing the compound with the structure formula $Rb_2CuBr_4 \cdot 2H_2O$, which has not been mentioned in literature until now. The results on the nuclear resonance experiments and the values of the elec-

tronic $\overset{\ddagger}{g}$ tensor components for this compound are analogous to those of the well-known compound $(NH_4)_2 \cdot CuBr_4 \cdot 2H_2O$. As also the external shape of the crystal corresponds to that of the ammonium compound, it can be concluded unambiguously that $Rb_2CuBr_4 \cdot 2H_2O$ is isomorphous to $(NH_4)_2CuBr_4 \cdot 2H_2O$.
The X-ray diffraction experiments provide the data concerning the positions of all atoms in the unit cell, apart from those of the hydrogen atoms. Itoh et al.[13] have determined the positions of the hydrogen atoms by studying the proton-proton dipolar interaction with nuclear resonance techniques. This experiment yields the direction and length of the line connecting the two protons within a water molecule. Recently Chidambaram et al.[14] have carried out a structure analysis of $K_2CuCl_4 \cdot 2H_2O$ using neutron diffraction. Their results confirm the earlier data from X-ray work and proton magnetic resonance, and yield a refinement of the atomic positions.

All compounds have tetragonal symmetry with space group $P4_2/mnm$, with two formula units in the unit cell. The crystallographic c axis is only about 5% longer than the a axes. In fig. 5 the unit cell of $K_2CuCl_4 \cdot 2H_2O$ is shown.

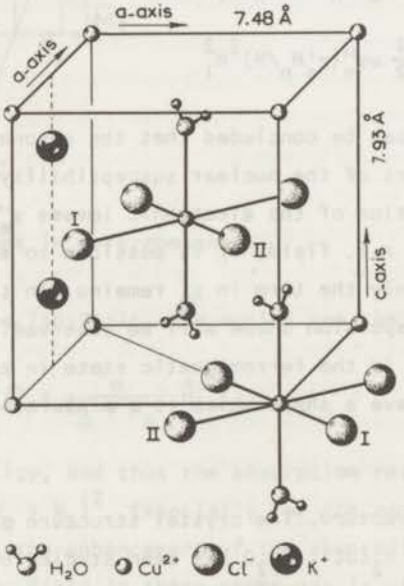

Fig. 5. Crystal structure of $K_2CuCl_4 \cdot 2H_2O$.

The copper ions are situated at the corner (0,0,0) and body center $(\frac{1}{2},\frac{1}{2},\frac{1}{2})$

positions of the unit cell; both sites have inversion symmetry. The copper ion at (0,0,0) is surrounded by four chlorine ions and two water molecules in a distorted octahedral arrangement. The chlorine ions form a rhombohedron in the (a-a) plane, with two ions at a large distance to the copper ion, denoted by Cl(I), and two at a short distance, which will be referred to as Cl(II). The water molecules are situated along the c axis; the line connecting the two protons of the water molecule is directed parallel to the Cu-Cl(II) bond. The octahedron about $(\frac{1}{2},\frac{1}{2},\frac{1}{2})$ is related to that about (0,0,0) by a rotation of 90° in the (a-a) plane. The potassium ions are situated in the (a-c) planes at the four-fold screw axes, which are parallel to the c axis.
In table 3 the unit cell dimensions for the different compounds are given, together with the positions of the atoms in $K_2CuCl_4 \cdot 2H_2O$ as determined by neutron diffraction.

Table 3
Unit cell dimensions and atomic positions

compound	a(Å)	c(Å)	Atomic positions in $K_2CuCl_4 \cdot 2H_2O$ [14]
$K_2CuCl_4 \cdot 2H_2O$ [14]	7.477	7.935	Cu : (0,0,0)
$(NH_4)_2CuCl_4 \cdot 2H_2O$ [12]	7.60	7.95	Cl(I) : $(\pm 0.274, \pm 0.274, 0)$
$Rb_2CuCl_4 \cdot 2H_2O$ [12]	7.60	8.04	Cl(II): $(\pm 0.216, \mp 0.216, 0)$
$Cs_2CuCl_4 \cdot 2H_2O$ [12]	7.92	8.24	O : $(0,0,\pm 0.248)$
$(NH_4)_2CuBr_4 \cdot 2H_2O$ [11]	7.98	8.41	H : $\pm(\pm 0.074, \mp 0.074, 0.318)$
$Rb_2CuBr_4 \cdot 2H_2O$	-	-	K : $(0,\frac{1}{2},\frac{1}{4}),(\frac{1}{2},0,\frac{1}{4})$

The positions of the atoms belonging to the octahedron about $(\frac{1}{2},\frac{1}{2},\frac{1}{2})$ are related to the given positions by the symmetry operations of the four-fold screw axis 4_2.
From the crystal structure it can be seen that the potassium ion is surrounded by a distorted cube consisting of four Cl(I) and four Cl(II) ions at approximately the same distance. The watermolecule is triagonally coordinated. There are two equivalent bent O-H.....Cl(I) hydrogen bonds, while the "lone pair" coordination is of type D, i.e. the bisector of the lone pairs is directed towards the copper ion [15]. The H-O-H angle of 109.7° is significantly larger than the value of 104.5° determined for the free water molecule.

Table 4

Interatomic distances and bond angles in $K_2CuCl_4 \cdot 2H_2O$

The Cu octahedron			
2 x Cu - O	1.971 Å	O...Cu...Cl(I)	90.0°
2 x Cu - Cl(I)	2.895	O...Cu...Cl(II)	90.0°
2 x Cu - Cl(II)	2.285	Cl(I)..Cu...Cl(II)	90.0°
The K polyhedron (cube)			
4 x K - Cl(I)	3.315 Å	Cl(I)...K...Cl(I)	106.3°
4 x K - Cl(II)	3.325		
The water molecule and the hydrogen bond			
O - H	0.966 Å	H-O-H	109.7°
H - H	1.580		
O...Cl(I)	3.116	Cl(I)...O...Cl(I)	100.3°
H...Cl(I)	2.165	H-O...Cl(I)	4.7°

Further discussions concerning the detailed surrounding of the various atoms will be given in connection with the experimental results on the magnetic hyperfine and electric quadrupole interaction of their nuclei.

5.6. Nuclear resonance spectra. The nuclear resonance experiments have to produce the directions of the principal axes of the interaction tensors, and the values of their components, of the nuclei of the different atoms in the unit cell. Because of the complexity of the total spectrum, it is useful to discuss the number of different resonance spectra which can be expected to be observed in view of the crystal symmetry. This knowledge will facilitate the identification of the large amount of resonance lines.

From the crystal structure it can easily be seen that all alkali ions are chemically as well as magnetically equivalent. We will thus always observe only one alkali resonance spectrum, except in the rubidium compounds where, due to the presence of two well abundant isotopes ^{85}Rb and ^{87}Rb which have different values for I, γ and Q, two resonance spectra appear. As the alkali ions are situated at the four-fold screw axes, it can be concluded that the transferred

hyperfine as well as the quadrupole interaction tensors will have axial symmetry about the crystallographic c axis.
As the copper site is an inversion center, the atoms centered about (0,0,0) are chemically and magnetically equivalent in pairs. So, from the four halide atoms in one rhombohedron, only two resonance spectra, apart from a doubling because of the presence of two isotopes, will be observed. The two pairs of halide atoms centered about $(\frac{1}{2},\frac{1}{2},\frac{1}{2})$ are chemically equivalent to the corresponding ions near (0,0,0), i.e. the values of the corresponding components of their nuclear interaction tensors are equivalent. The direction of the principal axes of these tensors however are rotated 90° in the (a-a) plane with respect to the corresponding axes of the ions centered about (0,0,0). Therefore, for an arbitrary direction of the external magnetic field with respect to the crystal axes, the halide nuclei about $(\frac{1}{2},\frac{1}{2},\frac{1}{2})$ will give rise to two resonance spectra which are different from those of the halide nuclei about (0,0,0). There will thus be observed in general four different halide resonance spectra, with a doubling of the number because of the presence of two isotopes (^{35}Cl and ^{37}Cl; ^{79}Br and ^{81}Br). Only for the external field parallel to the a and c axis, the four resonance spectra coincide in pairs.
The same arguments also hold for the copper ions and for the protons of the waters of hydration. Two copper resonance spectra are expected to be observed, with a doubling due to the isotopes ^{63}Cu and ^{65}Cu. All hydrogen atoms are chemically equivalent, but not magnetically. Because of the symmetry relations between the proton sites, in general four proton resonance lines will be observed. Each of these lines shows a fine structure due to proton-proton dipolar interaction.

To obtain a unique definition of the direction of principal axes of interaction tensors of the nuclei belonging to an octahedron, in fig. 6 the two crystallographic [110] axes are distinguished by denoting them by γ and γ'. We will always relate the principal axes to these γ and γ' directions to obtain a direct connection with the site symmetry of the nuclei.
The resonance experiments in the ferromagnetic state in zero field indicate that in the bromine compounds the direction of the spontaneous magnetization within the Weiss domains is parallel to the c axis. So only one resonance spectrum per set of chemically equivalent atoms is observed. In the chlorine compounds however the Weiss domains are magnetized along the [110] or [1$\bar{1}$0] axes, and two spectra per set of chemically equivalent atoms will be detected. To distinguish these zero field resonance spectra, in fig. 6 the atoms belonging to the two different octahedra are labelled by A and B. The nuclear resonance

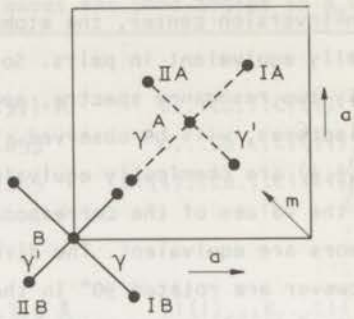

Fig. 6. Projection of the two magnetically non-equivalent octahedra on the (a-a) plane. The direction of the γ and γ' axes are given, together with the notation for the zero field spectra.

spectra originating from the nuclei belonging to the octahedra for which the magnetization $\vec{m}$ points along the γ' axis are denoted by A, while the spectra from the nuclei for which $\vec{m}//\gamma$ are denoted by B.

References.

1) Cohen, M.H. and Reif, F., Solid State Phys. 5 (1957) 321.
2) Abragam, A., The principles of nuclear magnetism (Oxford Univ. Press, 1961) p. 183.
3) Suhl, H., J. Phys. Rad. 20 (1959) 333.
4) Brown, L.C. and Parker, P.M., Phys. Rev. 100 (1955) 1764.
5) Das, T.P. and Hahn, E.L., Solid State Physics Suppl. I (Academic Press, New York-London, 1958).
6) Narath, A., Phys. Rev. 140 (1965) A552.
7) Suzuki, H. and Watanabe, T., Phys. Lett. 26A (1967) 103.
8) Velu, E., Renard, J-P. and Dupas, C., Solid State Commun. 11 (1972) 1.
9) Portis, A.M. and Lindquist, R.H., Magnetism IIA, eds. Rado, G.T. and Suhl, H., (Academic Press, New York-London, 1965) p. 360.
10) Chrobak, L., Z. Kristallogr. 88 (1935) 35.
11) Wyckoff, R.W.G., Crystal structures Vol. III, 2nd ed., Interscience Publishers (New York-London, 1948).

12) Peret, L., Bull. Soc. Chim. de France no. 10 (1966) No. 539.

13) Itoh, J., Kusaka, R., Yamagata, Y., Kiriyama, R. and Ibamoto, H., Physica 19 (1953) 415.

14) Chidambaram, R., Navarro, Q.O., Garcia, A., Karsono Linggoatmodja, Lin Shi-Chien, Il-Hwan Suh, Sequeira, A. and Srikanta, S., Acta Cryst. B26 (1970) 827.

15) Coulson, C.A., Research 10 (1957) 149.

Chapter 6

EXPERIMENTS IN THE PARAMAGNETIC STATE

In this chapter the results of the experiments which yield the (transferred) hyperfine interaction and the quadrupole interaction tensors of the various nuclei will be presented. As the used experimental techniques and the methods to analyse the resonance spectra have been discussed already in the preceding chapter, in general little attention will be given here to these subjects. Only in those cases where the analysis of the spectrum deviates from the normal procedures as given in section 5.2 the used method will be outlined. From the nuclear resonance experiments the values for the quadrupole interaction constants ν_q and η, the direction of the principal axes of the interaction tensors and the total internal field at the nuclei can be determined. The internal field is found from eq. (5.6) to be

$$\vec{H}_t - \vec{H}_o = \frac{2\pi g \overleftrightarrow{A} \langle \vec{S} \rangle}{g_e \gamma} + \vec{H}_{dip} + \vec{H}_L + \vec{H}_{dem} + \vec{H}_{nn}$$

The value of $|\vec{H}_t - \vec{H}_o|$ clearly depends on the temperature and the magnitude of the external field, as the first four terms depend on the value of the time averaged magnetic moment of the paramagnetic ions, which is proportional to $\langle S \rangle$. To be able to determine from an experiment at finite temperature and in a finite external field the value of the components of $\overleftrightarrow{A}$, we need to know the value of $\langle S(T,H) \rangle$ and the components of $\overleftrightarrow{g}$. The latter can be measured in an electron resonance experiment. The value of $\langle S(T,H) \rangle$ for temperatures well above the transition temperature can be determined graphically from a Brioullin curve for $S = \frac{1}{2}$ if the Curie-Weiss temperature θ is known. For the experiments at lower temperatures where this method of determination of $\langle S(T,H) \rangle$ cannot be used, a different procedure has been followed. The internal field at a nucleus, from which the resonance spectrum can be observed at all temperatures - for instance a hydrogen or alkali nucleus - is determined at a temperature T_1 and a field H_1 for which $\langle S(T_1,H_1) \rangle$ can be calculated with the Brioullin curve. The internal field at the nucleus, if corrected for $\vec{H}_{nn}$, is proportional to $\langle S \rangle$, provided that the direction of the external field is fixed. So by comparing the internal field at that nucleus for the desired temperature T_2 and

field H_2 with that for T_1, H_1 the value of $\langle S(T_2,H_2)\rangle$ can be obtained readily. From symmetry considerations as well as from the experimental data presented hereafter it can be deduced that for all nuclei, except for the protons, the directions of the principal axes of the hyperfine, dipole and quadrupole interaction tensors coincide with the (110), $(1\bar{1}0)$ and c axis of the crystal. The principal axes of $\overleftrightarrow{g}$ also are parallel to these axes. The used crystal samples have always rotational symmetry about one of these three axes. Therefore with $\vec{H}_o$ parallel to the (110), $(1\bar{1}0)$ or c axis all contributions to the total internal field $\vec{H}_t$ simply add scalarly. As the magnitudes of $\vec{H}_L$, $\vec{H}_{dem}$ and $\vec{H}_{nn}$ for these field directions can be calculated easily, we can obtain the values for the components of the frequency shift tensor $\overleftrightarrow{F}$, which are defined by

$$F_{ii} = \left[\frac{g_{ii}}{g_e}\langle S\rangle A_{ii} + \frac{\gamma}{2\pi}(H_{dip})_{ii}\right]_{T=0,H\neq 0} \qquad (i = x,y,z)$$

The indices i will always refer to the coordinate system set up by the principal axes of the EFG tensor of the nucleus in question. g_{ii} is the component of the electronic g-tensor of that copper ion with which the nucleus has a hyperfine interaction. It must be noted that therefore the coordinate systems of two different nuclear sites need not be equivalent.
In chapter 8 the dipole interaction tensors will be calculated, making use of the approximated unpaired spin density at the ligand ions by means of an iteration procedure. Thereafter the components of the transferred hyperfine interaction tensors can be calculated which yield the spin transfer coefficients for the different ligand orbitals.

6.1. Electronic g-values and crystal field splittings E. From the crystal structure it can be concluded that the $\overleftrightarrow{g}$ tensor of the copper ion at (0,0,0) is related to that at $(\frac{1}{2},\frac{1}{2},\frac{1}{2})$ by a rotation over 90° about the c-axis. Symmetry considerations show that the principal axes of the $\overleftrightarrow{g}$ tensor have to be parallel to the γ, γ' and c axes. As the surrounding of the copper ion has no rotational symmetry about the c-axis, the g-value in the (a-a) plane will be anisotropic. Therefore in general in an E.S.R. experiment one expects to observe two electron resonance lines when the external field rotates in the (a-a) plane, However due to the exchange interaction J_1 between the two dissimilar copper ions the two resonance lines coalescence if $2J_1 \geq |\Delta g|\mu_B H_o$, where Δg is the difference in g-value between the two dissimilar copper ions for the given direction of the external field $\vec{H}_o$ [1].
Only for $K_2CuCl_4 \cdot 2H_2O$ and $(NH_4)_2CuBr_4 \cdot 2H_2O$ electron resonance experiments have

been reported until now. Especially on the potassium compound a large number of E.S.R. experiments have been performed. The most important of these are those by Okuda et al.[2], Seidel et al.[3] and Kennedy et al.[4] who all studied the temperature dependence of the electron resonance line at different microwave frequencies. At high temperatures ($T > 250$ K) for frequencies above 30 GHz they observe two resonance lines for the magnetic field along the (110) axis. To lower temperatures and/or lower frequencies these two lines coalescence. From the temperature at which the coalescence occurs for different frequencies a strong temperature dependence of the exchange interaction J_1 between dissimilar copper ions could be determined. The problem of the anomalous temperature dependence of the nearest neighbour exchange interaction, together with the information which can be obtained from it, will be dealed with extensively in chapter 8. The results on the $\overleftrightarrow{g}$ tensor components at high temperature and high frequency are: $g_c = 2.06$, $g_\gamma = 2.35$, $g_{\gamma'} = 2.12$ according to Kennedy[4] and $g_c = 2.06$, $g_\gamma = 2.32$ and $g_{\gamma'} = 2.10$ according to Okuda[2]. The amalgamated g-value in the (a-a) plane is found to be $g_a = \frac{1}{2}(g_\gamma + g_{\gamma'})$ independent on temperature. The ground state wave function for the copper ion has been argued to be $(x^2 - y^2)$ with a small rhombic component with $Z//\gamma$, $Y//c$ and $X//\gamma'$. Van Santen et al.[5] have measured the components of the amalgamated $\overleftrightarrow{g}$ tensor at a frequency of 9.5 GHz for all six isomorphous compounds at liquid nitrogen temperatures. Their results are given in table 5. The values for $K_2CuCl_4 \cdot 2H_2O$ and

Table 5

Electronic g-values and crystal field splittings E.

compound[a]	g_a	g_c	$E(cm^{-1})$
KCl	2.215	2.047	11.900
NH_4Cl	2.219	2.052	12.050
RbCl	2.208	2.044	12.050
CsCl	2.208	2.051	-
NH_4Br	2.193	2.041	12.580
RbBr	2.193	2.044	12.420

a) In all tables from now on the compounds will be characterized only by the indication of the alkali ion and the halide ion.

$(NH_4)_2CuBr_4 \cdot 2H_2O$ agree rather well with those given in references 2 and 4. In table 5 also the data on the crystal field splittings E are given as

determined by Reedijk et al.[6]. The E values have been obtained from a powder spectrum at roomtemperature. Therefore only the mean value of the three possible crystal field transitions could be measured. Because of the very rapid dehydration of the caesium compound it appeared to be impossible in that case to determine the crystal field splitting. From the values of g_a, g_c and E the values of the components of the true $\overleftrightarrow{g}$ tensor and the spin-orbit coupling constant λ_{cov} will be calculated, using the expressions for the g components given in eq. (4.9).

6.2. Resonance spectrum of the protons of the water of hydration. This resonance spectrum is rather important as the angular dependence of the resonance pattern provides a perfect tool to obtain the necessary information concerning the orientation of the sample (see section 5.3.2). In fig. 7 a typical rotational diagram of the proton spectrum for $Cs_2CuCl_4 \cdot 2H_2O$ is shown. The external field H_o rotates in the crystallographic (110) plane. When $\vec{H}_o \| c$-axis all protons

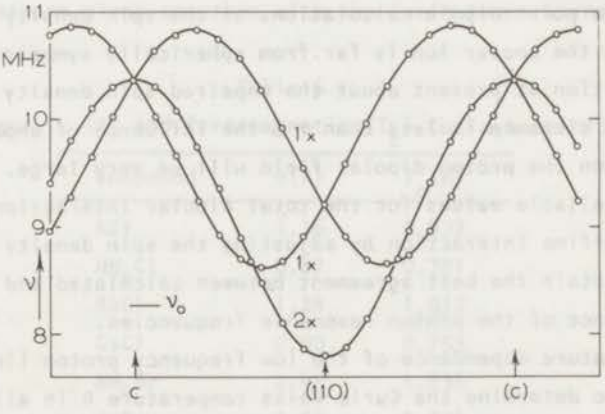

Fig. 7. Rotational diagram in the (110) plane of the proton spectrum in $Cs_2CuCl_4 \cdot 2H_2O$. H_o = 1.94 kOe, T = 1.2 K.

are magnetically equivalent as is required by crystal symmetry. For $\vec{H}_o$ along the (110) axis two pairs of resonance lines are observed. The proton-proton dipolar splitting Δ_{pp} which is not shown in the figure enables us to identify the resonance lines[7,8]. For the highest frequency line (with $\vec{H}_o \| (110)$) the dipolar splitting is Δ_{pp} = 84 kHz, while for the low frequency resonance transition Δ_{pp} = 42 kHz. This leads to the conclusion that the high frequency

resonance line originates from the protons belonging to the copper octahedron for which the external field is directed along the γ' axis ($\vec{H}_t$ is approximately parallel to the proton-proton connection line within the water molecules). The low frequency line originates from the water molecules for which $\vec{H}_o \| \gamma$. For the latter protons the external field rotates in the (γ - c) plane which is a mirror plane for the water molecule in question. Therefore these protons are magnetically equivalent for each direction of $\vec{H}_o$ in that plane, which explains the observation of only one resonance line for these protons. This symmetry property of this resonance line has been used to orientate the crystal whenever placed in the sample holder. The rotational diagrams of the proton spectrum in all other compounds are completely equivalent to the one shown in fig. 7. No attempt has been made to determine the transferred hyperfine interaction tensor for the protons. First of all the major part of the internal field at the proton site is of dipolar character and therefore very accurate calculations of the dipolar interaction tensor would be necessary to obtain a reasonable estimate for the transferred hyperfine interaction. So we cannot confine ourselves to simple point-dipole calculations as the spin density distribution of for instance the copper ion is far from spherically symmetric. Secondly we have no information at present about the unpaired spin density at the oxygen ion. As the O-H distance is less than 1 Å the influence of unpaired spin at the oxygen ion on the proton dipolar field will be very large. We don't think we can obtain reliable values for the total dipolar interaction and thus for the proton hyperfine interaction by adjusting the spin density on the oxygen ions so as to obtain the best agreement between calculated and experimental angular dependence of the proton resonance frequencies.

The temperature dependence of the low frequency proton line for $\vec{H}_o \| (110)$ has been used to determine the Curie-Weiss temperature θ in all compounds. From symmetry considerations it can be argued that the internal field is essentially parallel to the external field. The frequency shift of this resonance line is therefore perfectly proportional to the magnetization of the crystal. Inspection of the theoretically determined reduced magnetization as a function of field and temperature shows that for $T > 2\theta$ and $H_o < 1.5$ kOe the temperature dependence of the magnetization in a constant magnetic field is proportional to the temperature dependence of the zero field susceptibility χ_o. This zero field susceptibility for $T > 2\theta$ is given by the Curie-Weiss expression $\chi_o = C/T - \theta$. So by plotting the inverse frequency shift of the mentioned proton resonance line versus the temperature the value of θ can be obtained after correction for the demagnetizing field. For the chlorine compounds these

measurements have been performed in the temperature range $2\theta < T < 4.2$ K in a field of 1.25 kOe. For the bromine compounds however a different method has been used as $2\theta \approx 5$ K and it was not well possible to measure in the temperature interval 5 K - 10 K. Besides, as will be shown in section 6.6 possibly measurements at liquid hydrogen temperatures can lead to a wrong value of θ. The fact is that we have observed a change of the quadrupole interaction of the rubidium nuclei between 20 K and 4.2 K, which may indicate that there are also changes in the magnetic interactions in that temperature range. Actually from measurements for 13 K < T < 20 K we have obtained for $Rb_2CuBr_4 \cdot 2H_2O$ a value for θ which is about 0.35 K lower than the value determined at T = 4.2 K. At ^4He temperatures θ has been determined as follows. For T = 1.2 K and $H \approx 10$ kOe the magnetization of the bromine crystals is found to be saturated within the experimental accuracy. By comparison of the frequency shift of the mentioned proton line at this temperature and field with that at T = 4.2 K in a large external field where the magnetization is far from saturation the value for θ can be determined graphically from the Brioullin curve. In table 6 the Curie-Weiss temperatures are given together with the Curie temperatures T_c for comparison.

Table 6

Paramagnetic (θ) and ferromagnetic (T_c) Curie temperatures

compound	θ(K)	T_c(K)
KCl	1.16	0.877
NH_4Cl	0.87	0.701
RbCl	1.24	1.017
CsCl	0.90	0.753
NH_4Br	2.44	1.836
RbBr	2.54	1.874

It must be noted that as the θ-values are obtained from a high temperature extrapolation these values are much less accurate than the values for T_c. The error in the θ-values is estimated to be $\pm$ 0.02 K.

6.3. Chlorine (I) and bromine (I) ions. In chapter 5 in the discussions of the number of resonance spectra which is expected to be observed in the paramagnetic state, it has been mentioned already that there are two chlorine isotopes ^{35}Cl and ^{37}Cl both with a nuclear spin I = 3/2 with a natural abundance of respectively 75.4% and 24.6%. As it is found experimentally that from the resonance spectra of both isotopes exactly the same information is obtained concerning

the direction of the principal axes of the interaction tensors and the spin transfer coefficients, only the interaction parameters of the most abundant isotope ^{35}Cl will be presented. From the two bromine isotopes which are about equally abundant the interaction parameters of ^{79}Br will be given.

In zero field in the paramagnetic state for temperatures below 4.2 K in each compound one pure quadrupole resonance (PQR) transition per isotope for the halide (I) nuclei has been observed. The PQR frequencies for the $^{35}Cl(I)$ nuclei in the chlorine compounds and for the $^{79}Br(I)$ nuclei in the bromine compounds are given in table 7. The PQR frequencies are found to be independent of temperature for $T \leq 4.2$ K within the experimental accuracy ($\pm$ 0.2 kHz for $^{35}Cl(I)$ and $\pm$ 1 kHz for $^{79}Br(I)$). The ratio of the frequencies of the pure PQR transitions of the two chlorine isotopes ^{35}Cl and ^{37}Cl in the same compound is determined to be 1.2693 (4) which agrees perfectly well with the ratio of the scalar quadrupole moments as given in literature[9]. The width of the $^{35}Cl(I)$ resonance line is approximately 5 kHz, nearly independent of temperature down to the Curie temperature. Although we searched for it, we have not observed a clear critical broadening of the resonance line near T_c as predicted by Moriya[10]. This is probably due to the fact that the components of the frequency shift tensor $\overleftrightarrow{F}$ are very small. The ratio of the corresponding PQR frequencies for the ^{79}Br and ^{81}Br isotopes in the bromine compounds is 1.197 which also agrees with the ratio of the quadrupole moments[9]. The line width of the PQR transitions at $T = 4.2$ K is about 20 kHz and increases to lower temperatures to a value of 80 kHz very near T_c. It is not surprising that these resonance lines do exhibit a critical broadening as it can be seen from table 7 that the components of the frequency shift tensor for the bromine nuclei are about an order of magnitude larger than for the chlorine nuclei.

Experiments in small external fields indicate that for all compounds the F_{ii} values are much smaller than the quadrupole interaction constant ν_q. The determination of the principal axes of the EFG tensor and of $\overleftrightarrow{F}$, together with the values of their components have been performed in small external fields. Because $F_{ii} << \nu_q$ we always deal in that case with the situation $\nu_q >> \nu_L$ which facilitates very much the analysis of the resonance spectra. For $T = 4.2$ K the angular dependence of the resonance spectra have been measured with an external field $\vec{H}_o$ of the order of 100 Oe rotating in the (a-a) plane and in the (110) plane. For this temperature and field strength the magnetization of the crystal is very small so the internal fields at the nuclei are nearly zero, which provides that mainly the effects due to the anisotropy of the EFG tensor are observed. In fig. 8 two of such rotational diagrams for $(NH_4)_2CuCl_4 \cdot 2H_2O$ are shown.

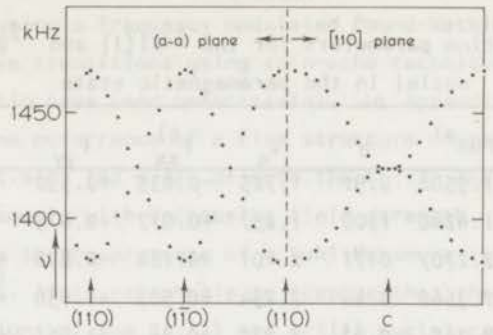

Fig. 8. Rotational diagram of the α-transitions of $^{35}Cl(I)$ in the (a-a) and (110) planes for $(NH_4)_2CuCl_4 \cdot 2H_2O$. H_o = 100 Oe, T = 4.2 K.

Only the so-called α-transitions have been detected; the β-transitions are mostly to weak to be observed. The analysis of the angular dependence yields the direction of the principal axes of the EFG tensor and the value of the asymmetry parameter η. For all chlorine as well as bromine compounds the direction of the principal axes has been calculated to be: X||c and Y and Z parallel to the (110) axes. These results are compatible with the point symmetry of the halide (I) ions. Although it is impossible to relate the Y ans Z axes to the local γ and γ' directions from the experimental results, it will be argued in chapter 8 that it is most probable that the Z axis is related to the γ direction and the Y axis to the γ' direction. The calculated values for ν_q and η are listed in table 7.

For $(NH_4)_2CuCl_4 \cdot 2H_2O$ only one pair of α-transitions is observed as is shown in fig. 8, although two pairs, originating from the two dissimilar Cl(I) sites, should be expected. For these Cl(I) nuclei however η = 1.00 as can be seen in table 7. That means that the Y and Z axes of the EFG tensor are equivalent. As in an external field of 100 Oe at T = 4.2 K the internal fields are practically zero, the two pairs of α transitions coincide for all field directions.

From the experiments in small external fields at lower temperatures where the internal fields are of the same order of magnitude as the applied field, the direction of the principal axes of the frequency shift tensors and the value of the components F_{ii} have been determined. In fig. 9 a typical rotational diagram for the α-transitions in $K_2CuCl_4 \cdot 2H_2O$ is shown; $\vec{H}_o$ rotates in the (110) plane. The two sets of α resonance lines can be clearly distinguished. The

Table 7

Interaction parameters for the $^{35}Cl(I)$ and $^{79}Br(I)$ nuclei in the paramagnetic state

	PQR[a]	η	ν_q	F_{xx}[b]	F_{yy}	F_{zz}
KCl	1.9508	0.91	1.725	-0.035	+0.550	-0.126
NH_4Cl	1.4240	1.00	1.237	+0.017	+0.673	-0.102
RbCl	2.2707	0.71	2.101	+0.184	+0.876	+0.010
CsCl	2.3666	0.44	2.294	+0.509	+1.050	+0.200
NH_4Br	8.345	0.92	7.375	+0.84	+3.55	+0.29
RbBr	14.342	0.63	13.483	+1.43	+4.77	+1.18

a) all interactions are given in MHz, unless otherwise indicated.

b) the indices refer to the EFG tensor coordinate system. $X \| c$; $Y \| \gamma'$; $Z \| \gamma$

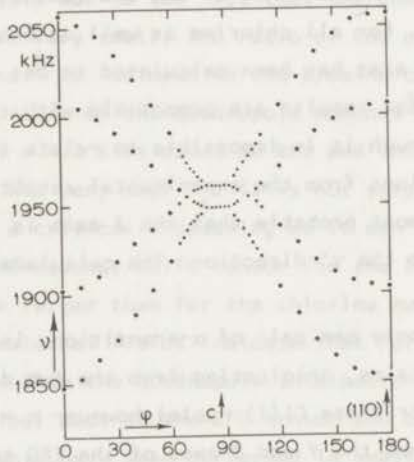

Fig. 9. Rotational diagram of the $^{35}Cl(I)$ α-transitions in the (110) plane for $K_2CuCl_4 \cdot 2H_2O$. H_o = 160 Oe, T = 1.2 K.

principal axes of $\overleftrightarrow{F}$ are calculated from this type of diagram to be parallel to the c, (110) and $(1\bar{1}0)$ axes for all halide (I) site nuclei in all compounds. Using the first order perturbation theory expressions from eq. (5.16) the frequency shift components have been calculated; the values are listed in table 7.

6.4. Chlorine (II) and bromine (II) ions. In the paramagnetic state in zero field no pure quadrupole resonance transition for the Cl(II) and Br(II) nuclei could be detected using a frequency modulated Pound-Watkins oscillator. Also the search for these transitions using spin-echo techniques to obtain a better signal to noise ratio have been unsuccessful. In Appendix A it will be shown that, apart from the occurrence of a fine structure on the Cl(II) resonance lines in external field, the width of both the Cl(II) and Br(II) resonance lines increases strongly with decreasing field strength. This low field broadening probably points to the presence of a Suhl-Nakamura interaction between nuclear spins[11,12]. It is reasonable to suppose that therefore the linewidth of the PQR transitions of the Cl(II) and Br(II) nuclei can be very large compared to that of the Cl(I) and Br(I) nuclei. Moreover the presence of chlorine impurities in the bromine compounds causes a notable increase of the Br(II) resonance linewidths (see Appendix B). It can thus be concluded that probably the failure to observe these PQR transitions is due to a too large width of the resonance lines which causes the resonance signals to be very weak.

The information concerning the frequency shift tensor and the EFG tensor has been obtained therefore from experiments in large external fields. The direction of the principal axes of both the frequency shift and EFG tensors are deduced from rotational diagrams of the $\Delta m_I = +\frac{1}{2} \rightarrow -\frac{1}{2}$ transitions. In fig. 10 such a diagram for $\vec{H}_o$ in the (110) plane is shown for $K_2CuCl_4 \cdot 2H_2O$; also a $\Delta m_I = +\frac{1}{2} \rightarrow +\frac{3}{2}$ transition has been observed. The resonance lines originate from those Cl(II) nuclei for which the magnetic field rotates in the (γ - c) plane. The resonance transitions for the other Cl(II) nuclei for which H_o rotates in

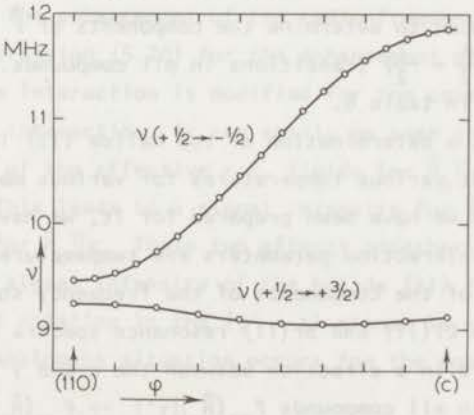

Fig. 10. Rotational diagram of the ^{35}Cl(II) resonance lines in the (110) plane for $K_2CuCl_4 \cdot 2H_2O$. H_o = 7.5 kOe, T = 1.2 K.

the (γ'- c) plane can only be observed for $\vec{H}_o$ nearly parallel to the c-axis. If $\vec{H}_o$ is rotated from the c-axis towards the (110)-axis the signal intensity of this second spectrum decreases drastically, so that for $\vec{H}_o$ about 10° from the c-axis these resonance lines cannot be detected anymore. The same holds for the bromine compounds, where however only the $(+\frac{1}{2} \rightarrow -\frac{1}{2})$ transition can be observed. In all compounds this resonance spectrum can be detected again if the applied field is parallel or nearly parallel to the γ' direction, but with a very low signal intensity. From the rotational diagrams together with the field dependence of the resonance frequency of the $(+\frac{1}{2} \rightarrow -\frac{1}{2})$ transitions it is deduced that the principal axes of both the EFG and $\overleftrightarrow{F}$ tensors are parallel to the (110), $(1\bar{1}0)$ and c axis. For the EFG tensor it is found that the Y-axis is parallel to the c axis and that the X and Z axes are directed along the (110) and $(1\bar{1}0)$ axes. Because the Cl(II) and Br(II) ions are strongly bonded to the copper ion along the γ' axis it can be concluded unambiguously that, due to the expected large σ spin transfer, $Z \| \gamma'$ and $X \| \gamma$.

The value for ν_q has been determined from the spectrum with $\vec{H}_o \| \gamma'$. In the chlorine compounds at T = 0.3 K all three allowed transitions ($\Delta m_I = 1$) can be detected, which yields directly the value of ν_q. In the bromine compounds for T = 1.2 K only two allowed transitions have been observed. Due to the fact that $H_o \| Z$ and that the asymmetry parameter is found to be small, an accurate determination of ν_q can be obtained from these two resonance frequencies. The value of η for the Cl(II) nuclei has been determined from the ratio of the frequencies of the two observed transitions for $\vec{H}_o \| \gamma$, and for the Br(II) nuclei from the field dependence of the $(+\frac{1}{2} \rightarrow -\frac{1}{2})$ transition for $\vec{H}_o \| \gamma$. In both cases the computer tables, which have been mentioned in chapter 5.2, have been employed. They have also been used to determine the components of $\overleftrightarrow{F}$ from the resonance frequencies of the $(+\frac{1}{2} \rightarrow -\frac{1}{2})$ transitions in all compounds. The interaction parameters are given in table 8.

The experiments for the determination of the halide (II) interaction parameters have been performed at various temperatures for various magnitudes of the applied field. Although we have been prepared for it, we have not found a clear indication that the interaction parameters are temperature or field dependent.

From the values of the components of the frequency shift tensor it can now be understood why the Cl(II) and Br(II) resonance spectra cannot be detected for the magnetic field in a direction between the c-and γ'-axis. From table 8 it can be seen that in all compounds $F_{zz}(\vec{H}_o \| \gamma') >> F_{yy}(\vec{H}_o \| c)$. Therefore if $\vec{H}_o$ points in a direction between the c- and γ'-axis, the magnitude and direction of the internal field at the nuclei are mainly determined by the Z

Table 8

Interaction parameters of the ^{35}Cl(II) and ^{79}Br(II) nuclei in the paramagnetic state

	ν_q	η	F_{xx} [a)]	F_{yy}	F_{zz}
KCl	9.465	0.198	+3.07	+ 3.94	+ 27.42
NH_4Cl	9.430	0.250	+3.72	+ 4.51	+ 27.74
RbCl	10.300	0.155	+3.10	+ 3.99	+ 27.45
CsCl	11.150	0.168	+2.71	+ 3.75	+ 27.35
NH_4Br	75.88	0.31	+6.98	+10.48	+129.3
RbBr	81.80	0.22	+6.04	+ 8.22	+126.2

a) $X \| \gamma$; $Y \| c$; $Z \| \gamma'$

component of $\vec{\vec{F}}$. So $\vec{H}_t - \vec{H}_o$ is approximately parallel to the γ' direction. At the low temperatures at which the experiments have been performed to obtain a sufficiently large signal intensity, the internal field is then much larger than the external field $\vec{H}_o$, and thus $\vec{H}_t$ is about parallel to the γ' direction. As the 600 Hz modulation field which is used to detect the resonance signals, in our experimental set-up is always parallel to $\vec{H}_o$, this modulation field is not at all parallel to $\vec{H}_t$. The modulation therefore becomes very ineffective with as a result a rapid decrease of the signal intensity if $\vec{H}_o$ is rotated away from the c-axis.

A second effect which also causes a decrease of the signal intensity is the angular dependence of the enhancement of the radio frequency field acting on the nuclei. If the expression (5.20) for the enhancement of the r.f. field for an isotropic hyperfine interaction is modified for the case of a strongly anisotropic hyperfine interaction, it can easily be seen that for the halide (II) nuclei the ratio of the effective r.f. fields for $\vec{H}_o \| c$ and $\vec{H}_o \| \gamma'$ is approximately F_{zz}/F_{yy}. This leads to a signal intensity for $\vec{H}_o \| \gamma'$ which is only about 1/40 from that for $\vec{H}_o \| c$. These two effects together explain the anomalous behaviour of the signal intensity of the halide (II) resonance spectrum for the external field rotating in the (γ' - c) plane. It will be seen in the next section that an analogous situation occurs for the copper spectrum.

6.5. Copper ions. Also for the copper nuclei in zero field in the paramagnetic state no pure quadrupole resonance transitions have been detected. This is most probably due to the same effects as have been discussed for the case of the

Cl(II) and Br(II) PQR transitions. From rotational diagrams of the $(+\frac{1}{2} \rightarrow -\frac{1}{2})$ transition for both copper isotopes at T = 1.2 K and the field dependence of the resonance frequencies for $\vec{H}_o$ parallel to the (110) and c axis it has been concluded that the Y axis of the EFG tensor points along the c-axis while the X-axis is parallel to the (110) axis. A typical rotational diagram for $\vec{H}_o$ in the (110) plane is given in fig. 11 for $Rb_2CuBr_4 \cdot 2H_2O$. Analogously to the halide (II) resonance spectrum also here only the resonance transition for that copper site for which the external field rotates in the (γ' - c) plane (i.e. X-Y plane of the EFG tensor) can be observed for $\vec{H}_o$ between the (110) and c axis. The spectrum for the external field along the Z axis of the EFG tensor could be detected in the bromine compounds at T = 1.2 K. In the chlorine compounds this

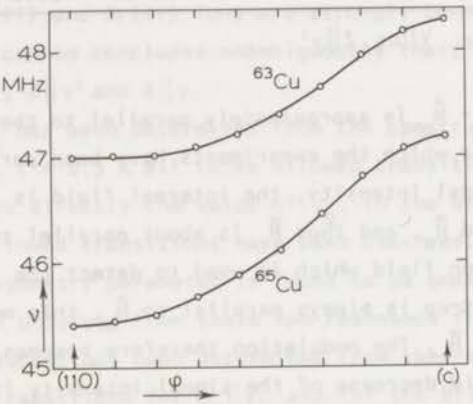

Fig. 11. Rotational diagram of the $(+\frac{1}{2} \rightarrow -\frac{1}{2})$ transitions of both copper isotopes in $Rb_2CuBr_4 \cdot 2H_2O$ in the (110) plane. H_o = 8.05 kOe, T = 1.2 K.

spectrum, even at T = 0.3 K could not be observed. This spectrum has only been detected at T = 0.3 K in zero field in the ferromagnetic state, where the spontaneous magnetization $\vec{m}_s$ is directed along the (110) axis.

For rhombic point symmetry of the magnetic copper ion it can be deduced that the principal axes of $\overleftrightarrow{g}$, $\overleftrightarrow{A}$ and the EFG tensor coincide[13]. Moreover from the expressions for the components of these tensors as given in chapter 4, it can be seen that the directions of maximum g-value and maximum hyperfine interaction always coincide with the Z-axis of the EFG tensor. According to Okuda et al.[2] the direction of the maximum g-component g_{zz} is parallel to the γ axis. So it can be concluded that for the direction of the principal axes of the EFG tensor holds $Z \| \gamma$, $Y \| c$ and $X \| \gamma'$.

The quadrupole interaction constant ν_q has been determined from the spectra

for which $\vec{H}_o$ respectively $\vec{m}_s$ are parallel to the Z axis where all three allowed transitions have been detected using the hybrid T spectrometer. Consequently for the chlorine compounds ν_q has been determined in zero field in the ferromagnetic state. For the sake of completeness these values are given in table 9 too. As for $\vec{H}_o \| Z$ the resonance frequencies are only very slightly dependent on the value of the asymmetry parameter, η had to be calculated from the field dependence of the $(+\frac{1}{2} \rightarrow -\frac{1}{2})$ transition of the ^{63}Cu isotope for $\vec{H}_o \| X$. The so obtained values for η are not very accurate (± 15%), but as η is rather small in all compounds, this error introduces only an extra uncertainty of about ± 1% in the values for F_{xx} and F_{yy}.

Table 9

Interaction parameters of the ^{63}Cu nuclei in the paramagnetic state

	ν_q	η	F_{xx} [a)]	F_{yy}	F_{zz}
KCl	46.25	∿0.20	-25.3	- 8.5	-229.0
NH_4Cl	43.60	∿0.20	-31.0	-11.7	-237.0
RbCl	43.71	0.16	-20.1	-14.1	-228.0
CsCl	38.60	∿0.20	-19.0	-17.7	-229.0
NH_4Br	41.30	0.20	-45.9	-32.8	-268.2
RbBr	40.80	0.17	-39.8	-36.2	-265.1

a) $X \| \gamma'$, $Y \| c$, $Z \| \gamma$. Frequencies in MHz

The observation of the copper resonance lines in the paramagnetic state is seriously hampered by the fact that the internal field at the nucleus is large and oppositely directed to the applied external field. Because of the negative internal field it does occur many times that for certain temperature and field intervals for $\vec{H}_o \| X$ or $\vec{H}_o \| Y$ the total field H_t at the copper nucleus is nearly field independent, due to the cancellation of the increase of the external field by the increase of the negative internal field. The width of the resonance lines is too large to be able to detect the resonance signals with frequency modulation, which implies that field modulation has to be used. As the total field H_t is about field dependent it is not possible in this situation to observe the resonance lines. Therefore mostly a large number of experiments for different temperatures and field strengths has been necessary to find the resonance lines for the desired direction of the external field.
The width of the $(+\frac{1}{2} \rightarrow -\frac{1}{2})$ transitions of the ^{63}Cu isotope in the chlorine compounds is found to be about 120 kHz for $\vec{H}_o$ parallel to the X and Y axes, and

500 kHz for $\vec{H}_o \| Z$ for the K, Rb and Cs compounds and 200 kHz and 1 MHz respectively for the NH_4 compound. The explanation for the larger linewidth in the NH_4 compound will be given in the next section while discussing the spectra of the NH_4 molecule. In the bromine compounds the linewidths for $\vec{H}_o \| X$ and Y are somewhat larger, probably due to the presence of chlorine impurities.

6.6. Alkali ions. In chapter 5 in discussing the crystal structure we have already mentioned that all alkali ions in the unit cell are chemically as well as magnetically equivalent. Because the ions are situated at four-fold screw axes which are parallel to the c-axis, all interaction tensors must have rotational symmetry about the c-axis. Essentially this is what we have observed experimentally in all compounds. As all interactions are isotropic within the (a-a) plane, all information concerning the magnitude of the interaction can be obtained from one rotational diagram in the (110) plane. All experiments have been performed in large external fields because the quadrupole interaction constants for all alkali nuclei are found to be too small to be able to carry out pure quadrupole resonance experiments. The resonance spectra are always characterized by $\nu_L >> \nu_q$ and have therefore been analyzed using first and second order perturbation theory expressions for the resonance frequencies. These analytical expressions are readily available as the asymmetry parameter η equals zero[14].

Potassium. In fig. 12 the angular dependence of the resonance frequencies of the three allowed transitions of the only abundant potassium isotope $^{39}K(I = 3/2)$ is shown for the external field in the (110) plane. The frequency difference between the outermost resonance lines $(\pm\frac{1}{2} \rightarrow \pm\frac{3}{2})$ is described exactly by the angular dependence $\Delta\nu = \nu_q(3\cos^2\theta - 1)$ with $\theta = 0$ for $\vec{H}_o \| c$. From eq. (5.17) it can be seen that then the asymmetry parameter equals zero and that the Z-axis of the EFG tensor is parallel to the c-axis, which confirms the theoretical predictions. The width of the resonance lines is only 3 kHz. The signal intensity however is so small that only experiments for $T \leq 4.2$ K could be performed. The values for the quadrupole interaction constant ν_q and for the components of the frequency shift tensor are given in table 10.

Rubidium. For the two rubidium compounds the spectra of both the $^{85}Rb(I = 5/2)$ and $^{87}Rb(I = 3/2)$ isotopes have been detected at ^{4}He temperatures. As the information deduced from the spectra of the two isotopes is found to be completely analogous, only the interaction parameters for the experimentally more convenient ^{87}Rb isotope will be discussed. In fig. 13 the rotational diagram of

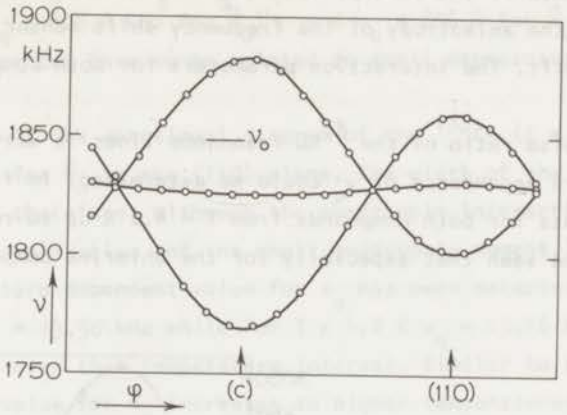

Fig. 12. Rotational diagram of ^{39}K resonance transitions in $K_2CuCl_4 \cdot 2H_2O$ in the (110) plane. H_o = 9.3 kOe, T = 4.2 K.

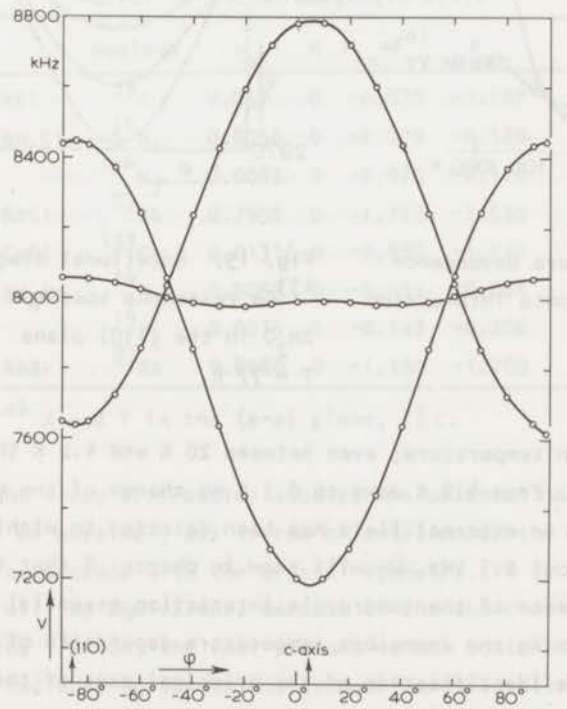

Fig. 13. Rotational diagram of the ^{87}Rb resonance spectrum for $Rb_2CuBr_4 \cdot 2H_2O$ in the (110) plane. H_o = 6.0 kOe, T = 4.2 K.

the ^{87}Rb resonance spectrum in $Rb_2CuBr_4\ 2H_2O$ for $\vec{H}_o$ in the (110) plane is shown. The angular dependence of the central line ($+\frac{1}{2} \rightarrow -\frac{1}{2}$ transition) is due to the combined effect of the anisotropy of the frequency shift tensor and the second order quadrupole shift. The interaction parameters for both compounds are listed in table 10.

As the signal to noise ratio of the ^{87}Rb resonance lines is very large, also an accurate temperature dependence of ν_q could be determined. In fig. 14 the results of these measurements for both compounds from T = 4.2 K up to room temperature are shown. It can be seen that especially for the chlorine compound ν_q very

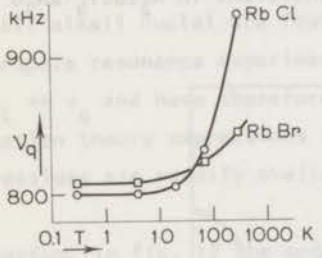

Fig. 14. Temperature dependence of the ^{87}Rb quadrupole interaction

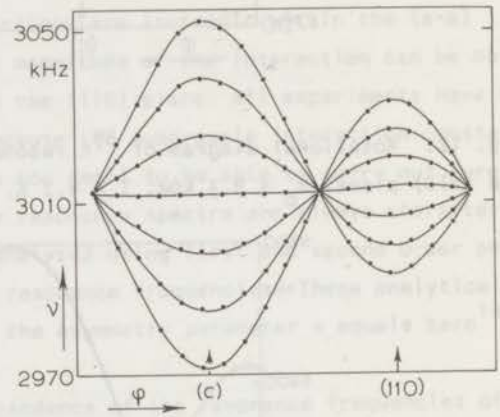

Fig. 15. Rotational diagram of the ^{133}Cs resonance spectrum for $Cs_2CuCl_4 \cdot 2H_2O$ in the (110) plane. H_o = 5.44 kOe, T = 77 K.

strongly depends on temperature; even between 20 K and 4.2 K the value of ν_q still changes 0.7%. From 4.2 K down to 0.3 K no change of the quadrupole interaction constant in external field has been detected to within the experimental accuracy of about 0.3 kHz. We will show in chapter 8 that from this strong temperature dependence of the quadrupole interaction essential information can be obtained concerning the anomalous temperature dependence of the exchange interaction and the identification of the principal axes of the Cl(I) and Br(I) EFG tensor.

At ^4He temperatures it has been observed that there exists a small difference between the value for ν_q measured with $\vec{H}_o$ along the (110) axis and the value

for $\vec{H}_o \| c$. For $Rb_2CuCl_4 \cdot H_2O$ we have determined ν_q = 799.5 kHz for $\vec{H}_o \| c$ and ν_q = 796.3 kHz for $\vec{H}_o \| (110)$. In the bromine compound this difference is somewhat smaller: ν_q = 808.0 kHz for $\vec{H}_o \| c$ and ν_q = 806.8 for $\vec{H}_o \| (110)$. We think that these differences have to be related to small magnetostriction effects.

Caesium. In fig. 15 the rotational diagram of the ^{133}Cs (I = 7/2) spectrum is presented, again for $\vec{H}_o$ in the (110) plane. The width of the resonance lines is only 1.5 kHz and therefore, although the quadrupole interaction is very small due to the large spin value and the small quadrupole moment, also for these nuclei a temperature dependent value for ν_q has been detected. For T = 77 K it is found that ν_q = 13.50 kHz while for T ≤ 4.2 K ν_q = 13.16 kHz which represents a change of 2.6% over that temperature interval. Similar to the Rb quadrupole interaction the value for ν_q increases to higher temperatures.

Table 10

Interaction parameters of the alkali nuclei in the paramagnetic state

	nucleus	ν_q	η	$F_{xx}=F_{yy}$ [a]	F_{zz}
KCl	^{39}K	0.057	0	-0.070	-0.107
NH_4Cl	$^{14}N_1$	0.0050	0	-0.020	-0.120
	$^{14}N_2$	0.0083	0	-0.070	-0.170
RbCl	^{87}Rb	0.7995	0	-1.220	-1.530
CsCl	^{133}Cs	0.01316	0	-0.880	-1.070
NH_4Br	$^{14}N_1$	0.0053	0	-0.033	-0.084
	$^{14}N_2$	0.0075	0	-0.147	-0.206
RbBr	^{87}Rb	0.8080	0	-1.330	-1.700

a) X and Y in the (a-a) plane, Z||c.

Ammonium. From the X-ray diffraction studies the orientation of the ammonium molecules cannot be obtained, but if the orientation of the molecules in the unit cell is in accordance with the crystal symmetry, it is clear that all nitrogen nuclei will be equivalent. Because of the cubic arrangement of the protons around the ^{14}N ion, the four protons do not contribute to the EFG tensor at the nitrogen nucleus. So equivalent symmetry considerations as for the EFG tensor of the alkali nuclei predict that the EFG tensor at all nitrogen nuclei will be equivalent and that this tensor will have axial symmetry around the c-axis. To determine the quadrupole interaction, rotational diagrams of the

nitrogen resonances were made at T = 4.2 K with an external field rotating in the (110) plane and the (a-c) plane. As the nitrogen nuclear spin is I = 1 one expects to observe two resonance lines.

The observed nitrogen spectrum in both compounds consists of two separated groups of resonance lines, with resonance frequencies which are lower than the free ^{14}N resonance frequency in that applied field. The fine structure in each group originates from the proton-nitrogen dipolar interaction, which is appreciable as the proton-nitrogen distance is about 1 Å. As there are four protons surrounding each nitrogen ion, this fine structure is very complicated. The resonance lines within each group are of unequal intensity and overlap each other frequently in the rotational diagram which makes it hard to analyze the angular dependence of the resonance frequencies.

However, with the field in the direction of the a-and c-axes this complicated structure of the two groups of resonance lines reduces to only two separated doublets. By observing the temperature dependence of the resonance frequencies of these doublets, it is apparent that they belong to two magnetically inequivalent N sites. Clearly this is not expected from the crystal symmetry, which leads to the conclusion that the symmetry of the N sites does not reflect the symmetry of the rest of the unit cell.

As the nitrogen spectra by their complexity are not suitable to give enough information about the two crystallographic sites and the orientations of the NH_4 tetrahedra, the spectrum of the protons of the NH_4 group has been studied.

In quite the same way as the study of the proton-proton dipolar interaction between the protons of a water molecule can give the information about the direction of the proton-proton connection line, the angular dependence of the much more complicated proton-proton splittings of the resonance lines from the protons of the NH_4 group yields the orientation of the proton tetrahedra The best procedure would be to study the resonance spectrum at high temperatures where the induced magnetization is negligible compared to the proton-proton interaction. At room temperature and at T = 77 K, however, only one intense resonance line with a linewidth of about 20 kHz, without fine structure, was observed. This is due to reorientations or torsional motions of the NH_4 group with frequencies much higher than the Larmor frequency of the protons, which lead to motional narrowing of the resonance spectrum. However, at T = 20 K the fine structure of the NH_4 proton resonance line can be observed, and the angular dependence of the spectrum has been studied. With the external field in the direction of the a-axis and of the c-axis the observed spectra are equivalent. This spectrum consists of five resonance lines with equal spacing of 20 kHz and an intensity

ratio of 1:2:2:2:1 (see fig. 16). By a simple calculation it can be deduced from this spectrum that the three two-fold rotational axes of the NH_4 group are parallel to the c- and a-axes of the crystal. From the value of the splitting the H-H distance is calculated to be 1.65 Å while the N-H distance is 0.99 Å.

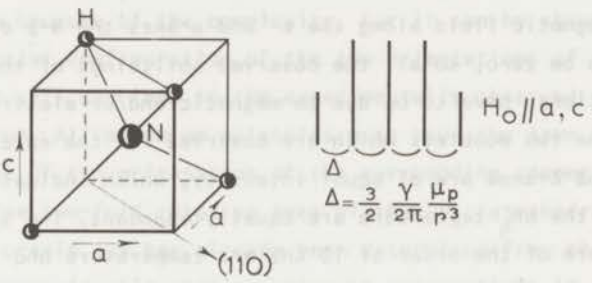

Fig. 16. The orientation of the NH_4 molecule in the unit cell and the schematic proton spectrum for $\vec{H}_o \| a$ or c at T = 20 K.

There are then two possible orientations for the NH_4 tetrahedra: first of all the protons can be directed towards the nearest Cl(I) or Br(I) ions. Secondly the protons can be directed towards the Cl(II) or Br(II) ions (see fig. 34 for the surrounding of the alkali ions).

At ^4He temperatures the magnetic interactions of the NH_4 protons are studied to get information about the two possible orientations of the tetrahedra with respect to the nearby Cu ions. For the field along the c-axis all the protons appear to be magnetically equivalent as only the above-mentioned quintet has been observed, shifted to lower frequency.

The spectrum with the field along the a-axis, however, splits up by the magnetic interaction into two separate groups of resonance lines. It can be calculated that, if the NH_4 tetrahedra at the various crystal sites were oriented according to the crystal symmetry, all the protons would have equivalent magnetic interactions when the magnetization is directed along the a-axis. So we have to conclude that both possible orientations of the NH_4 tetrahedra are present in the unit cell.

The magnetic and electric interactions of the NH_4 tetrahedra with the surrounding halide ions and water molecules will be different for these two orientations. This will lead to different magnetic interactions for the NH_4 protons in the two orientations. Because of the distortion of the NH_4 tetrahedron by the

surrounding ions, and because of covalency effects, which will also be different for the two orientations, also the magnetic and electric-quadrupole interactions of the ^{14}N nuclei will be different for the two orientations, leading to two nitrogen spectra.

Using the determined orientations of the NH_4 proton tetrahedra the observed nitrogen spectra at ^4He temperatures can now be analysed.

With the magnetic field along the c- and a-axes the N-p dipolar interaction is calculated to be zero, so all the observed splittings of the ^{14}N spectra for those directions, have to be due to magnetic and/or electric quadrupole interactions. The two doublets which are observed for the external field parallel to the a- and c-axes are of equal intensity, which indicates that both orientations of the NH_4 tetrahedra are equally abundant. The splittings of both doublets which are of the order of 10 kHz are temperature and field independent and have thus to be due to electric quadrupole interaction. Although no complete rotational diagram of the doublet splittings can be determined because of the complicated N-p dipolar splittings, it is found that for the external field at 55° from the c-axis the quadrupole splittings for both nitrogen spectra equals zero. As for $\vec{H}_o \| a$ the respective doublet splittings are half the value of those for $\vec{H}_o \| c$ it can be concluded that the EFG tensor at both nitrogen sites (in the chlorine as well as in the bromine compound) has axial symmetry about the c-axis. From the experiments with $\vec{H}_o$ along the a- and (110)-axis it is deduced that also the frequency shift tensors for both nitrogen sites have rotational symmetry about the c-axis. The interaction parameters determined from both resonance spectra are given in table 10.

It appears to be possible to conclude whether the two possible orientations of the NH_4 molecules are distributed randomly or whether they are distributed systematically over the crystal. Careful examination of the proton resonance spectrum of the waters of hydration demonstrates that the high frequency resonance doublet for $\vec{H}_o \| (110)$ (see fig. 7) in the ammonium compounds is not a single one as observed in all other compounds. At low temperatures and high field where the magnetization is near its saturation value it appears that this transition consists of two doublets, each with a proton-proton dipolar splitting of 84 kHz. The difference of the mean Larmor frequencies of the two doublets is proportional to the reduced magnetization m(T,H). For m(T,H) = 1 this difference in both compounds is only about 70 kHz. It is clear that this small difference in magnetic interaction for the otherwise similar protons has to be due to the presence of the two different orientations of the NH_4 tetrahedra. As the proton-proton splitting for both doublets has the maximum value of 84 kHz, the total

magnetic field at the two protons within one water molecule (for which $\vec{H}_o \| \gamma'$) have to be equal, as otherwise for these two protons the maximum value of Δ_{pp} would only be $\frac{2}{3}$ x 84 kHz = 56 kHz[7]. So there have to be two magnetically different types of water molecules for which $\vec{H}_o \| \gamma'$, i.e. $\vec{H}_o$ is parallel to the proton-proton connection line within the water molecule. However the two protons belonging to the same water molecule are magnetically equivalent. It will not be reasoned here because of the complexity, but it can be shown unambiguously that only one special configuration of the two orientations of the NH_4 molecules in the unit cell can lead to the experimentally observed spectrum of the waters of hydration. All ammonium molecules must have the same spatial orientation independent of the orientation of the surrounding copper octahedra. Naturally the three two-fold rotation axes of the NH_4 tetrahedra are directed along the a- and c-axis, as has already been determined from the spectrum of the ammonium protons. As this configuration of orientations is in contradiction with the crystal symmetry $P4_2/mnm$ also two nitrogen spectra have to be observed. The local symmetry at each of the two nitrogen sites however is still so as to have rotational symmetry about the c-axis for the nuclear interaction tensors. In principle all other resonance spectra in these ammonium compounds have to be two-fold too. Only for the protons of the waters of hydration and for the NH_4 protons this doubling has been observed actually. For all other resonance spectra this break-down of the crystal symmetry is reflected by an increase of the width of the resonance lines with respect to the linewidths in all other compounds. (See section 6.5 for the width of the copper resonance lines.)

References.

1) Anderson, P.W. and Weiss, P.R., Rev. Mod. Phys. 25 (1953) 269.
2) Okuda, T. and Date, M., J. Phys. Soc. Japan 28-2 (1970) 308.
3) Seidel, G. and Choh, S.H., Bull. Amer. Phys. Soc. 11 (1966) 186.
4) Kennedy, T.A., Choh, S.H. and Seidel, G., Phys. Rev. B2 (1970) 3645.
5) Van Santen, J.A., Scholten, A.T.M. and Schumm, W., private communication.
6) Reedijk, J., private communication.
7) Bloembergen, N., Physica 16 (1950) 95. (Commun. Kamerlingh Onnes Lab., Leiden, No. 208c)
8) Wittekoek, S., Thesis, Leiden, 1967.
9) Lederer, C.M., Table of Isotopes, 6th ed., John Wiley and Sons (New York, 1968).
10) Moriya, T., Progr. Theor. Phys. 28 (1962) 371.

11) Suhl, H., Phys. Rev. 109 (1958) 606.
12) Nakamura, T., Progr. Theor. Phys. 20 (1958) 542.
13) Abragam, A. and Bleany, B., Electron paramagnetic resonance of transition ions, Clarendon Press (Oxford, 1970) p. 654.
14) Abragam, A., The principles of nuclear magnetism, Clarendon Press (Oxford, 1962) p. 233.

Chapter 7

EXPERIMENTS IN THE FERROMAGNETIC STATE

The ferromagnetic state is characterized by the existence of a non-zero time averaged value of the magnetic moments of the copper ions in zero external field. The direction of these magnetic moments depends on crystal anisotropies and/or anisotropy of the exchange interaction. The crystal sample is divided into a large number of domains which are magnetized alternately in opposite direction. This yields a decrease of the total magnetostatic energy of the crystal because the larger part of the magnetic flux circuit is completed within the crystal. Within each (Weiss) domain the magnetic moments are all directed along the preferred direction, or easy axis, producing a local spontaneous magnetization $M_s(T)$. In describing the experiments, we will always use the value of the reduced spontaneous magnetization $m_s(T)$, defined by $m_s(T) = M_s(T)/M_s(T=0)$, i.e. $0 \leq m_s(T) \leq 1$ for $T_c \geq T \geq 0$, where T_c is the ferromagnetic transition temperature. The Weiss domains are separated from each other by the so-called Bloch walls. The direction of the magnetic moments within these walls changes gradually from the direction of the magnetic moments in the one domain to that in the other domain.

For these compounds the magnetization per volume unit is rather small because of the small number of magnetic ions per volume unit ($M_s(0) \simeq 45$ Oe). Therefore the total volume which is occupied by the Weiss domains is much larger than that occupied by the Bloch walls. Although the n.m.r. signal enhancement (see chapter 5) for nuclei inside Bloch walls is larger than for nuclei within domains[1], the much larger number of nuclear spins within the domains does cause the signal intensity of the n.m.r. transitions from these nuclei to be much larger than those originating from the nuclei inside walls. Moreover the resonance signals of the wall nuclei are expected to be much broader due to the combined effect of the strong anisotropy of the frequency shift and EFG tensors of the nuclei and the gradual change of the direction of the magnetic moments in the Bloch walls. As a result, apart from one Cl(II) resonance line, only n.m.r. transitions originating from nuclei within the domains have been detected.

7.1. Determination of the Curie temperature and the anisotropy field. In zero external field various criteria can be applied for the determination of the temperature at which the transition from the paramagnetic into the ferromagnetic state occurs. This "Curie" temperature can be determined from the maximum in the specific heat versus temperature curve, from the temperature of maximum susceptibility, or from the occurrence of spontaneous magnetization. We have used the last two criteria to obtain an accurate value for T_c in all six compounds.

The temperature at which $m_s(T)$ springs up can be determined by observing the PQR transition of the halide (I) nuclei as the temperature is lowered. For $T \leq T_c$ the single PQR line splits up by the magnetic interaction. Also by fitting the temperature dependence of the spontaneous magnetization just below T_c to the scaling law expression $m_s(T) = A(1 - T/T_c)^{\beta}$, the value of T_c can be obtained.

For the determination of T_c from the maximum of the susceptibility only relative values of $\chi(T)$ are needed, therefore such an experiment can be performed using a normal n.m.r. oscillator. The inductance L of the r.f. coil around the crystal depends on the temperature because of the temperature dependence of the crystal susceptibility: $L(T) = L(\infty)\{1 + 4\pi f\chi(T)\}$, where $L(\infty)$ is the coil inductance for $T = \infty$, i.e. for $\chi(T) = 0$, and f is the effective filling factor of the coil. If the capicitor of the LC circuit is fixed, the temperature dependence of the oscillator frequency is thus given by $\nu(T) = \nu(\infty)[1 + 4\pi f\chi(T)]^{-\frac{1}{2}}$. So the minimum of the oscillator frequency can be related to the maximum of the susceptibility of the crystal, occurring at the transition temperature. A second method to measure T_c from the maximum in the susceptibility is given by the possibility to observe the electron resonance line with a normal n.m.r. oscillator. For low frequencies, ν of the order of some Megahertz, the e.s.r. line can be observed for $H_o = 0$ with a small modulation field. As the signal intensity of the e.s.r. line is proportional to the electronic susceptibility, the temperature at which the maximum of the signal intensity is observed equals the transition temperature.

The values for T_c obtained using the various methods are found to agree within the experimental accuracy of about ± 0.2 mK; they are given in table II.

From the observation of the temperature dependence of the resonance field of the e.s.r. transition at low frequencies in the ferromagnetic state, the value of the anisotropy field H_A can be calculated. According to Suzuki et al.[2] the resonance condition for the electrons in a spherical sample for an external field perpendicular to the easy axis of magnetization is given by

$$(\omega/\gamma_e)^2 = H_o(H_o - H_A)$$

where $H_A = (A_{||} - A_{\perp}) M_s(T)$. $A_{||}$ and $A_{\perp}$ are the anisotropy molecular field constants. It is clear that for $\omega/\gamma_e \approx 0$, which holds fairly well for an oscillator frequency of some MHz, the e.s.r. line will be observed for $H_o \approx H_A$. The anisotropy fields, extrapolated to T = 0 K, have been determined by this method to be about 200 Oe for the chlorine and 300 Oe for the bromine compounds. The value of H_A for the bromine compounds agrees with that determined by Suzuki et al.[2] and Renard et al.[3].

By applying in the ferromagnetic state an external field perpendicular to the easy axis of magnetization, the magnetic moments of the ions within the Weiss domains will rotate into the direction of the external field, by that way producing a macroscopic magnetization of the sample. The apparent susceptibility, originating from the field dependence of this macroscopic magnetization, can be observed on the change of the frequency of the oscillator, as has been outlined already. For that field for which all magnetic moments are aligned along the field direction, the value of the apparent susceptibility will drop drastically to the small value of the normal paramagnetic susceptibility at that temperature and field. For larger fields the Weiss domain structure has disappeared and the crystal behaves in principle as a paramagnetic substance. The magnitude of H_o for which this "transition" occurs is found to be equal to the magnitude of H_A as determined by electron resonance at low frequency. The anisotropy field can thus be related to the transition from the ferromagnetic into the paramagnetic state for $T < T_c$.

7.2. Proton spectrum: the direction of the spontaneous magnetization in the Weiss domains.

7.2.1. Bromine compounds. In both bromine compounds only one resonance line from the protons of the water molecules has been observed in the ferromagnetic state in zero field. This resonance line shows a temperature independent fine structure which, after careful examination, is found to be six-fold. The mean Larmor frequency of this sextet at T = 0.3 K, where $m_s(T) \approx 1$, is about 6.4 MHz in both compounds. From the rotational diagram of the proton lines as given in fig. 7 it can be shown that a frequency shift of a proton line for $m(T,H) \approx 1$ can only be expected for the external field, and thus the magnetization, directed along the c-axis. Together with the observation of only one resonance

sextet, this indicates that the spontaneous magnetization in the ferromagnetic state has to be parallel to the crystallographic c-axis. This conclusion is confirmed by the analysis of the resonance spectra of all other nuclei in the bromine compounds. This direction of the spontaneous magnetization agrees with that determined by Wielinga[4] from macroscopic magnetization measurements in $(NH_4)_2CuBr_4 \cdot 2H_2O$.

Although we searched for it carefully, no extra proton resonance lines showed up at lower frequencies. That proves that there are no "closure" domains which are magnetized perpendicular to the c-axis. This has been confirmed again by the analysis of the other resonance spectra which indicates that always only one spectrum per set of chemically equivalent ions is observed. These two bromine compounds thus behave like uniaxial ferromagnets.

The static six-fold fine structure of the proton resonance line has not yet been understood. There are several possible explanations for this fine structure.

a) The internal fields at the two protons belonging to the same water molecule are equal in magnitude but have different directions. For such a situation Hardemann[5] has derived an expression for the proton-proton dipolar interaction for protons within a water molecule. However the maximum number of observable transitions is always four instead of the six observed transitions. Moreover, as the internal fields at the protons in both compounds are found to be nearly equal one would expect the fine structures for both resonance lines, if due to this effect, to be about equal. In table II, where the frequency differences between the successive fine structure lines is given, it can be seen that there is a large difference between the splitting patterns in both compounds.

b) Interaction with the two protons from the nearby water molecule. It can be calculated that the distance between the protons belonging to the water molecule at approximately (0,0,0.25) and those from the H_2O at (0,0,0.75) is small enough as to have a discrete dipolar interaction between them. The number of possible fine structure lines can be larger in this situation, as we deal now essentially with a four-particle system. As this interaction has to be present in the paramagnetic state too, we have examined the proton resonance transition for $\vec{H}_o \| c$ at T = 20 K. For that temperature the magnetic interaction with the copper ions is very small, and therefore mainly static dipolar interactions will be observed. The detected resonance transition consists of four lines with a ratio of the signal intensities of about 2:1:1:2. The frequency differences are approximately 13;26;13 kHz slightly different for the two compounds. The calculations show however that the dipolar interaction between the protons from different water molecules is too small to be able to explain

the observed fine structure splittings in both the paramagnetic and the ferromagnetic state.

c) The dipolar interaction of the protons with the nearby Br(I) nuclear magnetic moments has been found to be too small to produce the observed splittings too. It must be mentioned that also in the chlorine compounds in the paramagnetic state this four-fold fine structure of the proton line for $\vec{H}_o \| c$ has been observed. The search for the origin of these fine structures is one of the interesting problems which we will try to solve in the near future.

Table II

Larmor frequencies and fine structure splittings of the protons of the water molecules in the ferromagnetic state at T= 0 K

	T_c(K)	ν_L(MHz)	Δ_{pp}(kHz)
KCl	0.877	3.65	82
NH_4Cl	0.701	3.73	84
		3.79	84
RbCl	1.017	3.71	90
CsCl	0.753	3.79	84
NH_4Br	1.836	6.43	16- 7-22- 7-16
RbBr	1.874	6.46	10-11-14-11-10

7.2.2. Chlorine compounds. In all four chlorine compounds originally one proton resonance line, originating from the protons of the crystal waters, has been detected. The resonance frequency is about 3.5 MHz at T = 0.3 K. The proton-proton dipolar splitting has about the theoretically maximum value of 84 kHz, which proves unambiguously that in these compounds the spontaneous magnetization within the Weiss domains has to be parallel to the (110) direction (see the discussion in section 6.2). At low temperatures the H_2O proton doublet in the NH_4 compound splits up into two doublets, each with a proton-proton splitting of 84 kHz. This is due to the two possible orientations of the NH_4 molecules, as has already been outlined in section 6.6. The proton doublet which would be expected for the second H_2O for which $\vec{m}_s$ is perpendicular to its proton-proton connection line ($\vec{m}_s \| \gamma$) has not been observed. It can be calculated from the proton experiments in external field that the internal field at this proton site in the ferromagnetic state is less than 100 Oe. The resonance frequency of this transition is therefore too low to be able to observe this

doublet.

From the study of the proton doublet at T = 0.3 K in small external fields in the direction of the (110)-axis, with the r.f. field along the c-axis, it can be concluded whether the chlorine compounds are uniaxial ferromagnets or not. In fig. 17 the splitting pattern of the proton doublet for a weak field

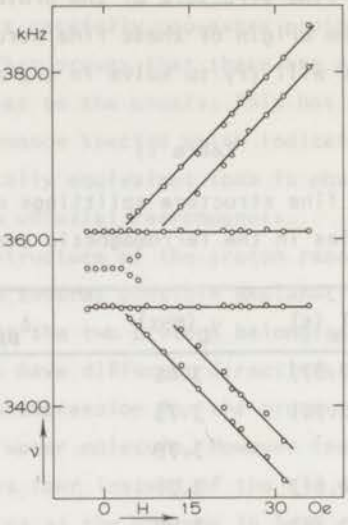

Fig. 17. $K_2CuCl_4 \cdot 2H_2O$. Field dependence of the splitting of the zero field proton doublet for $\vec{H}_o \| (110)$ at T = 0.3 K.

parallel to the (110)-axis is shown. The volume of the Weiss domains which are magnetized parallel to the applied field will increase at the cost of the domains which are magnetized antiparallel to $\vec{H}_o$ with increasing magnitude of H_o. Therefore the magnetic flux in both types of domains will become different, which results in a different total magnetic field at the protons within the two types of domains. The zero field proton doublet is thus expected to split up into two doublets in external field. This splitting actually is observed; however also a third doublet with a nearly field independent resonance frequency has been detected. The existence of this third doublet can only be explained by assuming that there also exist Weiss domains which are magnetized perpendicular to the external field, i.e. along the $(1\bar{1}0)$-axis. As these perpendicular magnetized domains are mutual magnetically equivalent, no splitting of the resonance doublet originating from the protons within these domains will occur by the applied field. This proves that the chlorine compounds are not uniaxial; the domains are magnetized along the (110) and $(1\bar{1}0)$ respectively. The occurrence

of these two preferred directions however will not influence the number of resonance spectra observed in zero field.

From the behaviour of these proton resonance lines and also of the Cl(II) resonance lines at T = 0.3 K for an external field in different crystallographic directions, it can be concluded that the a-axes are the hard directions of magnetization. It proves to be not possible to rotate the spontaneous magnetization into the direction of the a-axis by applying an external field of 100 Oe along this axis. If $\vec{H}_o$ is applied along the c-axis however, the direction of the spontaneous magnetization within the domains deviates already appreciably from the (110)-axis for H_o = 20 Oe.

In all compounds the temperature dependence of $m_s(T)$ can be determined straight forward from the temperature dependence of the proton resonance frequency, as this frequency is proportional to $m_s(T)$. The so determined magnetization curves have been used to facilitate the analysis of the very complicated resonance spectrum of the other nuclei.

7.3. Halide (I) spectra.

7.3.1. Bromine compounds. In both crystals in the ordered state at T = 0.3 K all six possible resonance transitions per isotope of the Br(I) site nuclei are observed. The linewidth of the +3/2 → -3/2 transition is about 10 kHz, while the width of all other resonance lines is 20 kHz. The lineshape of all transitions is that of a perfect absorption line, which indicates that the nuclear absorption susceptibility for these ions is not yet saturated by the enhanced radio frequency field. From the six resonance frequencies the appropriate energy level scheme can be constructed easily. In fig. 18 the temperature dependence of the resonance frequencies of the transitions of both isotopes in $Rb_2CuBr_4 \cdot 2H_2O$ is shown. As the intensity of the $(\pm\frac{1}{2} \rightarrow \pm\frac{3}{2})$ transitions was rather small, no attempt has been made to measure the temperature dependence of their resonance frequencies extensively.
The resonance spectra resemble the type of spectrum discussed in section 5.2.c for the case $\nu_L << \nu_q$. However, due to a second order frequency shift the β transitions are not situated symmetrically with respect to the PQR frequency. Therefore to analyze these spectra the Brown and Parker method has been applied. These BP calculations confirm that the direction of the spontaneous magnetization points along the c-axis. It is found that the values of the quadrupole interaction parameters deviate from those determined in the paramagnetic state. (see table 7). Moreover ν_q and η are slightly temperature dependent. We think

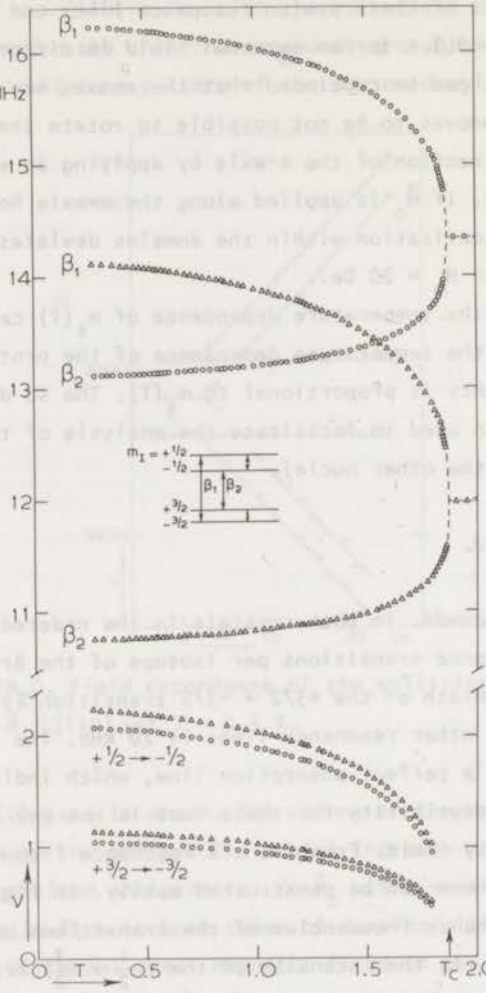

Fig. 18. $Rb_2CuBr_4 \cdot 2H_2O$. Temperature dependence of the Br(I) resonance spectra in the ferromagnetic state. ⊙ ^{79}Br; △ ^{81}Br.

that this effect points to the presence of minor spontaneous magnetostriction effects. The values of the interaction parameters of the $^{79}Br(I)$ nuclei, which have been extrapolated to T = 0 K, are given in table 12. The value of F°_{ii} given in the table is defined by $F^{\circ}_{ii} = \nu_L(T)/m_s(T)$, where the indices i indicate the principal axis of the EFG tensor, along which the spontaneous magnetization

Table 12

Interaction parameters of the halide (I) nuclei in the ferromagnetic state at T=0 K (^{79}Br and ^{35}Cl)

	spectrum	$\nu_q(1+\eta^2/3)^{\frac{1}{2}}$	ν_q	η	F°_{ii}
KCl	B[b]	1.9527	1.720	0.93	0.071
NH_4Cl	B	1.4261	1.235	1.00	0.023
RbCl	A[a]	2.2731	2.103	0.71	0.948
	B	2.2718	2.093	0.73	0.107
CsCl	A	2.3715	2.300	0.44	1.100
	B	2.3688	2.301	0.42	0.298
NH_4Br	c)	8.334	7.400	0.897	0.967
RbBr		14.349	13.459	0.640	1.568

a) $\vec{m}_s // Y$; b) $\vec{m}_s // Z$; c) $\vec{m}_s // X$

is directed.

The signal to noise ratio of the β resonance lines at T = 0.3 K is about 10^4. Because of their large intensity these lines are appropriate to search accurately for any other transitions originating from these Br(I) nuclei, which would indicate the existence of closure domains magnetized in a direction perpendicular to the c-axis. As has already been mentioned in section 7.2 no such transitions have been detected.

In section 7.7 it will be shown that the difference in resonance frequency of the two β transitions $\Delta\nu_\beta$ is always exactly equal to two times the Larmor frequency. Therefore from the temperature dependence of $\Delta\nu_\beta$ the critical behaviour of the spontaneous magnetization near T_c has been determined. The results of these measurements will be discussed in section 7.7.

In the course of the experiments it has been observed that in the bromine compounds a notable amount of chlorine impurities can be present. The influence of these impurities on the Br(I) resonance spectrum will be discussed in Appendix B.

7.3.2. Chlorine compounds. As the spontaneous magnetization within the Weiss domains is directed along the (110)-axis in the chlorine compounds, we will expect to observe two resonance spectra per chlorine isotope. According to the

notation for the zero field spectra in the ferromagnetic state, as introduced in chapter 5.6, these two different spectra are denoted by Cl(I)A and Cl(I)B. The Cl(I)A spectrum originates from those nuclei for which the spontaneous magnetization is parallel to the γ' direction, which is the Y-axis of the Cl(I)EFG tensor. The Cl(I)B spectrum originates from the nuclei for which $m_s \| \gamma'$, i.e. parallel to the Z-axis of the EFG tensor.

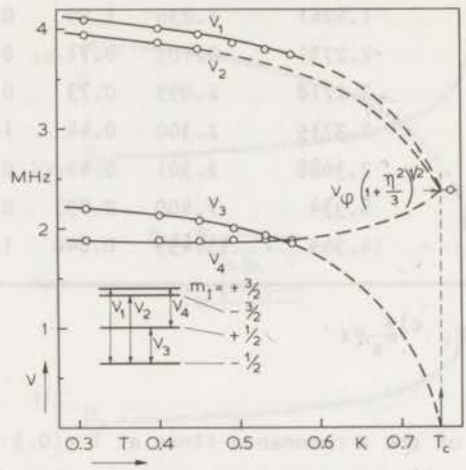

Fig. 19. $Cs_2CuCl_4 \cdot 2H_2O$. Temperature dependence of the $^{35}Cl(I)A$ resonance spectrum in the ferromagnetic state.

Cl(I)A.

In fig. 19 the temperature dependence of the frequencies of the $^{35}Cl(I)A$ resonance transitions in $Cs_2CuCl_4 \cdot 2H_2O$ is shown. The signal intensity of these resonance lines is rather small, which prevents an accurate determination of the temperature dependence near T_c. The energy level diagram however can be constructed easily. Also in the Rb compound the Cl(I)A spectrum has been detected, although the signal intensity of the resonance lines is very small. In the K and NH_4 compounds, surely due to still smaller signal intensities, the Cl(I)A spectra could not be observed. For the Rb and Cs compound the values of the interaction parameters extrapolated to T = 0 K are given in table 12. By comparison of the values given in this table with those of table 7 it can be concluded that the quadrupole interaction parameters calculated from the Cl(I)A spectra differ from those determined in the paramagnetic state. This difference,

like for the Br(I) nuclei in the bromine compounds, has to be due again to spontaneous magnetostriction effects.
The resonance lines have an absorption shape with a width of about 10 kHz.

Cl(I)B.

In all four chlorine compounds the Cl(I)B spectrum for both isotopes has been observed. The spectrum consists of two intense α transitions and two very weak β transitions. In fig. 20 the temperature dependence of the α resonance frequencies in the rubidium compound is shown, together with the energy level diagram. At T = 0.3 K in the Rb and Cs compound the $+\frac{3}{2} \rightarrow -\frac{3}{2}$ transitions have also been detected at respectively 295 kHz and 836 kHz. In the Cs compound even the $+\frac{1}{2} \rightarrow -\frac{1}{2}$ transition at a frequency of 267 kHz has been observed with a good signal to noise ratio.
The interaction parameters for T = 0 K are given in table 12. It is seen that also for these spectra the quadrupole interaction constants differ from those

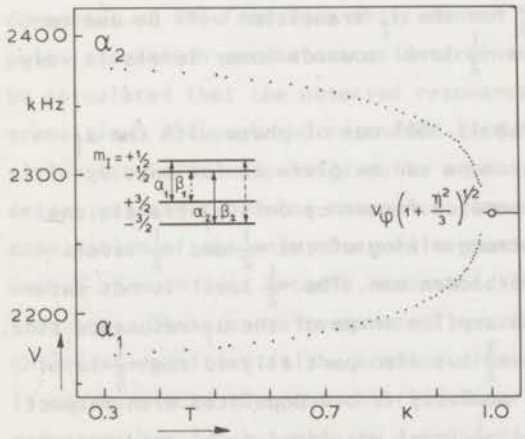

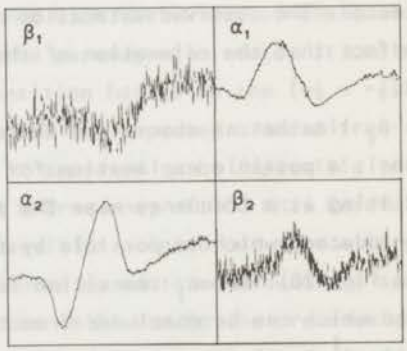

Fig. 21. $Rb_2CuCl_4 \cdot 2H_2O$. Shape of the Cl(I)B resonance lines.

Fig. 20. $Rb_2CuCl_4 \cdot 2H_2O$. Temperature dependence of the $^{35}Cl(I)B$ spectrum in the ferromagnetic state. Only the α transitions are shown.

determined in the paramagnetic state and even from those calculated from the Cl(I)A spectra. It must be noted that the separate values for ν_q and η can be determined less accurately than the value of $\nu_q(1 + \eta^2/3)^{\frac{1}{2}}$. Therefore these differences in the EFG between paramagnetic and ferromagnetic state, attributed to spontaneous magnetostriction effects, can be demonstrated the best by

comparing the values for $\nu_q(1 + \eta^2/3)^{\frac{1}{2}}$ for the different zero field spectra with the PQR frequency. It can then be seen that in the chlorine compounds this value in the ferromagnetic state is always higher by a few kHz than in the paramagnetic state.

Because the lineshape of the α and β transitions in all four compounds is very peculiar, in fig. 21 a recorder trace of the second derivative of the experimentally observed spectrum in $Rb_2CuCl_4 \cdot 2H_2O$ at T = 0.3 K is shown. For the observation of the β resonance lines a ten times larger sensitivity of the lock-in amplifier has been used than for the α lines. The shape and phase of the α_1 resonance line agrees with the shape of the proton and Cl(I)A resonance lines and is therefore evidently an example of a normal absorption line. The dispersion shape of the α_2 line (in the Cs compound even all three zero passages of the second derivative can be observed) undoubtedly is caused by the saturation of the nuclear absorption susceptibility χ_n'' for the $\Delta m_I = -\frac{3}{2} \rightarrow -\frac{1}{2}$ transition, because of the enhancement of the r.f. field. As has been outlined in chapter 5.4, in such cases a resonance line with a dispersion shape can be detected. The observed saturation of χ_n'' for the α_2 transition will be due to the fact that the relaxation of the $m_I = -\frac{1}{2}$ level towards lower levels is very bad.

The β_1 line has an absorption shape which is 180° out of phase with the α_1 signal; a possible explanation for this shape can be given as follows. By radiating at a frequency near the β_1 resonance frequency only α_1 transitions are induced, which is possible by the strong mixing of the $+\frac{1}{2}$ and $-\frac{1}{2}$ levels (see fig. 20). The β_1 transition is a forbidden one. The $+\frac{1}{2}$ level is not saturated which can be concluded from the absorption shape of the α_1 resonance line. If the $+\frac{1}{2}$ level not only relaxes to the $+\frac{3}{2}$ but also partially to the $-\frac{1}{2}$ level due to the strong mixing, this $-\frac{1}{2}$ level probably is overpopulated with respect to the $+\frac{3}{2}$ level as the relaxation of the $-\frac{1}{2}$ level was found to be very bad. By changing the oscillation frequency to the β_1 resonance frequency a stimulated emission will occur, leading to the observed shape of the β_1 line. From the observation of a normal absorption shape for the $\Delta m_I = +\frac{1}{2} \rightarrow -\frac{1}{2}$ transition in the Cs compound it can be concluded that there is indeed a good relaxation from the $+\frac{1}{2}$ level towards the $-\frac{1}{2}$ level. When the amplitude of the r.f. field is increased, the intensity of the β_1 resonance line increases with respect to that of the α_1 line. This is in accordance with the change in intensity ratio which can be expected for this mechanism.

The 180° out of phase dispersion shape of the β_2 transition cannot be explained using similar arguments. We think that this shape is caused by cross relaxation

between the saturated α_2 line and the β_2 line, but even a qualitative explanation of the shape of β_2 is not yet possible.
From the temperature dependence of the difference in resonance frequency of the two α transitions $\Delta\nu_\alpha$, the temperature dependence of $m_s(T)$ near T_c has been determined in the Rb and Cs compound (see section 7.7). Because of the too small value for $\Delta\nu_\alpha$ in the K and NH_4 compounds no attempt has been made to measure $m_s(T)$ near T_c in these compounds, as overlap of the resonance lines near T_c will hamper the accurate determination of $\Delta\nu_\alpha$.

7.4. Halide (II) spectra.

7.4.1. Bromine compounds. Originally in the two bromine compounds in the ferromagnetic state only one Br(II) resonance line per isotope has been detected at approximately 20 MHz at T = 1.2 K. The width of this resonance line is about 200 kHz; the signal to noise ratio with which the resonance line at T = 1.2 K is detected is estimated to be of the order of 10^4. From the value of the Y component of the frequency shift tensor together with the values of the quadrupole interaction parameters as determined in the paramagnetic state, it could be calculated that the observed resonance transition had to be the $(+\frac{1}{2} \rightarrow -\frac{1}{2})$ transition. Although the resonance frequencies of the expected α and β transitions could be calculated quite accurately it appeared to be impossible to detect any other bromine resonance line up to a frequency of 100 MHz. Careful examination of the only observed resonance transition pointed out that a large number of much less intense resonance lines showed up centered around the same frequency. These extra resonance lines are found to be due to the presence of chlorine impurities at the bromine sites as will be discussed in Appendix B.
It can be argued that the chlorine impurities not only lead to discrete extra resonance spectra but also to a broadening of the Br(II) resonance lines. Especially the α and β transitions for which the resonance frequency is mainly determined by the quadrupole interaction, will be very much influenced by these impurities. In the crystals with much less chlorine impurities which have been grown afterwards, the α and β transitions have been observed. Field modulation has to be used as the width of these resonance lines is approximately 1.5 MHz, which is much too large to observe these signals with frequency modulation. In fig. 22 the temperature dependence of the resonance spectrum in the NH_4 compound is shown. The analysis of the Br(II) spectra in both compounds show that the interaction parameters for the Br(II) nuclei in the ferromagnetic state are about equal to those in the paramagnetic state. It must be noted that due

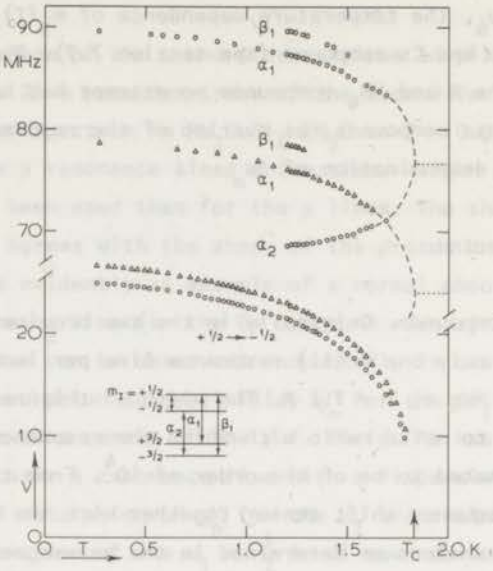

Fig. 22. $(NH_4)_2CuBr_4 \cdot 2H_2O$. Temperature dependence of the Br(II) resonance spectrum in the ferromagnetic state. ⊙ ^{79}Br; △ ^{81}Br.

to the very large linewidth of the α and β transitions the interaction parameters in the ferromagnetic state cannot be calculated very accurately. For the same reason it has not been possible to decide whether any temperature dependence of the quadrupole interaction, which would point to magnetostriction effects, exist. The interaction parameters are listed in table 13.

7.4.2. Chlorine compounds. As expected from the direction of the spontaneous magnetization, two Cl(II) resonance spectra per isotope have been observed. The Cl(II)A spectrum originating from those chlorine nuclei for which the spontaneous magnetization is directed parallel to the local γ'-axis (Z-axis of the Cl(II) EFG tensor) and the Cl(II)B spectrum for the nuclei for which $\vec{m}_s // \gamma$ (X-axis).

Cl(II)A. The Cl(II)A spectrum consists of the three allowed $\Delta m_I = 1$ transitions. The temperature dependence of the resonance frequencies in the

Table 13

Interaction parameters of the $^{35}Cl(II)A$, $^{35}Cl(II)B$ and $^{79}Br(II)$ nuclei in the ferromagnetic state at T=0 K

	spectrum	ν_q	η	F^o_{ii}
KCl	A[a]	9.465	0.20	27.50
	B[b]	5.94	0.56	4.61
NH_4Cl	A	9.430	0.25	27.74
	B	5.43	0.63	4.76
RbCl	A	10.300	0.16	27.45
	B	6.62	0.53	4.23
CsCl	A	11.150	0.17	27.35
	B	6.62	0.57	3.46
NH_4Br	c)	75.5	0.31	10.93
RbBr		81.6	0.22	9.30

a) $\vec{m}_s // Z$; b) $\vec{m}_s // X$; c) $\vec{m}_s // Y$

rubidium compound is shown in fig. 23. The quadrupole interaction parameters and the component of the frequency shift tensor for these nuclei in all four compounds are determined to be exactly equal to those measured in the paramagnetic state. The value for ν_q is found to be temperature independent within the experimental accuracy of about ± 10 kHz in the considered temperature interval. The resonance lines have an absorption shape with a width of 40 kHz when detected using a very weak r.f. field. If the amplitude of the r.f. field is increased the shape of the resonance line changes gradually from an absorption to a dispersion shape. This clearly demonstrates the influence of saturation effects on the lineshape as discussed in chapter 5.4. In the near future a study of these relaxation effects will be made.

Cl(II)B. In the frequency interval 1-40 MHz only those chlorine resonance lines are considered for the Cl(II)B spectrum from which the temperature dependence of the resonance frequencies are plotted in fig. 24. In fact there is one more line with a frequency equal to the sum of ν_1 and ν_4. This resonance line,

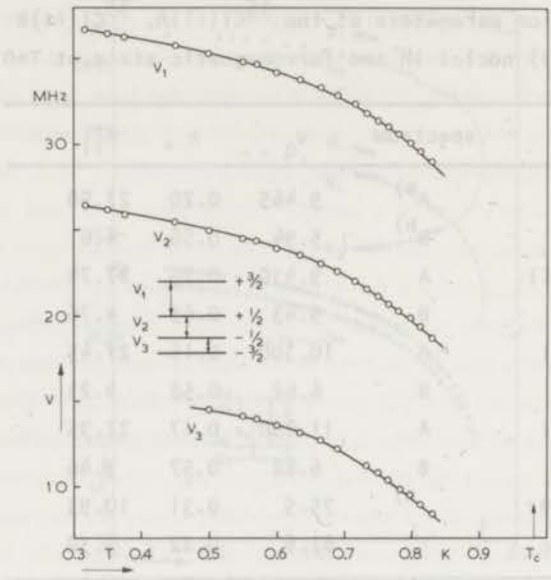

Fig. 23. $Rb_2CuCl_4 \cdot 2H_2O$. Temperature dependence of the ^{35}Cl(II)A spectrum in the ferromagnetic state.

however, is only determined at a few temperatures because of the low signal intensity. The resonance lines 2, 3 and the sum transition have an absorption shape with a width of about 50 kHz for the ^{35}Cl isotope. Line 1, however, has a dispersion shape and also a width of 50 kHz, while the linewidth of transition 4 is about 100 kHz and the shape is a mixture of absorption and dispersion character. The observation of the mentioned sum transition indicates that ν_1 and ν_4 are transitions within the same energy level scheme, and this fixes the relative position of three of the four levels. It appears to impossible to construct an energy-level diagram, starting with ν_1 and ν_4, so that both ν_2 and ν_3 belong to the same level scheme. So one of the resonance lines ν_2 or ν_3 does not belong to the Cl(II)B spectrum. To determine the level scheme, the following procedure has been used.

We start with the 3 levels determined by ν_1 and ν_4. Next all twelve possible level schemes using ν_2 or ν_3 as third transition have been constructed for both isotopes. By using the Brown and Parker method the interaction para-

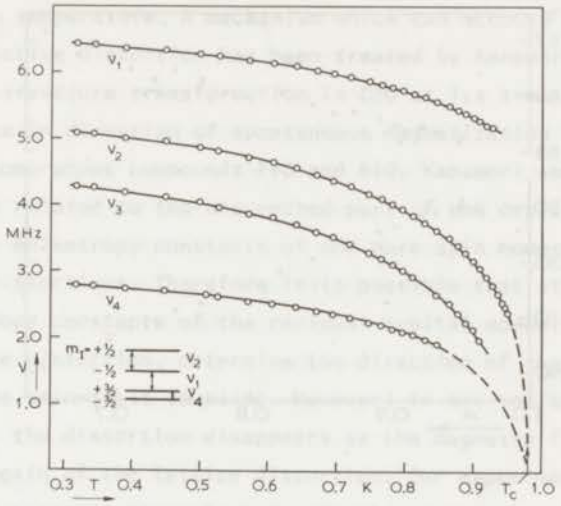

Fig. 24. $Rb_2CuCl_4 \cdot 2H_2O$. Temperature dependence of the $^{35}Cl(II)B$ resonance transitions in the ferromagnetic state.

meters for all twelve schemes have been calculated. The only assumption made is that the magnetic interaction is parallel to one of the EFG principal axes. The so determined parameters (ν_q, η, ν_L, principal axis) are used for a computer calculation of the resonance spectrum which belongs theoretically to each set of parameters. For only one level scheme the experimental and calculated spectrum are identical, which indicates the physical relevance of only that scheme. All other calculated spectra differ very much from the experimental spectrum. The so determined level diagram with ν_2 as third transition is given in fig. 24. The internal magnetic field is found to be parallel to the X axis of the EFG tensor, as expected, but the quadrupole interaction parameters differ largely from those calculated from the Cl(II)A spectrum in zero field (see table 13). Moreover, ν_q and η are strongly temperature dependent as is shown in fig. 25. The frequency shift tensor component $F^{\circ}_{xx} = \nu_L(T=0)$ is only very slightly temperature dependent but does differ much from the value F_{xx} determined in the paramagnetic state. The temperature dependence of the resonance frequencies has been checked in the already mentioned way by computer calculations. The experimental and recalculated spectrum are always identical within 10 kHz. From

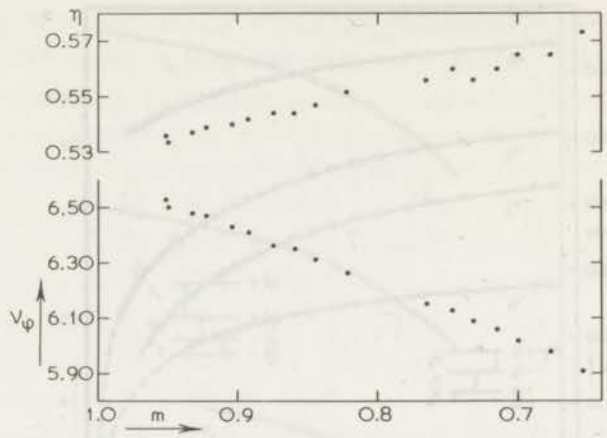

Fig. 25. $Rb_2CuCl_4 \cdot 2H_2O$. The $^{35}Cl(II)B$ quadrupole interaction parameters as a function of the reduced spontaneous magnetization m_s.

the plot of ν_q and η versus the reduced spontaneous magnetization m_s it seems as if these parameters for $m_s \to 0$ i.e. $T \to T_c$ do not extrapolate to the values found for the Cl(II) spectrum in the paramagnetic state.

To get more information about the Cl(II)B spectrum especially with regard to possible magnetostriction effects an external field in the (110) direction has been applied at T = 0.3 K. Only line 2 can be observed in a large external field. The intensity of the other Cl(II)B resonance lines decreases very sharply with increasing field; the lines disappear completely for fields above about 300 Oe.

It appears that the field dependence of ν_2 at T = 0.3 K cannot be explained making use of the zero-field values for ν_q, η and F°_{xx} of the Cl(II)B spectrum, although the magnetization at that temperature is nearly saturated, and therefore no appreciable change of these parameters is expected. For $H_o > 2$ kOe the field dependence of ν_2 can only be described theoretically when we assume that the quadrupole interaction parameters as determined for the Cl(II)A spectrum will also be appropriate for the Cl(II)B spectrum in strong field. Moreover, a different value for the frequency shift tensor component is determined.

It can thus be concluded that the distortion of the crystal lattice which has

to be the origin of the large change of the interaction parameters for the Cl(II)B-site nuclei, is present only in the ferromagnetic state in zero (or small) external field. Moreover, this distortion probably disappears discontinuously at the transition temperature. A mechanism which can account for this spontaneous magnetostrictive distortion has been treated by Kanamori[6,7] for the explanation of the structure transformation in CoO at its transition temperature and the difference in direction of spontaneous magnetization in CoO with respect to that in the isomorphous compounds FeO and NiO. Kanamori shows that the anisotropy constants related to the unquenched part of the orbital moment, in contrast with the anisotropy constants of the pure spin moment, strongly dependent on lattice distortions. Therefore it is possible that at the Curie temperature the anisotropy constants of the residual orbital moment, enlarged by a favourable lattice distortion, determine the direction of the spontaneous magnetization via the spin-orbit coupling. However, in not too small external fields for $T < T_c$ the distortion disappears as the magnetic field energy overcomes the energy gain of the lattice distortion. Our experimental data on the Cl(II)B resonance spectrum strongly suggests the occurrence of such spin-orbit distortions in these chlorine compounds. The difference in direction of the spontaneous magnetization in the chlorides with respect to the bromides also indicate such a mechanism.

The origin of transition ν_3 is not yet clear. The ratio of the frequencies of the two resonance lines belonging to the two isotopes is about that of the gyromagnetic ratios. As a function of increasing temperature this resonance frequency ν_3 decreases slightly faster than the spontaneous magnetization. It is not possible to get more information about the origin of this resonance by applying an external field in the direction of the (110) axis, as also for this resonance line the signal intensity decreases too fast with increasing field so that for H > 300 Oe the signal cannot be detected anymore.
There are several possible origins for this resonance line. The resonance transition can originate from nuclei inside closure domains which are magnetized along the c-axis or from nuclei within domains at the edges of the crystal sample. Also possibly it can be a transition from nuclei inside a Bloch wall. Because of the two preferred directions in the crystal we can distinguish two types of Bloch walls: a 90° wall between two domains magnetized along the (110) and $(1\bar{1}0)$ axis respectively and a 180° wall between two antiparallel magnetized domains.
It can be excluded that ν_3 is a resonance transition from nuclei inside a 90° Bloch wall, because for such a transition a resonance frequency of about 15 MHz

has to be expected in view of the values for the frequency shift components as determined in the paramagnetic state.
By applying an external field of 150 Oe in the direction of the c-axis, all Cl(II) resonance frequencies including ν_3 change about 1 MHz, due to the rotation of the magnetization in the Weiss domains. So it is not likely either that this extra chlorine resonance originates from small closure domains magnetized along the c axis. For such a line from a closure domain one should expect a nearly field independent resonance frequency.
Careful examination of the Cl(II)A spectrum shows that all three resonance lines of fig. 23 have a weak satellite line shifted about 100 kHz to lower frequency (T = 0.3 K). The temperature dependence of this extra set of resonance lines is equal to that of the main spectrum. We think that these extra resonance lines originate from nuclei inside domains at the edges of the crystal or from nuclei inside single-domain particles in enclosures inside the crystal. These nuclei inside such domains do feel a demagnetizing field, unlike nuclei in regular domains, which results in a somewhat smaller total magnetic field at these nuclei. The spontaneous magnetization in these deviating domains can also be a little smaller because of the demagnetizing field. The frequency difference of 100 kHz between the main lines and the satellites can be estimated quantitatively to be caused by these effects. In the Cl(II)B spectrum also an extra resonance line has been detected, but only for the $(+\frac{1}{2} \rightarrow -\frac{1}{2})$ transition (ν_2); the frequency difference agrees approximately with a decrease of the Larmor frequency of about 100 kHz. So it is not likely that the origin of transition ν_3 can be explained by this type of effect.

We think that, after the exclusion of the mentioned possible origins of the extra chlorine resonance transition, this resonance line may be due to nuclei inside 180° Bloch walls. The time-averaged magnetic moments of the copper ions in the middle of such walls are parallel to the (110) axis. Therefore it is very well possible that ν_3 is the $(+\frac{1}{2} \rightarrow -\frac{1}{2})$ transition of the Cl(II)B spectrum from chlorine nuclei in these walls. The value of the time-averaged magnetic moment of Cu ions within a Bloch wall will be somewhat smaller than that for a Cu ion within a normal domain at the same temperature. Together with the presence of demagnetizing fields inside the Bloch wall this yields a smaller internal field at the chlorine nuclei in the walls. Furthermore it can be expected[8] that the Larmor frequency of these nuclei decreases faster with increasing temperature than the spontaneous magnetization in the domains. Both effects are observed for the ν_3 resonance line. As the fractional r.f. energy absorption for nuclei in Bloch walls is about a factor 50 larger than for nuclei within the domains[1],

the small amount of nuclei inside the walls still can give an observable resonance signal. The observed intensity ratio of the Cl(II)B ν_2 and ν_3 signals is larger than 50.

7.5. Copper spectra.

7.5.1. Bromine compounds. In both compounds two resonance transitions per isotope have been observed. One rather intense resonance line with a dispersion shape and a width of 1.5 MHz at about 50 MHz (T = 1.2 K) and one weak transition with an absorption shape and a width of approximately 2 MHz at 100 MHz. From the temperature dependence of these two transitions, shown in fig. 26 for the Rb compound, it has been calculated that these resonance lines originate from respectively the $(+\frac{1}{2} \rightarrow -\frac{1}{2})$ and $(+\frac{1}{2} \rightarrow \frac{3}{2})$ transitions. The quadrupole interaction

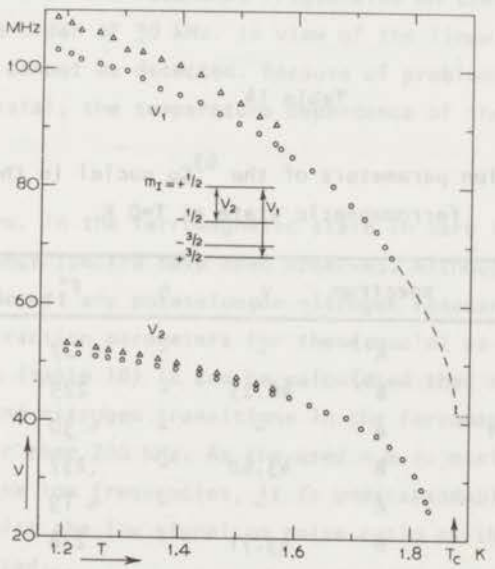

Fig. 26. $Rb_2CuBr_4 \cdot 2H_2O$. Temperature dependence of the copper resonance transitions in the ferromagnetic state. ⊙ ^{63}Cu; △ ^{65}Cu.

constants and the value for the frequency shift tensor component have been calculated from these two resonance lines using the computer tables. As the width of the lines is very large no accurate determination of these interaction

parameters is possible. By comparison of the values for ν_q and F_{yy} given in table 9 for the paramagnetic state with those for the paramagnetic state in table 14, it can be seen that within the experimental accuracy no difference between the interaction parameters in the ferromagnetic and paramagnetic state has been observed.

7.5.2. Chlorine compounds. Also for the copper ions two spectra per isotope are expected in the ferromagnetic state. First of all the Cu(A) spectrum originating from those copper nuclei for which $\vec{m}_s$ is parallel to the X axis of the EFG tensor. In all four compounds only one resonance transition of this spectrum has been observed. For T = 0.3 K this very broad resonance line has been detected at approximately 35 MHz; it appears to be the composition of the ^{63}Cu and ^{65}Cu $+\frac{1}{2} \rightarrow -\frac{1}{2}$ transitions. Indications have been found from other transitions of this spectrum, but because of the overlap of the resonance lines from both isotopes, the signals are very broad and therefore too weak to be observed properly.

Table 14

Interaction parameters of the ^{63}Cu nuclei in the ferromagnetic state at T=0 K

	spectrum	ν_q	η	F°_{ii}
KCl	A[a]	-	-	∿ 27
	B[b]	46.25	-	229
NH_4Cl	A	-	-	∿ 30
	B	43.60	-	237
RbCl	A	-	-	∿ 19
	B	43.71	-	228
CsCl	A	-	-	∿ 19
	B	38.60	-	229
NH_4Br	c)	41.3	0.20	32.2
RbBr		41.0	0.17	36.4

a) $\vec{m}_s$//X; b) $\vec{m}_s$//Z; c) $\vec{m}_s$//Y.

The second spectrum, Cu(B) ($\vec{m}_s // Z$), has been observed easily in all four compounds. Because of the high frequencies involved, the resonance lines have been detected with a hybrid T spectrometer using field modulation. Both the ^{63}Cu and ^{65}Cu spectra can be observed nicely. For the ^{63}Cu isotope the resonance frequency at T = 0.3 K of the $(+\frac{1}{2} \rightarrow -\frac{1}{2})$ transition is found to be about 220 MHz. The two $(\pm\frac{1}{2} \rightarrow \pm\frac{3}{2})$ transitions are observed at 220 ± 40 MHz. The width of these resonance lines is 500 kHz in the K, Rb and Cs compounds, while in the NH_4 compound the linewidth is found to be 1 MHz. This larger linewidth in the ammonium compound again reflects the loss of crystal symmetry due to the two orientations of the NH_4 molecules. From this Cu(B) spectrum the quadrupole interaction constant ν_q can be calculated easily, as the spontaneous magnetization and thus the internal field is directed along the Z axis of the EFG tensor. The frequency difference between the $(+\frac{1}{2} \rightarrow +\frac{3}{2})$ and the $(-\frac{1}{2} \rightarrow -\frac{3}{2})$ transitions exactly equals $2\nu_q$. The value of the asymmetry parameter η however cannot be determined from this spectrum; the dependence of the resonance frequencies on the value of η for $\eta \approx 0.2$ is only of the order of 30 kHz. In view of the linewidth of 500 kHz these small differences cannot be detected. Because of problems with radio frequency heating of the crystal, the temperature dependence of the spectrum has not been determined.

7.6. Alkali spectra. In the ferromagnetic state in zero field only the rubidium and caesium resonance spectra have been observed. Although we have searched for it, we could not detect any potassium or nitrogen resonance lines. From the values of the interaction parameters for these nuclei as determined in the paramagnetic state (table 10) it can be calculated that the resonance frequencies of all potassium and nitrogen transitions in the ferromagnetic state in zero field will be lower than 200 kHz. As the used n.m.r. oscillators are not sensitive enough at the low frequencies, it is understandable that these K and N resonance lines, with the low signal to noise ratio as they have normally, could not be detected.

7.6.1. Rubidium. In the bromine compound, where the magnetization is directed along the Z-axis of the rubidium EFG tensor only two ^{87}Rb resonance lines have been observed. From the temperature dependence of the resonance frequencies the resonance lines have been determined to be related to the $(+\frac{1}{2} \rightarrow -\frac{1}{2})$ and the $(+\frac{1}{2} \rightarrow +\frac{3}{2})$ transitions. Although from these two resonance frequencies the frequency for the missing $(-\frac{1}{2} \rightarrow -\frac{3}{2})$ transition can be calculated accurately, even no indication of a resonance signal at the calculated frequency has been

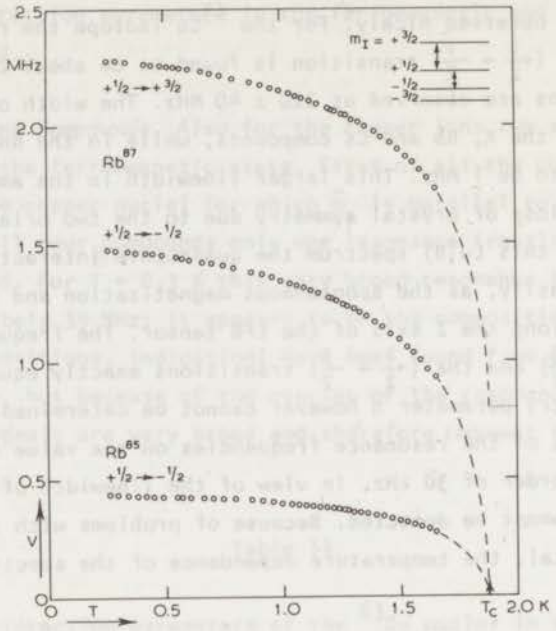

Fig. 27. $Rb_2CuBr_4 \cdot 2H_2O$. Temperature dependence of the observed ^{87}Rb and ^{85}Rb resonance transitions in the ferromagnetic state.

found. The quadrupole interaction constant ν_q is determined to be exactly equal to the value obtained from the experiments in the paramagnetic state. This indicates that the small magnetostrictive effects, which are probably the origin of the temperature dependence of the Br(I) quadrupole interaction, do not influence the Rb quadrupole interaction. In fig. 27, apart from the temperature dependence of the two observed ^{87}Rb resonance lines, also that of the ^{85}Rb $(+\frac{1}{2} \rightarrow -\frac{1}{2})$ transition is shown.

In the chlorine compound plenty of rubidium resonance lines have been observed. The resonance signals are rather intense; the linewidth is about 10 kHz for the ^{87}Rb and 5 kHz for the ^{85}Rb transitions. Because of the complexity of the total resonance pattern, only by the determination of an extensive temperature dependence of all resonance frequencies, it appears to be possible to identify all resonance transitions. For the sake of clarity the temperature dependence of the ^{87}Rb and the ^{85}Rb spectra are shown separately in figs. 28 and 29

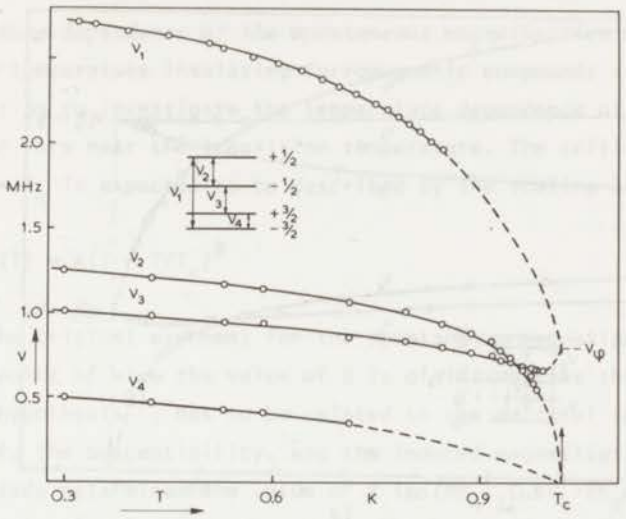

Fig. 28. $Rb_2CuCl_4 \cdot 2H_2O$. Temperature dependence of the ^{87}Rb spectrum in the ferromagnetic state.

respectively. The quadrupole interaction constant for ^{87}Rb is calculated from this spectrum to be ν_q = 802 kHz which is slightly different from the value in the paramagnetic state. As in the bromine compound this difference has not been observed, it is probable that this change of the Rb quadrupole interaction is related to the magnetostrictive distortion, which is assumed to be the origin of the large difference of the Cl(II)B quadrupole interaction in the ferromagnetic state, rather than to the distortion which leads to the small changes in Cl(I) and Br(I) quadrupole interactions.
In fig. 29 it can be seen that for the ^{85}Rb isotope the spectrum consists of two sets of "α" transitions. Apart from the here shown transitions, also the $(+\frac{1}{2} \rightarrow +\frac{5}{2})$ could be detected at low temperatures.

7.6.2. Caesium. The ^{133}Cs resonance spectrum has been observed over a large temperature range. The spectrum consists of the seven allowed transitions (Δm_I = 1). The frequency difference between successive resonance lines is only 6.6 kHz. Because of the small linewidth, only 1.5 kHz at T = 0.3 K, the signals are very well separated. For temperatures near T_c however, $T_c - T \leq 50$ mK, the

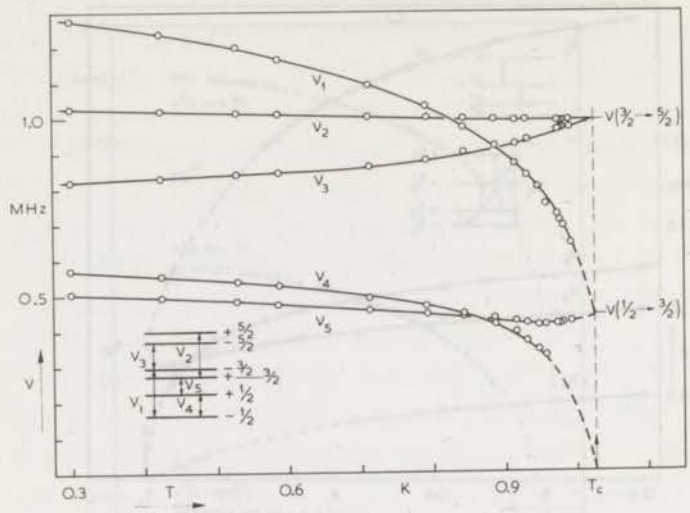

Fig. 29. $Rb_2CuCl_4 \cdot 2H_2O$. Temperature dependence of the ^{85}Rb resonance spectrum in the ferromagnetic state.

Table 15

Interaction parameters of the alkali nuclei in the ferromagnetic state at T=0 K

	ν_q	η	F°_{zz}
$^{87}RbCl$	0.802	0	0.900
$^{133}CsCl$	0.0132	0	0.710
$^{87}RbBr$	0.808	0	1.475

resonance lines start to overlap each other due to the critical broadening of the signals, which causes a very rapid decrease in signal intensity. The quadrupole interaction is found to be equal to that in the paramagnetic state. It must be mentioned however that for the ^{133}Cs nuclei a relative change of the value of ν_q, as observed for the ^{87}Rb nuclei in $Rb_2CuCl_4 \cdot 2H_2O$, cannot be detected because of the experimental accuracy. Therefore it cannot be excluded that

also for the caesium nuclei a small influence of magnetostrictive effects on the quadrupole interaction exists.

7.7. Temperature dependence of the spontaneous magnetization near T_c. As only very few low temperature insulating ferromagnetic compounds are known, it is very interesting to investigate the temperature dependence of the spontaneous magnetization very near the transition temperature. The critical decrease of $m_s(T)$ for $T \to T_c$ is expected to be described by the scaling law expression

$$m_s(T) = A(1 - T/T_c)^{\beta}$$

where β is the critical exponent for the spontaneous magnetization. From a theoretical point of view the value of β is of interest as this value, following the scaling hypothesis[8], has to be related to the critical indices for the specific heat, the susceptibility, and the induced magnetization for $T = T_c$. Wielinga already determined the value of β in $(NH_4)_2CuBr_4 \cdot 2H_2O$ by means of macroscopic magnetization measurements[4]. The large disadvantage of this method however originates in the necessity to apply an external magnetic field to allow the determination of the magnetization with all Weiss domains aligned It is not well known experimentally whether the value of the reduced magnetization is influenced by the applied field, apart from the increase due to a finite susceptibility. We think it is preferable to use magnetic resonance techniques to determine the value of β. The advantages are very clear: the experiments can be performed in zero field where the true ferromagnetic ordering is preserved. For this n.m.r. determination no theoretical relations, which depend on the temperature, have to be assumed to relate the measured macroscopic magnetization in external field to the value of the spontaneous magnetization in zero field, as necessary in the case of macroscopic methods. Moreover the accuracy of a nuclear resonance determination of the temperature dependence of $m_s(T)$ is larger by an order of magnitude.
The halide (I) spectra in the ferromagnetic state can be used extremely well to study the critical behaviour of $m_s(T)$. The magnetic interactions of both the Br(I) and Cl(I) nuclei are relatively small, which ensures that only a very small critical broadening of the resonance lines, if any, will occur very near the transition temperature. Moreover the resonance frequencies of the Br(I) β transitions and the Cl(I)B α transitions extrapolate to the finite PQR frequency if the spontaneous magnetization tends to zero. Therefore the resonance lines can always be observed properly, which would not be the case for for

instance a proton resonance line for which the resonance frequency goes to zero if $m_s(T) \rightarrow 0$.

From the numerical computer calculations it has been found that for the Br(I) spectrum the frequency difference between the two β transitions, $\Delta\nu_\beta$, exactly equal two times the bromine Larmor frequency. The frequency difference $\Delta\nu_\alpha$

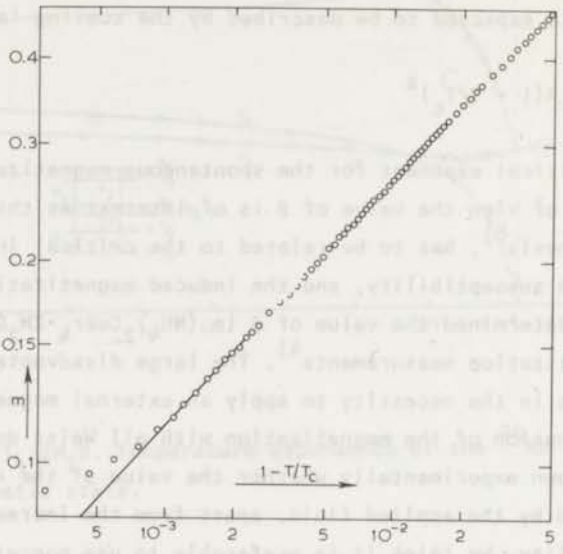

Fig. 30. $(NH_4)_2CuBr_4 \cdot 2H_2O$. Temperature dependence of the spontaneous magnetization near T_c, plotted on a double logarithmic scale.

between the α resonance lines for the Cl(I)B spectrum also equals $2\nu_L$. So the value of $m_s(T)$ at each temperature is given straightforward by $m_s(T) = \Delta\nu_\beta(T)/\Delta\nu_\beta(0)$ and $m_s(T) = \Delta\nu_\alpha(T)/\Delta\nu_\alpha(0)$ for the bromine and chlorine compounds respectively.

The temperature dependence of the quadrupole interaction parameters in the ferromagnetic state of the halide (I) nuclei as discussed in section 7.3. does not influence at all the relations between $\Delta\nu_\beta$, $\Delta\nu_\alpha$ and m_s. It would be possible however that these changes of the quadrupole interaction are accompanied by temperature dependent changes of the magnetic interaction parameters F°_{ij}. By comparing the temperature dependence of the Br(I) and Cl(I)B Larmor frequencies with that for the proton and alkali Larmor frequencies in corresponding compounds, it has been concluded that for $m_s > 0.5$ within the experimen-

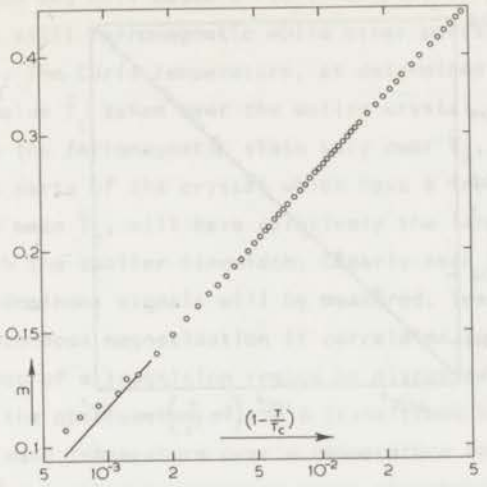

Fig. 31. $Rb_2CuBr_4 \cdot 2H_2O$. Temperature dependence of the spontaneous magnetization near T_c, plotted on a double logarithmic scale.

tal accuracy no temperature dependence of the halide (I) frequency shift components occurs. It is therefore very likely that also for $0 \leq m_s < 0.5$ the influence of a temperature dependence of F°_{ii}, if any, on the determination of the value of the critical exponent will be far within the experimental accuracy.

The transition temperatures in the various compounds have been measured from the maximum in the susceptibility, using the methods outlined in section 7.1. The exactness of the determination of T_c on a relative temperature scale is better than 0.2 mK. In section 5.3.3. the determination and stabilization of the temperature has already been discussed.

In figs. 30, 31 and 32 the temperature dependence of the spontaneous magnetization in respectively $(NH_4)_2CuBr_4 \cdot 2H_2O$, $Rb_2CuBr_4 \cdot 2H_2O$ and $Rb_2CuCl_4 \cdot 2H_2O$ are shown. The value of $m_s(T)$ is plotted versus $(1 - T/T_c)$ on double logarithmic scale. It can be seen that the temperature dependence of $m_s(T)$ is described very well by the expression $m_s(T) = A(1 - T/T_c)^{\beta}$. The values for A and β are listed in table 16. The values for β are determined from the experimental points for $10^{-3} < 1 - T/T_c < 50.10^{-3}$ in the bromine compounds and for $2.10^{-3} < 1 - T/T_c < 50.10^{-3}$ in the chlorine compounds. For $K_2CuCl_4 \cdot 2H_2O$ and $(NH_4)_2CuCl_4 \cdot 2H_2O$ no accurate temperature dependence of $m_s(T)$ near T_c could be measured as, due to

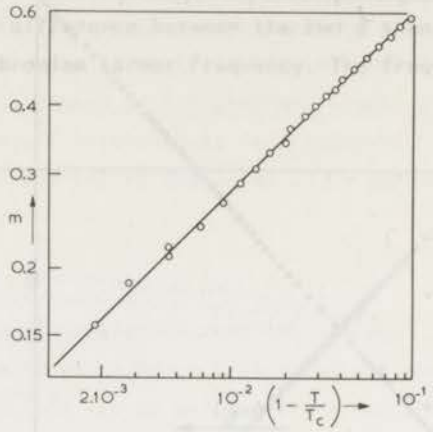

Fig. 32. $Rb_2CuCl_4 \cdot 2H_2O$. Temperature dependence of the spontaneous magnetization near T_c, plotted on a double logarithmic scale.

Table 16

Curie temperatures and the values of the scaling law parameters

	T_c(K)	A	
RbCl	1.017	1.39	0.346(10)
CsCl	0.753	1.37	0.354(10)
NH_4Br	1.836	1.47	0.369(3)
RbBr	1.874	1.44	0.367(3)

the very small frequency difference between the α transitions, the resonance lines do overlap each other for temperatures close to T_c. Moreover the intensity of the α resonance signals in these compounds is much less than in the Rb and Cs compound. In the two bromine compounds the observed magnetization very near T_c is found to be larger than that expected from the extrapolation of the scaling law. This is not due to the measuring accuracy, but is caused by a not

sharply-defined transition temperature for the entire crystal. Impurities in the crystal such as chlorine ions, and also stresses, will influence the super-exchange interaction and will cause a finite transition region in which parts of the crystal are still ferromagnetic while other parts are already in the paramagnetic state. The Curie temperature, as determined by a susceptibility method is a mean value $\bar{T}_c$ taken over the entire crystal. While observing the resonance lines in the ferromagnetic state very near $\bar{T}_c$, those signals associated with nuclei in the parts of the crystal which have a transition temperature which is higher than the mean $\bar{T}_c$, will have relatively the largest signal intensity in combination with the smaller linewidth. Clearly near $\bar{T}_c$ the resonance frequencies of these dominant signals will be measured, leading to too large a value for the spontaneous magnetization if correlated to the mean Curie temperature. The existence of a transition region as discussed has been confirmed experimentally by the observation of the β transitions together with the PQR transition at the same temperature over a temperature range of less than 0.5 mK on both sides of $\bar{T}_c$. In that temperature range the observed β resonance lines are asymmetrical; both lines have a broad tail at the "lower-frequency splitting" side, indicating the existence of the effect above discussed.
The same effect has been observed for the α transitions in the two chlorine compounds.
The values for the critical exponent in the chlorine compounds compare rather well with the theoretical value $\beta = 0.35$ for a Heisenberg ferromagnet with $S = \frac{1}{2}$ [9]. The difference between the theoretical value and the values determined for the bromine compounds, however, are far outside the experimental accuracy. It is however hard to say which is the origin of this discrepancy.

References.

1) Portis, A.M. and Lindquist, R.H., Magnetism IIA, G.T. Rado and H. Suhl, eds., Academic Press (New York, London 1965) p. 360.
2) Suzuki, H. and Watanabe, T., J. Phys. Soc. Japan 30 (1971) 367.
3) Velu, E., Renard, J.-P. and Dupas, C., Solid State Commun. 11 (1972) 1.
4) Wielinga, R.F., Thesis, Leiden, 1968.
5) Hardemann, G.E.G., Thesis, Leiden, 1957.
6) Kanamori, J., Progr. Theor. Phys. 17 (1957) 197.
7) Kanamori, J., J. Appl. Phys. Suppl. 31 (1960) 145.
8) Kadanoff, L.P., Rev. of Mod. Phys. 30 (1967) 395.
9) Baker, G.A., Eve, J., and Rushbrooke, G.S., Phys. Rev. B2 (1970) 706.

Chapter 8

ANALYSIS OF THE EXPERIMENTAL RESULTS AND DISCUSSION OF THE SPIN TRANSFER EFFECTS

8.1. Electronic g-tensor. In chapter 6.1 we have presented the results of the e.s.r. experiments in all six compounds. As outlined there, because of the large exchange interaction between dissimilar copper ions, it proved to be impossible to measure the true $\overleftrightarrow{g}$ tensor components. Instead, only the values for $g_c \equiv g_{yy}$ and $g_a \equiv \frac{1}{2}(g_{xx} + g_{zz})$ could be determined. However to be able to calculate the transferred hyperfine interaction tensors of the diamagnetic ions we need to know the values of the three principal g components.

In chapter 4 the expressions for the components of the g tensor, which are appropriate for a copper ion in a rhombic environment with covalent bonding, are given. From eq. (4.9) it can be seen however that three out of the five parameters involved - λ_{cov}, E_{xy}, E_{yz}, E_{xz} and ϕ - have to be known to calculate the values of g_{ii} from the experimental values for g_a and g_c. This is clearly impossible as from the crystal field splitting experiment only a mean value of E_{xy}, E_{yz} and E_{xz} is known. Because no detailed crystal field splitting determination of copper ions in a rhombic crystal field have been performed as far as we know, it is not possible to obtain reliable information about the relative values of E_{xy}, E_{yz} and E_{xz}. Therefore we decided to make the approximation $E_{xy} = E_{yz} = E_{xz} = E$, where E is the experimental value for the mean splitting as given in table 5. For the Cs compound, for which E could not be measured, we assumed that the value for E is equal to that of $Rb_2CuCl_4 \cdot 2H_2O$.

With this approximation we can now make a reasonable estimate of the values of the g components. From the expressions for $g_a = \frac{1}{2}(g_{xx} + g_{zz})$ and $g_c = g_{yy}$ (see eq. (4.9)) the two unknown parameters, λ_{cov}/E and the rhombic distortion parameter ϕ, can be calculated directly. Because E is known, these calculations also yield the value of λ_{cov}. In section 8.6 this experimental value of λ_{cov} will be compared with the value calculated from eq. (4.7) using the experimental spin transfer coefficients.

The rhombic distortion parameter in table 17 has been denoted by ϕ_g, to indicate that its value has been calculated from the electronic g-tensor. The analysis of the copper hyperfine interaction (section 8.5) will also yield a value for

Table 17

Calculated g-tensor components and the values for the parametric angle ϕ_g and for the spin-orbit coupling constant λ_{cov}

	ϕ_g (degrees)	λ_{cov} (cm^{-1})	g_{xx}	g_{yy}	g_{zz}
KCl	7.0	-490	2.115	2.047	2.316
NH_4Cl	6.0	-507	2.112	2.052	2.324
RbCl	7.4	-480	2.113	2.044	2.304
CsCl	5.7	-487	2.105	2.051	2.311
NH_4Br	7.2	-467	2.104	2.041	2.283
RbBr	6.6	-464	2.102	2.044	2.286

ϕ, denoted by ϕ_A. This distinction in ϕ_g and ϕ_A has to be made as it will appear that it is not possible to describe both the $\vec{g}$ and $\vec{A}$ tensor by a single value ϕ. This discrepancy will be discussed in section 8.6.

8.2. Halide (I) ions.

8.2.1. The principal axes of the EFG tensor. Before we can analyse the results on the halide (I) frequency shift tensors, we have to justify the choice of the direction of the principal axes of the EFG tensor - $Z//\gamma$ and $Y//\gamma'$ - as made in section 6.3. The justification cannot be obtained from simple point charge calculations of the EFG tensor. These calculations lead to completely wrong values of the quadrupole interaction constants as have been reported recently by Choh et al.[1] and Gupta et al.[2]. Their calculations yield that the Z-axis of the EFG tensor should be parallel to the γ' direction.
Choh et al.[2] have found from their n.m.r. experiments on $K_2CuCl_4 \cdot 2H_2O$ that the Cl(I) value of ν_q strongly decreases, while the η value increases, if the temperature increases from 4 K to 300 K. For the Cl(II) site nuclei the value of ν_q does not change in this temperature region, while the asymmetry parameter shows a slight increase with decreasing temperature. The magnitude of the temperature dependence of the Cl(I) quadrupole interaction parameters is much too large to be caused by volume effects.
Choh et al. have explained the anomalous behaviour of the Cl(I) EFG tensor by assuming the existence of a low frequency torsional motion of the $CuCl_4 \cdot 2H_2O$

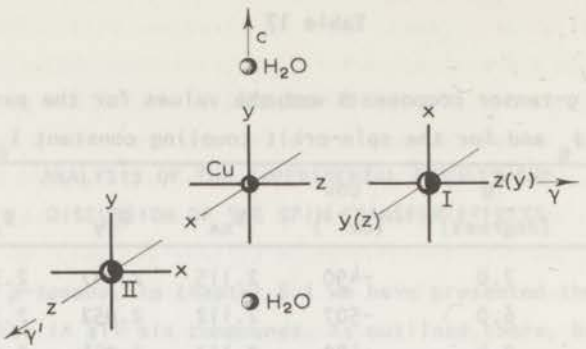

Fig. 33. Part of the $CuCl_4 \cdot 2H_2O$ octahedron. The principal axes of the EFG tensors of the various nuclei are indicated.

octahedron about the γ'-axis. They calculate that for such a torsional mode with a frequency of about 3.10^{12} Hz the temperature dependence of the Cl(I) and Cl(II) EFG tensors can be explained very well from the temperature dependence of the root mean square amplitude of the oscillations, if all calculations are normalized to the room temperature data. The essential condition however is that the Z-axis of the Cl(I) EFG tensor is directed along the Cu - Cl(I) bond (γ). With the Z-axis parallel to the γ' direction, the temperature dependence of the Cl(I) EFG tensor can only be explained by assuming a torsional oscillation about the c-axis. In that case however the Cl(II) quadrupole interaction constant ν_q has to show also a strong temperature dependence, which is in contradiction with the experimental results.

These arguments provide the justification of the choice of the direction of the Z-axis of the halide (I) EFG tensor. The existence of the proposed torsional motion of the octahedron about the γ'-axis is strongly supported by our determination of the temperature dependence of the rubidium quadrupole interaction in the paramagnetic state. (See fig. 14, section 6.6.) As can be seen in fig. 34 the Rb ions are surrounded by four Cl(II) and four Cl(I) ions in a nearly cubic arrangement. Therefore, if no oscillations of the octahedra are present, these nearby chlorine ions do give only a very small contribution to the EFG tensor of the Rb nucleus. By introducing a torsional motion of the octahedra about the γ'- or c-axis, the contribution of the chlorine ions to the Rb quadrupole interaction will become much larger. Gupta et al.[3] have calculated the EFG tensor for the Rb nuclei in $Rb_2CuCl_4 \cdot 2H_2O$ for a static arrangement of the ions; the Z component of the electric field gradient is found to have a positive value. Very simple considerations lead to the conclusion that the contribution of the

chlorine ions to the Z component of the Rb EFG tensor, due to a torsional motion of the octahedra about the c-axis, is negative. The contribution to ν_q for a torsional oscillation about the γ'-axis however is found to be positive. As the r.m.s. amplitude of the oscillations increase to higher temperatures, the experimentally observed increase of the Rb quadrupole interaction can only be explained by the existence of a torsional mode about the γ'-axis. The smaller increase of ν_q with increasing temperature, observed in the bromine compound, will be due to a larger moment of inertia of the $CuBr_4 \cdot 2H_2O$ octahedron than that of the $CuCl_4 \cdot 2H_2O$ octahedron. Therefore at the same temperature the r.m.s. amplitude of the torsional oscillations in the bromine compound will be smaller, leading to a smaller positive contribution of the nearby bromine ions to the Rb quadrupole interaction constant.

The neutron diffraction experiments on $K_2CuCl_4 \cdot 2H_2O$ do not indicate the existence of the assumed torsional motions[4]. However Mathieu et al.[5] studied the Raman spectra in $K_2CuCl_4 \cdot 2H_2O$, $(NH_4)_2CuCl_4 \cdot 2H_2O$ and $Rb_2CuCl_4 \cdot 2H_2O$. Although they can not assign a specific Raman line to the torsional motion of the octahedron about the γ'-axis, they conclude that the frequency of this torsional oscillation has to be between 2.10^{12} Hz and 4.10^{12} Hz. The agreement between this frequency and the frequency assumed by Choh et al. to fit their experimental data is surprisingly well.
We think that all these arguments provide a strong evidence for the correctness of the assignment of the Z-axis of the halide (I) EFG tensor to the γ direction. The discrepancy between the calculated and observed magnitude of ν_q is probably due to the influence of the hydrogen bonds which is not taken into account in the calculations.

8.2.2. Determination of the spin transfer coefficients. From the definition of the components F_{ii} of the frequency shift tensor given in chapter 6.3 it is found that the components of the (transferred) hyperfine interaction tensor $\overleftrightarrow{A}$ can be calculated from the expression

$$A_{ii} = \frac{4}{g_{ii}} [F_{ii} - (H_{dip})_{ii}]$$

The values of g_{ii} for all compounds are listed in table 17. The computation of the dipolar interaction tensor for all nuclear sites has been performed making use of the estimated unpaired spin density on the ligands. Because of the lack of data on the oxygen hyperfine interaction, any unpaired spin density on these oxygen ions has been left out of consideration. The contribution to the dipolar

interaction of all ions within a radius of 40 Å has been calculated. We have restricted ourselves to a simple point-dipole computation.

With these calculated values of the dipolar interaction components the transfered hyperfine interaction tensor can be determined. The separate contributions of the different electron orbits to the total $\overleftrightarrow{A}$ tensor can be deduced from the expressions given in eq. (3.21). It must be noted however that these expressions have been derived for the case of one magnetic ion surrounded by six equivalent ligands in an octahedral arrangement. As the actual situation is quite different, these expressions have to be modified. First of all the dipolar interaction term A_d in eq. (3.21) has already been included in the computed dipolar interaction tensor H_{dip}, and therefore can be left out of consideration. Secondly the contributions of the two p_π orbitals to $\overleftrightarrow{A}$ in general will be different and therefore have to be denoted by two different quantities.

The calculation of the spin transfer coefficients f is rather trivial (see chapter 3.5 for the required formulae) and it is therefore confusing to let it be accompanied by a large amount of tabulated data. Consequently we will not present the values of the hyperfine interaction components A_{ii} and the separate contributions of the various electron orbitals A_s, A_σ, $A_{\pi 1}$ and $A_{\pi 2}$ to the total hyperfine interaction. Only the spin transfer coefficients f will be tabulated.

To get an overall idea concerning the order of magnitude of the dipolar interaction tensors for the different nuclei, in table 18 typical values for these tensors are given. Because of the different gyromagnetic ratios for the chlorine

Table 18

Typical values of the components of the dipolar interaction tensors

	H_{xx} [a] (kOe)	H_{yy}	H_{zz}
Cu	+0.20	-0.10	-0.11
Halide (I)	-0.19	-0.34	+0.58
Halide (II)	-0.60	-0.53	+1.16
Alkali	+0.044	+0.044	-0.079

a) The indices refer to the principal axes of the respective EFG tensors

and bromine nuclei and for the various alkali nuclei the dipolar interaction

has been expressed in kOe. For the actual calculations of the spin transfer coefficients, the dipole tensors computed for the specific compound have been used naturally.

From fig. 33 and the known direction of the principal axes of the halide (I) EFG tensor it can be concluded that the contributions of the various electron orbitals to the halide (I) transferred hyperfine interaction tensor are given by

$$A_{zz} = A_s + 2A_\sigma - A_{\pi x} - A_{\pi y}$$

$$A_{yy} = A_s - A_\sigma - A_{\pi x} + 2A_{\pi y}$$

$$A_{xx} = A_s - A_\sigma + 2A_{\pi x} - A_{\pi y}$$

A_σ is the contribution from the p_z orbital; $A_{\pi x}$ and $A_{\pi y}$ are the contributions from the π orbitals p_x and p_y respectively. The indices x, y and z refer, as always, to the principal axes system of the EFG tensor. It can be seen from these expressions that it is impossible to calculate the values of all four contributions separately. The summation of the three A_{ii} values directly yields the value of A_s, but to get information about the values of the three p components certain assumptions have to be made. If strong σ bonding is present, as is the case for the halide (II) ions, A_σ definitely will be the leading p term, and can therefore be calculated easily by assuming that the two π terms are approximately zero. For the halide (I) ion however in first order no σ bonding is present as its p_σ orbit is directed towards the copper $(3z^2 - r^2)$ orbit which in first order does not possess unpaired spin density. Only in second order, due to the mixing of the copper $(x^2 - y^2)$ and $(3z^2 - r^2)$ orbitals a small σ spin density will occur. As also the presence of unpaired spin density in the p_π orbitals is due to a second order effect, probably the p_σ and p_π contributions to the hyperfine interaction will be of the same order of magnitude. To get information about the approximate spin transfer coefficients anyhow, we have assumed that the ratio of the spin density in the p_σ orbit and that in the s orbit, both due to the σ bonding, is equal to the ratio calculated for the halide (II) ions. From table 20 it can be seen that this ratio is 23 for the chlorine ions and 30 for the bromine ions. The spin transfer coefficients calculated under this assumption are given in table 19. The values for the hyperfine interaction constant used, are $A°(3s) = 6800$ MHz[6] and $A°(3p) = 205$ MHz[7] for ^{35}Cl and $A°(4s) = 31500$ MHz[6] and $A°(4p) = 884$ MHz[7] for ^{79}Br. Although possibly the magnitudes of the p_σ and p_π spin transfer coefficients

Table 19

Spin transfer coefficients for the halide (I) ions

	f_s(%)	f_σ(%)	$f_{\pi y}$(%)	$f_{\pi x}$(%)
KCl	$+ 3.7\ 10^{-3}$	+0.08	+0.41	+0.21
NH_4Cl	$+ 5.3\ 10^{-3}$	+0.12	+0.47	+0.24
RbCl	$+10.10^{-3}$	+0.23	+0.61	+0.38
CsCl	$+16.10^{-3}$	+0.37	+0.74	+0.56
NH_4Br	$+ 9.4\ 10^{-3}$	+0.28	+0.58	+0.38
RbBr	$+12.10^{-3}$	+0.36	+0.77	+0.51

are not all correct, we are of the opinion that the increase of the spin transfer coefficients with increasing unit cell dimension (i.e. on substitution of heavier alkali ions) does reflect the actual situation. This increase of covalent bonding is confirmed by the increase of f_s which value has been calculated straightforward without any assumption.

We can use another assumption to be able to calculate all four spin transfer coefficients. The analysis of the experimental results on the electronic g tensor yields the values of the rhombic distortion parameter ϕ and of the spin-orbit coupling constant λ_{cov}. Using these values, the parameters α, β and γ from eq. (4.3) which ascribe the admixture of resp. the Cu^{2+} (yz), (xz) and (xy) into the $(x^2 - y^2)$ orbital can be calculated. The unpaired spin densities in these t_{2g} orbitals, due to this admixture, have the relative values α^2, β^2 and γ^2. By assuming that the covalent bonding between the halide (I) p_x and the copper yz orbital is of equal strength as that between the halide (I) p_y and the copper xz orbital it can be seen that the spin transfer coefficients are related to each other by $f_{\pi x}/f_{\pi y} = \alpha^2/\beta^2$. The calculations of the halide (I) spin transfer coefficients based on this assumption yield negative values for f_σ, $f_{\pi x}$ and $f_{\pi y}$ which are equal for all chlorine compounds. Clearly this result is not at all consistent with the positive value of f_s and with the strong dependence of f_s on the compound. Therefore we have to conclude that this second assumption is totally irrelevant.

8.3. Halide (II) ions. The analysis of the hyperfine interaction tensors for the halide (II) nuclei is much less complicated. The contribution to $\overset{\leftrightarrow}{A}$ due to

the strong σ bonding is much larger than that from the two π orbitals. The contribution of the different halide electron orbitals to the $\overset{\rightarrow\rightarrow}{A}$ tensor are given by exactly the same expressions as those derived for the halide (I) ions

$$A_{zz} = A_s + 2A_\sigma - A_{\pi x} - A_{\pi y}$$

$$A_{yy} = A_s - A_\sigma - A_{\pi x} + 2A_{\pi y}$$

$$A_{xx} = A_s - A_\sigma + 2A_{\pi x} - A_{\pi y}$$

From fig. 33 it can be seen that the contributions A_s and A_σ are due to the spin transfer from the Cu^{2+} $3d(x^2 - y^2)$ orbit towards the halide (II) s and p_z orbits respectively. Because the unpaired electron of the copper ion is situated in this $3d(x^2 - y^2)$ orbital, the spin transfer coefficients f_s and f_σ will be relatively large. $A_{\pi x}$ and $A_{\pi y}$ are related to the spin transfer between the p_x and 3d(xz) orbitals and between the p_y and 3d(xy) orbitals respectively.

Table 20

Spin transfer coefficients of the halide (II) ions

	f_s(%)	$f_\sigma - f_{\pi x}$	$f_{\pi y} - f_{\pi x}$	ν_q(MHz)
KCl	+0.32	+7.31	+0.38	9.47
NH_4Cl	+0.33	+7.24	+0.37	9.43
RbCl	+0.32	+7.33	+0.39	10.30
CsCl	+0.32	+7.45	+0.40	11.15
NH_4Br	+0.29	+8.70	+0.32	75.88
RbBr	+0.28	+8.55	+0.22	81.80

In table 20 the spin transfer coefficients calculated for these ions are listed. For the p transfer coefficients only differences can be given.
As the covalent bonding of these halide (II) ions with the copper ion is much stronger than that of the halide (I) ions, surely the magnetic properties of the halide (II) ions can be described much better by the formalism outlined in chapter 3 than those of the halide (I) ions. Therefore we expect to obtain a reliable estimate of the ratio of the magnitudes of $f_{\pi x}$ and $f_{\pi y}$ for the halide (II) ions from the calculation of the admixture coefficients of the 3d(xy) and 3d(xz) orbitals following the same arguments as given in section 8.2 for the

halide (I) ions. For a typical value of the rhombic parameter ϕ and the spin-orbit coupling λ_{cov} we compute that the ratio of the values of γ (which determines the admixture of xy into the ground state) and β (xz) is about 2.2 That means that ratio $f_{\pi y}/f_{\pi x}$ can be estimated to be of the order of 5. It can thus be concluded that probably f_x can be neglected, even with respect to $f_{\pi y}$, so that in table 20 we can safely read f_σ and $f_{\pi y}$ instead of $f_\sigma - f_{\pi x}$ and $f_{\pi y} - f_{\pi x}$ respectively.

For comparison in table 20 again the experimentally determined quadrupole interaction constants are listed. As the total value of ν_q can be written as the sum of the contributions of all surrounding ions and of the covalent bonding, it is expected that the quadrupole interaction can yield analogous information about the spin transfer coefficients as does the magnetic hyperfine interaction. Choh et al.[11] calculated the ionic contribution to ν_q of Cl(II) in $K_2CuCl_4 \cdot 2H_2O$ to be approximately 6.6 MHz. For the other chlorine compounds for which the unit cell dimensions are larger the value of ν_q(ion) surely will be smaller. Following eq. (3.23) the covalent part of the quadrupole interaction is given by

$$\nu_q(\mathrm{cov}) = \frac{\frac{4}{5} e^2 Q \langle r^{-3} \rangle_p}{4I(2I-1)h} (f_\sigma - f_\pi)$$

Therefore the increase of the total value of ν_q which accompanies the increase of the unit cell dimensions of the chlorine compounds has to reflect the increase of $(f_\sigma - f_\pi)$. The estimated difference between the values of ν_q(cov) of the Cl(II) nuclei in the potassium and caesium compound is about 2.7 MHz. Using the value of 110.6 MHz for $\frac{4}{5} e^2 \langle r^{-3} \rangle_p / 4I(2I-1)h$ determined experimentally for the ^{35}Cl nucleus[7] it is found that in the Cs compound the value of $(f_\sigma - f_\pi)$ would be about 2.4% larger than in the K compound. However from the results on the magnetic hyperfine interaction tensors it has been concluded, as shown in table 20, that within the series of chlorine compounds the spin transfer coefficients are nearly constant. This apparent discrepancy will be discussed in section 8.6.

8.4. Alkali ions. In fig. 34 the surrounding of the alkali ions is shown. As can be seen, these ions will not have a direct interaction with the copper ions. There are two possible orientations for the outer p orbitals of the alkali ions. First of all the three p orbits can be directed along the c-axis and approximately along the two (110)-axes respectively. (This cannot be the situation for

the nitrogen ions, as because of the NH_4 molecule, the outer electron orbitals have to be hybridized sp^3 orbitals essentially.) In that case the orbit directed along the c-axis will be the p_z orbit; i.e. the electron orbit parallel to the z-axis of the alkali EFG tensor. The p_z electrons will interact with the nearest halide electrons, viz. with the halide (I) p_y and the halide (II) p_x electrons. As we have already calculated that there exists an unpaired spin density in these halide orbitals, this interaction will lead to the the occurrence of a fraction of unpaired spin in the alkali p_z orbital. Analogous the alkali p_x and p_y orbitals, which are equivalent because of the crystal symmetry, will contain an amount of unpaired spin, due to the interaction with the halide (I) p_x and the halide (II) p_y orbitals.

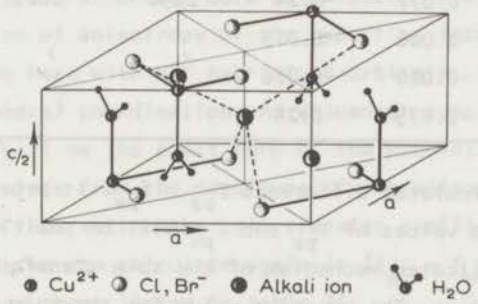

Fig. 34. Surrounding of the alkali ions.

The components of the transferred hyperfine interaction tensor are represented by

$$A_{zz} = A_s + 2A_{pz} - 2A_{px}$$

$$A_{yy} = A_{xx} = A_s - A_{pz} + A_{px}$$

where we have made use already of the fact that $A_{px} \equiv A_{py}$. In table 21 the values of the spin transfer coefficient, calculated from these relations, are listed. For the p orbits only the difference $f_{pz} - f_{px}$ can be computed naturally. Also the hyperfine interaction constants A_s° and A_p° for the various alkali ions are included in that table.

It can be seen that for all nuclei the value calculated for f_s is only approximately a factor 3 smaller than for $(f_{pz} - f_{px})$. On the analogy of the halide spin transfer coefficients, also for the alkali ions it is expected that the spin transfer coefficients for the p orbitals will at least be an order of magnitude larger than for the s orbital. Therefore probably f_{pz} and f_{px} are both

Table 21

Spin transfer coefficients and hyperfine interaction constants for the alkali ions

	f_s(%)	$f_{pz}-f_{px}$	A_s°(MHz)	A_p°
Cl-^{39}K	-0.068	-0.17	230[8]	6.0[9]
$^{14}N_1$	-0.007	-0.043	1560	93.6[10]
$^{14}N_2$	-0.013	-0.045		
^{87}Rb	-0.072	-0.17	3430[8]	84.8[9]
^{133}Cs	-0.077	-0.24	2298[8]	50.9[9]
Br-$^{14}N_1$	-0.006	-0.015		
$^{14}N_2$	-0.020	-0.026		
^{87}Rb	-0.079	-0.24		

large compared to the calculated difference $f_{pz} - f_{px}$. It proves to be very hard to argue whether the values of f_{pz} and f_{px} will be positive or negative, because of the very complicated mechanism of the spin transfer from the halide ions towards the alkali ions. The negative value for the spin transfer coefficient f_s can be due to a negative spin transfer as well as to a core polarization because of the unpaired spin in the p orbit, as discussed in section 3.5.

A second possibility for the outer alkali electron orbitals is that, because of the nearly tetrahedral arrangement of the four nearby halide (I) ions as well as of the halide (II) ions, the three p orbitals and the s orbital admix as to form hybridized orbitals. These four sp^3 orbitals can then be directed towards the four halide (I) ions or towards the four halide (II) ions. Although the distances between the alkali ion and both types of halide ions is nearly equal, as can be seen in table 4, most probably the sp^3 orbitals will be directed towards the halide (I) ions. The reason for this is that the negative electric charge at the halide (I) ions is much larger than at the halide (II) ions due to a much weaker covalent bonding with the copper ion. For the nitrogen ions however it has been concluded already in chapter 6.4 from the observation of two nitrogen resonance spectra that the sp^3 orbitals of successive nitrogen ions are directed towards the halide (I) and halide (II) ions alternately. The four prefectly tetrahedrally coordinated sp^3 orbitals are given by the expressions

$$sp_1^3 = \tfrac{1}{2}(s + p_x + p_y + p_z)$$

$$sp_2^3 = \tfrac{1}{2}(s + p_x - p_y - p_z)$$

$$sp_3^3 = \tfrac{1}{2}(s - p_x + p_y - p_z)$$

$$sp_4^3 = \tfrac{1}{2}(s - p_x - p_y + p_z)$$

The contribution from the three p orbitals to the transferred hyperfine interaction cancel identically in that case, and only the isotropic s contribution, due to the spin transfer and/or core polarization will be detected. The experimental observation of anisotropy of the hyperfine interaction indicates that, if we are dealing here with sp^3 hybridized orbitals, these orbitals have no prefectly tetrahedral coordination. As we cannot conclude from the crystal structure which will be the exact form of the hybridized orbitals, it is not possible to calculate from the magnitude of the anisotropic part of the transferred hyperfine interaction the spin transfer coefficients of the p orbitals. The only quantity we can calculate again is $(f_{pz} - f_{px})$, which naturally yields the same values as those listed in table 21.

Although it cannot be concluded from the nuclear resonance experiments, which is the appropriate bonding scheme for the alkali ions, we think that the formation of hybridized orbitals is the most probable one because of the energy gain due to a stronger covalent bonding with the nearby halide ions. This is confirmed by the fact that the normal alkali ions can be substituted easily by the tetrahedral NH_4 molecules, without the occurrence of changes of the crystal structure.

8.5. Copper ions. The experimental values of the components of the copper hyperfine interaction tensor have been analysed using the expressions for A_{ii} given in eq. (4.10). As can be seen, to calculate theoretically A_{ii} from these expressions, the value of a large number of parameters has to be known. For Δg_{ii} the values of the g-tensor components as given in table 17 have been used. For the computation of the parameters δ_i and ε_i we have used the experimental value of E (table 5) and the calculated value of λ_{cov} (table 17). Although from the analysis of the experimental g values the magnitude of the rhombic distortion parameter ϕ_g has been deduced, it proved to be impossible to use this value of ϕ_g in the analysis of the hyperfine interaction. Therefore the

angle ϕ has been treated as an adjustable parameter. The reduction parameters N_σ^2 and W which depend on the spin transfer coefficients and the overlap integral can be estimated indeed, but because the spin transfer coefficients for the oxygen ions are not known, it is hard to calculate these values exactly. Moreover only approximate values for the three overlap integrals S_s, S_σ and S_π (see eq. (3.8)) can be obtained. The exact wave functions of the outer electrons of the various ions are not known for the case of covalent bonding.

The use of the values for the overlap integrals which can be calculated from the free ion wave functions can lead to seriously wrong conclusions in this situation where strong covalent bonding is present[11]. As a consequence also N_σ^2 and W have been treated as adjustable parameters. However the values N_σ^2 and W can have,are restricted by the determined spin transfer coefficients. For the Cu^{2+} ion in first order the unpaired spin is situated only in the $(x^2 - y^2)$ orbit. Therefore the expressions which relate the spin transfer coefficients to the ligand admixture coefficients α as given in eq. (3.8) modify to $f_\sigma = \frac{1}{4} N_\sigma^2 \alpha_\sigma^2$; $f_s = \frac{1}{4} N_\sigma^2 \alpha_s^2$ and $f_\pi = \frac{1}{4} N_\pi^2 \alpha_\pi^2$.

If we suppose the spin transfer coefficients and overlap integrals for the oxygen ions to be approximately equal to those of the halide (II) ions we can estimate the values for $N_\sigma^2\alpha_\sigma^2$, $N_\sigma^2\alpha_s^2$ and $N_\pi^2\alpha_\pi^2$. Using reasonable values for the overlap integrals - $S_\sigma \approx 0.10$, $S_\pi \approx 0.10$, $S_s \approx 0.06$[11] - we can then calculate the approximate values of α_σ, α_s, α_π, N_σ^2, N_π^2 and W. In adjusting the values of N_σ^2 and W to obtain the best agreement between the experimental values of the hyperfine interaction and the values calculated from eq. (4.10) we have taken care that the values of N_σ^2 and W are very close to those estimated from the ligand spin transfer coefficients.

As has been discussed already in chapter 4.2 the value of $\langle r^{-3} \rangle_{3d}$ appropriate for the copper ion in the presence of covalent bonding may be smaller than that calculated for the free ion because of expansion of the 3d wave function. Therefore also the value of $P_{cov} = 2g_n\beta\beta_n\langle r^{-3} \rangle_{cov}$ needs to be adjusted. The only restriction for its value is that P_{cov} has to be smaller than $P_{ion} = 582$ MHz[11]. The core polarization parameter κ in any case has to be deduced from the experimental values of A_{ii} as this parameter depends on a number of complicated factors which makes that κ is essentially an adjustable parameter.

By successive approximation the values of the adjustable parameters, which give the closest agreement between theory and experiment, have been derived from the expressions (4.10). They are collected in table 22. The relative difference between calculated and experimental values of the components of the hyperfine interaction tensor is less than 1% in all compounds.

Table 22

Copper hyperfine interaction parameters

	P_{cov} (MHz)	κ	ϕ_A (degrees)	N_σ^2	W
KCl	480	0.382	4.2	0.93°	1.23
NH_4Cl	490	0.390	3.9	0.93°	1.20
RbCl	480	0.375	3.6	0.91°	1.23
CsCl	480	0.380	2.6	0.91^5	1.23
NH_4Br	501	0.411	3.8	0.90^5	1.24
RbBr	503	0.408	3.0	0.90°	1.24

From the values of N_σ^2 and W in table 22 the theoretical spin transfer coefficients can be calculated using the already mentioned values for the overlap integrals. For the chlorine compounds this yields approximately $f_\sigma(Cl(II))$ = 7.3%; $f_s(Cl(II))$ = 0.3% and f_π = 0.45%. For the bromine compounds the values for f_s and f_π are the same as for the chlorine compounds, while $f_\sigma(Br(II))$ = 8.4%. By comparing these theoretical values with the experimental ones given in tables 19 and 20 it can be seen that the agreement is very satisfactory.

8.6. Discussion of the spin transfer mechanisms

8.6.1. Crystal field splitting. In chapter 3 it has been shown that the magnitude of the crystal field splitting depends on the covalent bonding of the copper ion. Following eq. (3.9) the total splitting E can be approximated by

$$E = E_{ion} + (\alpha_\sigma^2 - \alpha_\pi^2)(E_d - E_p)$$

The admixture coefficient $\alpha_\sigma^2 = 4f_\sigma N_\sigma^{-2}$ of the Br(II) ions is found to be larger than that of the Cl(II) ions. As the π admixture coefficients for all halide (II) ions is about equal, it can be expected from this expression that the covalent part of the crystal field splitting in the bromine compounds will be larger than in the chlorine compounds. No calculations of E_{ion} for the Cu^{2+} ion have been performed until now, so that no quantitative discussion about the magnitude of E can be given. If we assume E_{ion} to be equal in the bromine and chlorine compounds, or perhaps slightly smaller in the bromine compounds due to

the larger unit cell dimensions, the total value of the crystal field splitting in the bromine compounds will be larger than in the chlorine compounds. As can be seen in table 5 the value of E in the bromides is 500 cm^{-1} larger than in the chlorides indeed.

8.6.2. Spin orbit coupling constant. A good test for the validity of the theoretical description of the properties of the Cu^{2+} ion can be found in the comparison of the values of the parameters obtained from the analysis of the copper hyperfine interaction with those obtained from the electronic g-tensor. As has been shown in the preceding section, the values of the reduction parameters N_σ^2 and W, as given in table 22, agree very well with those calculated from the halide spin transfer coefficients.
From the analysis of the g-tensor components in section 8.1 the value of the spin-orbit coupling constant λ_{cov} has been calculated for all compounds.
In eq. (4.7) the theoretical expression for λ_{cov} has been given. To account for the expansion of the 3d wave function an extra reduction factor has to be included in that formula. The value of this reduction factor $\langle r^{-3}\rangle_{cov}/\langle r^{-3}\rangle_{ion}$ is equal to the ratio P_{cov}/P_{ion} which can be obtained from the analysis of the copper hyperfine interaction. The experimentally determined spin-orbit coupling constant can thus be written as

$$\lambda_{cov} = N_\sigma^2 N_\pi^2 (\lambda_{ion} - \tfrac{1}{2}\alpha_\sigma\alpha_\pi\lambda_p) W^{-1} P_{cov}/P_{ion}$$

In table 23 the values for λ_{cov} which have been determined from the g-values are compared with those calculated from the above expression, using the values of the parameters as given in table 22. Because of the small π transfer coefficients, $N_\pi^2 = 1$. The values for the admixture coefficients α_σ and α_π are 0.56 and 0.14 respectively in the chlorine compounds and 0.61 and 0.14 in the bromine compounds. The values of the spin-orbit coupling constants are $\lambda(Cu) = -828\ cm^{-1}$, $\lambda(Cl) = -587\ cm^{-1}$, $\lambda(Br) = -2456\ cm^{-1}$ and $\lambda(O) = -75\ cm^{-1}$ [12,13]. For the calculation of the term $\frac{1}{2}\alpha_\sigma\alpha_\pi\lambda_p$ a weighted mean value of the λ values for the halide and oxygen ions has been used. It can be seen from table 23 that the agreement between the calculated and experimental values of λ_{cov} for all compounds is very satisfactory. This leads to the conclusion that the formalism outlined in chapters 3 and 4 gives a good description of the influence of the covalent bonding on the properties of the Cu^{2+} ion.
The small systematic differences between the calculated and experimental values of λ_{cov} can be due to the fact that we have not taken into account properly that

Table 23

Comparison of the calculated and experimental values of λ_{cov}

	P_{cov}/P_{ion}	λ_{exp} (cm^{-1})	λ_{theor} (cm^{-1})	ϕ_g (degrees)	ϕ_A	$\nu_q(Cu)$ (MHz)
KCl	0.824	-490	-505	7.0	4.2	46.2
NH_4Cl	0.842	-507	-529	6.0	3.9	43.6
RbCl	0.824	-480	-494	7.4	3.6	43.7
CsCl	0.824	-487	-497	5.7	2.6	38.6
NH_4Br	0.859	-467	-474	7.2	3.8	41.3
RbBr	0.864	-464	-474	6.6	3.0	40.8

the surrounding of the copper ion is not octahedral, and that the six ligands are not equivalent. However, as long as no results on the oxygen spin transfer coefficients are known, we have to use the mentioned approximations.

8.6.3. Rhombic distortion parameter ϕ. Less satisfactory is the systematic discrepancy between the magnitude of the rhombic distortion parameter ϕ_g as determined from the g-values and ϕ_A which has been obtained from the analysis of the magnetic hyperfine interaction (see table 23). There may be several origins for this difference. First of all in the analysis of the experimental g-values we have assumed that all three crystal field splittings E_{xy}, E_{yz} and E_{xz} are equal to the experimentally determined mean value E. The value of ϕ_g however depends on differences between the magnitudes of these three crystal field transitions. It can be calculated that especially the introduction of a smaller value for E_{xy} leads to a smaller calculated value for ϕ_g. Secondly, for the calculation of ϕ_g we have supposed that the σ spin transfer coefficients for the halide (II) and oxygen ions are equal, and that the π transfer coefficients for all six ligands have equal values. That means that the influence of the covalent bonding on the electronic g-tensor has been treated as if the Cu^{2+} ion has a perfectly octahedral coordination. To account for the departures from this idealized situation it is necessary to modify the expressions for the reduction factors occurring in eq. (4.7) for λ_{cov}. As a result, the theoretical expressions (4.9) for the components of the g-tensor have to be rewritten using a value for λ_{cov} which is different for each of the three g components. By using these two approximations in the analysis of the experimental g-values

systematic errors in the determination of ϕ_g are introduced. The magnitude of these errors is hard to estimate due to the lack of the oxygen spin transfer coefficients.

Consequently the calculated values of g_{xx} and g_{zz}, which are listed in table 17, will also show departures from the actual values. The influence of these errors on the analysis of the hyperfine interaction tensor will however not be very large. The terms in the expressions for the components of $\overset{\ddagger}{A}$ which depend on the value of the g components always contain the factor W. Therefore the errors in g due to the errors in the reduction factor W^{-1}, contained in λ_{cov}, will cancel. Moreover the determination of the value ϕ_A is found to be not strongly dependent on the precise values of the g components. Therefore the value ϕ_A for the rhombic distortion parameter will more accurately reflect the actual situation than does the value of ϕ_g. In the further discussion we will confine ourselves to the values of ϕ_A.

8.6.4. Spin transfer to the Cu^{2+} 4s and 4p orbitals. The isotropic part of the copper hyperfine interaction, described by the empirical core polarization factor κ, can yield valuable information concerning spin transfer from the ligands to the empty copper 4s and 4p orbitals. As can be seen from the expressions (4.10) the value of κ can be calculated from

$$\kappa = \frac{1}{3}(\Delta g_{xx} + \Delta g_{yy} + \Delta g_{zz})W - (A_{xx} + A_{yy} + A_{zz})/3P_{cov}$$

The first term is exactly equal to $\frac{1}{3}(\Delta g_c + 2\Delta g_a)W$ where g_c and g_a are the experimentally determined g-values (see sections 6.1 and 8.1). The value of P_{cov} is accurately known from the analysis of $\overset{\ddagger}{A}$. As the influence of small errors in the value of W do not seriously influence the value of κ because both right hand side terms add ($A_{ii} < 0$), the core polarization factor can be calculated quite accurately.

The value of the isotropic hyperfine interaction is not only due to core polarization but also to the presence of small amounts of unpaired spin in the empty 4s orbital. There is no direct admixture of the 4s orbital into the $3d(x^2 - y^2)$ orbital, but as the $3d(3z^2 - r^2)$ and the 4s orbitals belong to the same symmetry group, the 4s orbital will be admixed indirectly into the ground state via the $(3z^2 - r^2)$ orbital. This yields a small unpaired spin density in the 4s orbital which, via the Fermi-Dirac contact interaction, gives a positive contribution to the isotropic hyperfine interaction. The unpaired spin density in the 4s orbital will be larger as the admixture of the $(3z^2 - r^2)$

orbital into the ground state, and thus the rhombic distortion parameter ϕ_A, is larger. As the hyperfine interaction due to the core polarization is negative we will therefore expect that the value of κ will increase with decreasing magnitude of ϕ_A, if we assume that the core polarization remains constant. If we look at the values for ϕ_A and κ for the chlorine compounds (table 22) we do not observe the predicted simultaneous increase of κ and decrease of ϕ_A. From the much smaller value of ϕ_A in the Cs than in the K compound one should expect the κ value in the Cs compound to be significantly larger than in the K compound; both κ values are however practically equal. This apparent discrepancy can be explained by assuming that there occurs an extra spin transfer from the ligands towards the empty copper 4s orbital. In first order equal amounts of spin parallel and spin antiparallel to the unpaired spin in the $3d(x^2 - y^2)$ orbital will be transferred from the ligands to the empty copper 4s orbital, leaving no net unpaired spin in the 4s orbital. Due to exchange polarization (Hunds rule) however, spin parallel transfer becomes more favourable than spin antiparallel transfer, leading to a net amount of unpaired spin parallel to that in the ground state. This causes a large positive contribution to the isotropic hyperfine interaction. The nearly constant value of the isotropic part of the hyperfine interaction in the four chlorine compounds can thus be explained by assuming that the total amount of unpaired spin in the 4s orbital is about constant due to the simultaneous decrease of the 4s admixture into the $3d(x^2 - y^2)$ ground state and the increase of spin transfer from the ligands towards the 4s orbital.

The occurrence of this extra spin transfer and the increase of it with the increasing atomic number of the alkali ion is confirmed unambiguously by the experimentally observed dependence of the halide (II) quadrupole interaction constant on the alkali ion. As has been discussed already in section 8.3 the value of ν_q for the Cl(II) nuclei (apart from that in the NH_4 compound) increases systematically from 9.465 MHz in the potassium compound to 11.150 MHz in the Cs compound (see table 20). The contribution to ν_q from the ions which surround the Cl(II) nucleus decreases as the unit cell dimensions increase from the K to the Cs compound. The net increase of ν_q has therefore to be due to the increase of the covalent contribution to the quadrupole interaction. The practically constant value of the p_σ and p_π spin transfer coefficients however does not reflect this increase.

The transfer from the two Cl(II) p_z electrons to the copper 4s orbital, in first order does not induce an extra unpaired spin density in this p_z orbital, and will therefore not be observed in the values of f_σ. The only result of this

mechanism is the transfer of negative electric charge from the p_z orbit towards the copper 4s orbit. The contribution of spin transfer to the quadrupole interaction only depends on the unbalance of electric charge. Therefore the increase of the covalent part of the Cl(II) quadrupole interaction can be, and has to be, explained by the increase of the spin transfer from the Cl(II) p_z orbital towards the copper 4s orbital. The same effect is observed in the two bromine compounds.

For the Cl(II) quadrupole interaction in $(NH_4)_2CuCl_4 \cdot 2H_2O$ this argumentation does not hold very well as the value of ν_q is slightly smaller than that in the K compound. As also the value of κ for the isotropic copper hyperfine interaction is larger than in the other chlorine compounds we have to conclude that in this compound the spin transfer towards the copper 4s orbital is obviously smaller than in the other compounds. Probably this is due to the two different orientations of the NH_4 molecules.

The relative values of the copper quadrupole interaction constants in the various compounds will be shown to be explained by the occurrence of spin transfer from the ligands into the copper 4p orbitals.

The total quadrupole interaction of the copper nucleus is given by the sum of the large contribution due to the single electron in the $3d(x^2 - y^2)$ orbital and the smaller ionic contribution, with opposite sign, due to the surrounding ions. With increasing unit cell dimensions this second contribution will become smaller and thus it should be expected that the value of ν_q increases. The experimental values of ν_q in the chlorine compounds, given in table 23, however show an opposite behaviour.

The contribution from the single electron in the $(x^2 - y^2)$ orbital to ν_q is, according to eq. (4.11), given by

$$\nu_q(\mathrm{cov}) = \frac{e^2 Q \langle r^{-3} \rangle_{3d}}{7I(2I-1)} \cdot 2N_\sigma^2 \cos 2\phi$$

It can be seen from this expression that also from the decrease of the rhombic distortion parameter, a small increase of ν_q will be expected for increasing unit cell dimensions.

There are several possible origins for the observed decrease of ν_q. First of all an expansion of the 3d wave function will lead to a smaller value of $\nu_q(\mathrm{cov})$. From the values of P_{cov}/P_{ion} given in table 23 it can be seen, leaving $(NH_4)_2CuCl_4 \cdot 2H_2O$ out of consideration again, that no such expansion is observed in the series of chlorine compounds. Secondly the slight decrease of the value of the reduction parameter N_σ^2 (table 22) cannot account for the large relative

change (20%) of the value of ν_q. The only effect which can cause this large decrease of ν_q is the occurrence of an increasing spin transfer from the Cl(II) and oxygen ions into the empty copper $4p_x$ and $4p_y$ orbitals respectively. The presence of an electron density in these orbitals namely leads to an extra contribution to ν_q oppositely to the contribution of the single electron in the ground state. The assumption of the increase of this 4p spin transfer is consistent with the already discussed increase of the 4s spin transfer.

The influence of this spin transfer to the 4p orbit on the copper hyperfine interaction will be small, as only in second order a net unpaired spin density will result. The hyperfine interaction constant A°_{4p} is much smaller than A°_{4s}, so for about equal amounts of unpaired spin in both orbitals, the contribution from the 4p orbital to the total hyperfine interaction will be much smaller than that from the 4s orbital. For equal amounts of spin transferred into the $4p_x$ and $4p_y$ orbitals the contributions to A_{xx} and A_{yy} are equal and positive, while the contribution to A_{zz} is two times as large and negative. Because the exchange polarization mechanism for the 4s and 4p orbitals is not well known quantitatively we cannot estimate the spin transfer coefficient. For the halide (II) ions evidently the spin transfer to the 4p and 4s orbitals will yield a small extra negative spin density in the s and p_σ orbitals. Also here the magnitudes of the contributions to the hyperfine interaction cannot be estimated. The spin transfer coefficient f_σ for the Cl(II) ions is the sum of the positive coefficient f'_σ for the spin transfer towards the $3d(x^2 - y^2)$ orbital and the negative coefficient f''_σ for the spin transfer towards the copper 4s and 4p orbitals. As can be seen in table 20 the value of f_σ for Cl(II) shows a very small increase in the series NH_4, K, Rb and Cs. It can thus be concluded that, as the absolute value of f''_σ increases, the value of f'_σ will also increase in this series.

Because of the much weaker covalent bonding of the halide (I) ions it is difficult to conclude whether the differences of the quadrupole interaction parameters in the various compounds can be explained also by the effect of spin transfer towards the copper 4s and 4p orbitals. The increase of the halide (I) value of ν_q in the series NH_4, K, Rb and Cs may indicate the occurrence of this transfer effect. However as long as no proper information is obtained concerning the ionic contribution to the halide (I) quadrupole interaction (see section 8.4) the discussion of second order effects in the covalent contribution is senseless.

8.6.5. Spontaneous magnetostriction in the chlorine compounds. With the

knowledge about the spin transfer effects which influence the Cl(II) quadrupole interaction constants it is now possible to make some comments concerning the spontaneous magnetostriction observed in the chlorine compounds in the ferromagnetic state. As can be seen from table 8 and table 12 both the frequency shift component F_{xx} and the quadrupole interaction parameters of the Cl(II) nuclei determined in the paramagnetic state differ from those determined in the ferromagnetic state. To get information about differences of the values of the unpaired spin transfer coefficients in the paramagnetic and in the ferromagnetic state we need to know all three components of the frequency shift tensor in the ferromagnetic state in zero field. This is, unluckily, totally impossible as the spontaneous magnetization points along the (110)-axis in zero field, and the influence of the magnetostriction is only observed for those Cl(II) nuclei for which $\vec{m}_s$ is parallel to the X-axis of the EFG tensor. Therefore we can not obtain any information about the nature of the magnetostrictive distortion from the difference between the components F°_{xx} and F_{xx} of the frequency shift tensor in the ferromagnetic and paramagnetic state respectively.

From the resonance spectrum in the ferromagnetic state for $\vec{m}_s // X$ we are able to determine the components of the electric field gradient tensor as the analysis using the Brown and Parker method yield the values of ν_q and η. By comparing the values for ν_q determined in the ferromagnetic state with those in the paramagnetic state it can be seen that the value for ν_q in the ferromagnetic state is about 4 MHz smaller than in the paramagnetic state. As it seems impossible that this difference is due to a large change of the position of the Cl(II) ions in the unit cell, it has to be ascribed to a change in the covalent bonding with the copper ion. If we analyse the change in quadrupole interaction in terms of changes of the electric charge density in the Cl(II) 3p orbitals we obtain the following results. With respect to the paramagnetic state, the charge unbalance in the p_z orbit has been decreased by an amount of 0.055 e, while the charge unbalance in the p_x orbit has been increased by an amount of 0.018 e. Here e is the electric charge of the electron. These numbers hold for the potassium compound; in the caesium compound these quantities are 0.071 e and 0.024 e respectively.

This change in unbalance of the electric charge can be due to a change of the spin transfer to the copper 3d, 4s and 4p orbitals and can therefore be accompanied by a change of the unpaired spin density in the Cl(II) orbitals, which has been observed from the difference between F°_{xx} and F_{xx}.

It must be noted that, due to the change of the covalent bonding also the Sternheimer antishielding factor for the nucleus may be changed. So it is

possible that a part of the change of the EFG tensor may be caused by this effect rather than by the change of the spin transfer coefficients.
As we have not been able to observe the copper resonance spectrum for $m_s // \gamma$ in an external field we have no information about the influence of the magnetostrictive distortion on the copper interaction parameters. Probably the influence will be relatively much smaller than observed for the Cl(II) ions as for the copper ion the changes in the covalent bonding are second order effects in the electric and magnetic hyperfine interaction, while they are first order effects for the chlorine ions.
From the argument given above it can be seen that it is likely that the differences between the Cl(II) interaction parameters in the ferromagnetic and paramagnetic state are due to a (small) distortion of the copper wave functions. This distortion is probably caused by the ordering of the orbital magnetic moment at the transition temperature. The exact nature however cannot be established.

8.7. Discussion of the super exchange interactions. With the present knowledge concerning the microscopic aspects of super exchange interaction, it is rather precarious to discuss the magnitude of super exchange couplings in this type of compounds starting from microscopic quantities. Even for such simple structures as MnO it is still difficult to calculate the magnitude of the exchange interaction from microscopic quantities. Therefore we cannot expect at all to be able to present a quantitative discussion of the exchange couplings in these much more complicated compounds. We will only try to indicate the reasons for the differences between the exchange interactions in the various studied crystals. To that aim we will make use of the spin transfer coefficients which have been obtained from the experiments. In chapter 3.6 the relation between the exchange interaction J and the unpaired spin density f_σ at the ligands has been discussed for the situation of two magnetic ions with one intermediate ligand ion. It has been found that J is proportional to f_σ^2. All super exchange pathes in our compounds involve at least two diamagnetic ions, which are not even situated at one line with the two neighbouring copper ions. However the qualitative rule (see p. 27) that the magnitude of the super exchange interaction is proportional to the product of the relevant spin transfer coefficients, will also remain valid if more than one diamagnetic ion is present in the super exchange link.
The bonding angles do not vary significantly over the series of compounds, so we do not need to consider the influence of bond angles on the relative magnitudes of the super exchange interactions.

Nearest neighbour interactions J_1.

The super exchange interaction J_1 between the two nearest neighbour copper ions at (0,0,0) and $(\frac{1}{2},\frac{1}{2},\frac{1}{2})$ is the sum of at least two different interactions which occur via different intermediate diamagnetic ions. The first one, $J_1(I)$, is the interaction via the exchange path Cu_1-H_2O-halide(I)-Cu_2 (see fig. 5, p. 50). The dependence of $J_1(I)$ on the spin transfer coefficients involved can be written symbolically as

$$J_1(I) \sim f(\sigma,\pi x)_I \times f(I \rightarrow H_2O) \times f(O \rightarrow Cu)$$

$f(\sigma,\pi x)_I$ contains the proper combination of the halide (I) spin transfer coefficients f_σ and $f_{\pi x}$. The second term stands for the spin transfer between the halide (I) p_z and p_x orbitals and the oxygen sp^3 orbital which is directed towards the halide (I) ion, containing the hydrogen ion. f(O - Cu) denotes the appropriate combination of the spin transfer coefficient of the two oxygen "lone-pair" orbitals (see p. 51). Because of Hund's rule, the intra atomic exchange interaction between the lone-pair orbitals and the oxygen orbitals containing the hydrogen ions, will be positive, which results in a ferromagnetic exchange interaction between the copper ions via these diamagnetic ions.
In the series of chlorine compounds the values of f_σ and $f_{\pi x}$ for the Cl(I) ions (table 19) increase in going from the K- to the Cs compound. The second term of $J_1(I)$ will slowly decrease simultaneously due to the increasing distance between the Cl(I) ion and the water molecule. Although we have no information about the oxygen spin transfer coefficients, it is reasonable to assume that the value of f(O - Cu) is about constant, analogous to what has been observed for the, also strongly bounded, Cl(II) ions. It can thus be expected that the magnitude of $J_1(I)$ will be approximately constant or will show a maximum in going from the potassium to the caesium compound. In the bromine compounds $J_1(I)$ will probably be somewhat larger because of the systematic larger spin transfer coefficients for the Br(I) ions.

The second exchange interaction $J_1(II)$ takes place via the link

$$Cu_1 - \text{Halide (II)} - H_2O - Cu_2$$

As far as the halide (II) ions are concerned the relevant spin transfer coefficients are f_σ and $f_{\pi y}$. The coefficient $f(II \rightarrow H_2O)$ is probably much smaller than for the halide (I) ions, as the distance from the halide (II) ion to the water molecule is about 0.6 Å larger than the halide (I) - H_2O distance.

Besides the oxygen orbitals are not directed towards the halide (II) ions, which will cause a further decrease of $f(II \rightarrow H_2O)$ compared to $f(I \rightarrow H_2O)$. Therefore, although the halide (II) spin transfer coefficients are much larger than those of the halide (I) ions, $J_1(I)$ and $J_1(II)$ will be of the same order of magnitude. Because the spin transfer mechanism leading to $J_1(II)$ is analogous to that of $J_1(I)$, $J_1(II)$ will also be ferromagnetic. In the chlorine compounds the values of f_σ and $f_{\pi y}$ for the Cl(II) ions increase slightly in the series NH_4, K, Rb and Cs. As discussed in the preceding section, f_σ is the difference of the two transfer coefficients, $f_\sigma = f'_\sigma - f''_\sigma$, where f'_σ and f''_σ stand for the spin transfer from the p_z orbital to the copper $3d(x^2 - y^2)$ and 4s orbitals respectively. Both f'_σ and f''_σ were found to increase, which causes only a very slight increase of f_σ. In the deduction of the magnitude of the super exchange interaction, we have to consider these two transfer mechanisms separately. The simultaneous transfer of an electron from the oxygen ion to the Cu_2 4s orbital and of an electron from the Cl(II) ion to the Cu_1 4s orbital (correlation super exchange) will give a ferromagnetic contribution to $J_1(II)$. As also the spin transfer to the copper 3d orbitals leads to a ferromagnetic interaction we have to conclude that the influence of the σ spin density at the Cl(II) ions, on the super exchange interaction is proportional to $f'_\sigma + f''_\sigma$ rather than to $f'_\sigma - f''_\sigma$. So the increase of $J_1(II)$ due to the interactions of the Cl(II) ions is much larger than can be estimated from the increase of f_σ in the series NH_4, K, Rb and Cs. The coefficient $f(II \rightarrow H_2O)$ will decrease with increasing unit cell dimension, thus following the series K, NH_4, Rb and Cs. As for the value of $J_1(I)$, probably $J_1(II)$ will show a maximum in this series (or remain about constant). However for the ammonium compound it can be seen that both $f(\sigma,\pi y)_{II}$ and $f(II \rightarrow H_2O)$ will be smaller than in the potassium compound, from which it can be concluded that $J_1(II)$ in the NH_4 compound is smaller than in the K compound.

Possibly a third mechanism contributes to J_1. This exchange interaction $J_1(A)$ takes place via the linkage

$$Cu_1 - \text{Halide (I)} - \text{Alkali} - \text{Halide (I)} - Cu_2$$

As can be seen from fig. 34 two such linkages exist between two neighbouring copper ions. This interaction is about equal to the next-nearest neighbour interaction $J_2(A)$ between similar copper ions via the alkali ion. This interaction $J_2(A)$ will be shown to be ferromagnetic and to increase in the series NH_4, K, Rb and Cs. $J_1(A)$ evidently shows the same behaviour.

In the bromine compounds all spin transfer coefficients are larger than

in the chlorine compounds, and therefore all exchange interactions will be larger. Qualitatively the same difference between the super exchange interactions in the NH_4 and Rb compound, as discussed for the chlorine compounds, will exist. Summarizing we can say that for the series chlorine compounds K, Rb and Cs the total value of J_1 will probably show a maximum due to the combined effect of increasing spin transfer coefficients for the chlorine and alkali nuclei and the decreasing interaction between the chlorine ions and the water molecules.

Next-nearest neighbour interaction J_2.

The n.n.n. super exchange interaction of the copper ion is not equivalent for all six next-nearest neighbours. The interaction $J_2(c)$ with the two copper ions along the crystallographic c-axis takes place via the linkage

$$Cu - OH_2 - \text{Halide (I)} - H_2O - Cu$$

As we have no information about the oxygen spin transfer coefficients, which mainly determine the magnitude of this exchange interaction, it is not possible to discuss the differences of the interaction in the various compounds.
The n.n.n. interaction between the copper ions in the (a-a) plane, $J_2(A)$, occurs via the linkage

$$Cu - \text{Halide (I)} - \text{Alkali} - \text{Halide (I)} - Cu$$

There are two of such linkages between the copper ions.
Because both copper ions transfer unpaired spin to different alkali orbitals this interaction is ferromagnetic. Although the analysis of the alkali hyperfine interaction has not yielded clear information about the spin density in their p orbits, the increase of the s-orbital spin density reflects the increase of the p-orbital spin density in the series K, Rb and Cs. Therefore it is expected that the value of J_2 increases in going from the K compound to the Cs compound. In the NH_4 compounds the two n.n.n. exchange pathes between two copper ions are different, as the one link involves halide (I) ions and the other halide (II) ions. Both exchange interactions however are ferromagnetic. It is hard to see if the correspondence between the NH_4 molecule and the alkali ions is such that the values of the spin transfer coefficients f_s can be compared straight forward. If so, we can conclude that J_2 in the ammonium compounds must be smaller than in all other compounds.

Comparison of J_1 and J_2 with the values of θ and T_c.

In principle it is possible to calculate the values of J_1 and J_2 from the experimentally determined values of θ and T_c; using the following expressions which are appropriate for a b.c.c. Heisenberg ferromagnet with $S = \frac{1}{2}$ and $J_2/J_1 > 0$ (see chapter 2).

$$k\theta = 4J_1 + 3J_2$$

$$kT_c = b_0 J_1 + b_1 J_1/J_2$$

where $b_0 = 2.60$ and $b_1 = 2.45$[14].

Applying these formulae to the values of θ and T_c given in table 6 it is found that the so calculated value of J_2 is much larger than J_1. This result is clearly in contradiction to what has been discussed before.

There may be several reasons, theoretical as well as experimental, for this discrepancy.

a) In the expressions for θ and T_c the n.n.n. exchange interaction has been treated to be equivalent for all six nearest neighbours. This is not the situation in these compounds.

b) The influence of third nearest neighbour interaction on θ and T_c has not been included. Especially the interaction via Cu-Hal(I)-HOH-Hal(I)-Cu between similar copper ions along the (110)-axis can have an appreciable magnitude.

c) From the experiments it is known that there is a small anisotropic exchange interaction present in these crystals. In table 1 (p. 14) it can be seen that any anisotropy influences the relation between T_c and J_1, but not in such a way as to be able to ascribe the mentioned discrepancy to the occurrence of a small anisotropic exchange interaction. (The influence of anisotropy on other macroscopic quantities however is much larger. For instance the large discrepancy between the experimental value for $(E_\infty - E_c)/kT_c$ and the theoretical one for nearest-neighbour interaction only, respectively 0.384 and 0.460 can be explained already by the assumption of an anisotropy of only 4%.)

d) The value of θ is determined by extrapolation of experimental data for $T > 2\theta$. It is possible that systematic errors in this extrapolation procedure cause a wrong value of θ. Moreover, as has been discussed in chapter 6.6, the exchange interactions still change between liquid hydrogen and liquid helium temperature. It is quite possible that, although we did not observe it from the nuclear interaction parameters, the exchange interactions in external field show a temperature dependence, even for $T < 4.2$ K. That may be due either to

the torsional oscillation of the copper octahedron as discussed in chapter (8.2) or to the occurrence of magnetostriction. Magnetostriction could influence both the exchange interactions and the nuclear interaction parameters of the protons, from which the temperature dependence of the resonance frequency has been used to determine θ.

Qualitatively however, it can be seen that the conclusions about the relative values of the exchange interactions in the series of compounds are in accordance with the values of T_c and θ.

From the expressions given before it is found that for increasing value of J_2/J_1 the ratio T_c/θ increases too. As we have no reliable information about the value of J_2 in the NH_4 compounds relative to that in the other compounds we can only compare the values of T_c/θ for the series of chlorine compounds K, Rb and Cs. These values are respectively 0.756, 0.820 and 0.836. Although these values are not very accurate, the trend is obvious: an increasing value of J_2 in going from the K to the Cs compound. This confirms the conclusions drawn with respect to the relative values of the alkali spin transfer coefficients. The larger values of T_c for the bromine than for the chlorine compounds is clearly reflected by the larger spin transfer coefficients for the bromides. The relative magnitudes of the n.n.n. exchange interactions with respect to the n.n. exchange interactions in the bromides is smaller than in the corresponding chlorides as the values of T_c/θ are smaller. That can be understood as the substitution of the chlorine by bromine ions mainly changes the value of J_1 as can be seen from the values of the spin transfer coefficients. The value of T_c in $RbCuBr_4 \cdot 2H_2O$ is slightly larger than that of the NH_4 compound probably due to the larger n.n. interactions because of larger spin transfer from the Br(II) ions to the copper 4s and 4p orbitals and the larger Br(I) transfer coefficients. The effect of the smaller spin transfer to the copper 4s and 4p orbitals, probably together with the smaller n.n.n. exchange interaction in $(NH_4)_2CuCl_4 \cdot 2H_2O$ is reflected very clearly by its low value of T_c as compared to that of the other chlorine compounds. The transition temperature of the Rb compound is higher than that of the K compound which is in accordance with the discussed larger value of both J_1 and J_2 in the Rb compound. The much lower transition temperature for the Cs compound is surely due to the large decrease of the interaction between the chlorine ions and the water molecules, which is not compensated by the increase of the spin transfer coefficients.

Summarizing we can conclude that the qualitative arguments, based on the experimentally determined spin transfer coefficients, explain the relative values of T_c for the various compounds rather well.

References.

1) Choh, S.H. and Stager, C.V., Canad. J. Phys. 49 (1971) 144.
2) Gupta, L.C. and Radnakrishna Setty, D.L., Ind. J. Pure and Appl. Phys. 8 (1970) 754.
3) Gupta, L.C. and Radnakrishna Setty, D.L., Chem. Phys. Lett. 4 (1969) 263.
4) Chidambaram, R., Navarro, Q.O., Garcia, A., Karsona Linggoatmodja, Lin Shi-Chien, Il-Hwan Suh, Sequeira, A. and Srikanta, S., Acta Cryst. B26 (1970) 827.
5) Mathieu, J.-P. and Couture-Mathieu, L., J. Chim. Phys. 50 (1953) 573.
6) Schoemaker, D., Phys. Rev. 149 (1966) 693.
7) Nuclear Data Tables 5, 5-6 (1969) 433-616.
8) Tterlikkis, L., Mahanti, S.D. and Das, T.P., Phys. Rev. 176 (1969) 10.
9) Schmieder, R.W., Lurio, A. Happer, W. and Khadjavi, A., Phys. Rev. A2-4 (1970) 1216.
10) McGarvey, B.R., J. Phys. Chem. 71 (1967) 51.
11) Clementi, E., IBM Journal of Res. Develop. Suppl. 9 (1965) 2.
12) Moore, C.E., Atomic Energy Levels, Nat. Bur. Stand., Circular 467 (1949).
13) Shenstone, A.G. and Wilets, L., Phys. Rev. 83 (1951) 104.
14) Swendsen, R.H., Phys. Rev. B-5 (1972) 116.

APPENDIX A

Finestructure of the Cl(II) resonance lines in external field. During the experiments in the paramagnetic state at T = 1.2 K in an external field, for the determination of the components of the field-shift tensor of the Cl(II) site nuclei, an extra finestructure of the Cl(II) resonance lines in all four compounds has been observed. At that temperature only the $\Delta m_I = +\frac{1}{2} \rightarrow +\frac{3}{2}$ and the $\Delta m_I = +\frac{1}{2} \rightarrow -\frac{1}{2}$ transitions of that Cl(II) site, for which the external field is rotating in the X-Y plane of the EFG tensor, can be detected. Due to the lack of intensity the resonance signals for the magnetic field parallel to the Z-axis cannot be observed. The shape of the finestructure of the resonance lines in the X-Y plane strongly depends on the magnitude and direction of the external field and on temperature. Moreover, the pattern of the finestructure of the $(+\frac{1}{2} \rightarrow -\frac{1}{2})$ transition differs from that of the $(+\frac{1}{2} \rightarrow +\frac{3}{2})$ transition. The finestructure of the $(+\frac{1}{2} \rightarrow +\frac{3}{2})$ resonance line is asymmetric and most times fourfold. The $(+\frac{1}{2} \rightarrow -\frac{1}{2})$ transition, however, shows a nearly symmetric splitting pattern which is threefold for the magnetic field along the Y-axis (c-axis). In fig. 35 two recorder traces of the second derivative of the lineshape of the $(+\frac{1}{2} \rightarrow -\frac{1}{2})$ transition for $\vec{H}_o \| X$ axis are shown. The number of, not well separated, resonance lines gradually changes from six for high field and low temperature to four and then to two for low field and/or high temperature.

The ratio of the splittings $\Delta\nu$ of the ^{35}Cl and ^{37}Cl $(+\frac{1}{2} \rightarrow -\frac{1}{2})$ transitions for $\vec{H}_o \| X$ (T = 1.2 K, H_o = 5 kOe) in the potassium compound is found to be 1.22. As for this temperature and fieldstrength the Cl(II) Larmor frequency ν_L is smaller than the quadrupole interaction constant ν_q $(\nu_L/\nu_q \simeq \frac{1}{4})$, the resonance frequency of the $(+\frac{1}{2} \rightarrow -\frac{1}{2})$ transition can be approximated by a second-order perturbation theory expression

$$\nu = \alpha\nu_L - \beta \frac{\nu_L^2}{\nu_q}$$

α and β depend on the ratio ν_L/ν_q, the asymmetry parameter η and the direction of the total magnetic field with respect to the EFG principal axes. The ratio of the γ values and of the quadrupole moments of the two isotopes are, respectively, $\gamma^{35}/\gamma^{37} = 1.201$ and $Q^{35}/Q^{37} = 1.269$. Using these data it can easily be calculated that if the finestructure is due to different values of the quadrupole interaction the ratio of the splittings for corresponding $(+\frac{1}{2} \rightarrow -\frac{1}{2})$

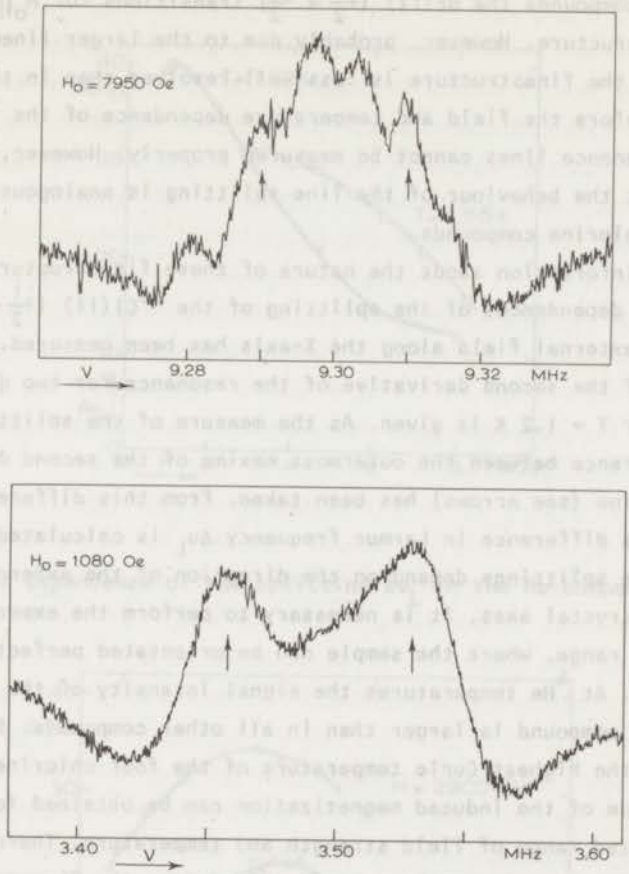

Fig. 35. Recorder traces of the second derivative of the $^{35}Cl(II)$ $(+\frac{1}{2} \rightarrow -\frac{1}{2})$ transition in $Rb_2CuCl_4 \cdot 2H_2O$ with the magnetic field parallel to the X-axis, (T = 1.2 K) for two different values of H_o.

transitions of the two isotopes will be $\Delta\nu^{35}/\Delta\nu^{37} < 1.201$, whereas if the splittings are caused by the changes of the Larmor frequency $\Delta\nu^{35}/\Delta\nu^{37} > 1.201$. So it can be concluded that the observed finestructure has to be due to small differences in the Larmor frequency. In all four chlorine compounds these splittings have been observed; the pattern are analogous and the magnitude of the splittings in the various compounds under the same conditions differs only slightly. The magnitude and shape of the finestructure is found to be independent of crystal shape, and reproduces exactly for different samples of the same

compound. These splittings are not observed at any other resonance line. In the bromine compounds the Br(II) $(+\frac{1}{2} \rightarrow -\frac{1}{2})$ transitions for $\vec{H}_o \| X$ axis also exhibit a finestructure. However, probably due to the larger linewidth of these resonance lines the finestructure is less well resolved than in the chlorine compounds. Therefore the field and temperature dependence of the splitting of the bromine resonance lines cannot be measured properly. However, it has been established that the behaviour of the line splitting is analogous to that observed in the chlorine compounds.

To obtain information about the nature of these finestructures the temperature and field dependences of the splitting of the $^{35}Cl(II)$ $(+\frac{1}{2} \rightarrow -\frac{1}{2})$ transition with the external field along the X-axis has been measured. In fig. 35 a recorder plot of the second derivative of the resonance for two different magnetic fields for T = 1.2 K is given. As the measure of the splitting $\Delta\nu$ the frequency difference between the outermost maxima of the second derivative of the resonance line (see arrows) has been taken. From this difference in resonance frequency $\Delta\nu$ the difference in Larmor frequency $\Delta\nu_L$ is calculated.

Because the splittings depend on the direction of the external field with respect to the crystal axes, it is necessary to perform the experiment in the ^4He temperature range, where the sample can be orientated perfectly in the desired direction. At ^4He temperatures the signal intensity of the Cl(II) resonance lines in the Rb compound is larger than in all other compounds. Besides, the Rb salt possesses the highest Curie temperature of the four chlorine compounds, so the largest value of the induced magnetization can be obtained for this compound within the limited range of field strength and temperature. Therefore most of the line-splitting experiments have been performed on the Rb compound.

In fig. 36 the field dependence in the Rb compound of $\Delta\nu_L$ for two different temperatures is given $(\vec{H}_o \| X)$. In fig. 37 the temperature dependence in two different fields is plotted, whereby instead of the temperature the measured reduced magnetization is used as the variable. From both plots it can be seen that the magnitude of the splitting does not depend in a simple way on the magnetization or on the strength of the applied field. Therefore the possibility of twin crystals, the presence of impurities or the existence of isotope effects as origins of the finestructure can be excluded. In all these cases the splitting would be directly proportional to the magnetization. Also any classical dipolar interaction with surrounding nuclei can be left out of consideration, as these interactions are temperature and field independent. It seems that both the temperature and field dependence of the splitting $\Delta\nu_L$ can be described to be, not linearly, dependent on the parameter $m(dm/dH_o)$ (m = reduced magnetization, H_o =

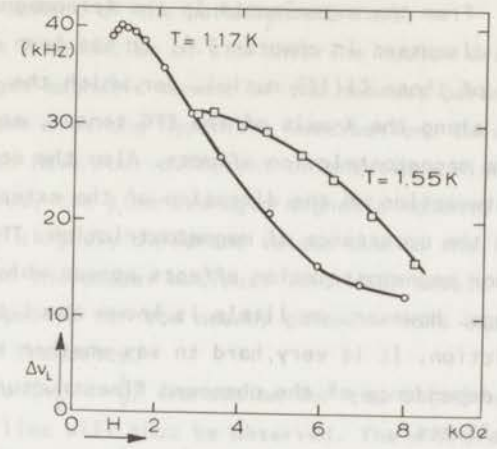

Fig. 36. Field dependence of the splitting $\Delta\nu_L$ in the Rb compound. $\vec{H}_o \| X$ axis.

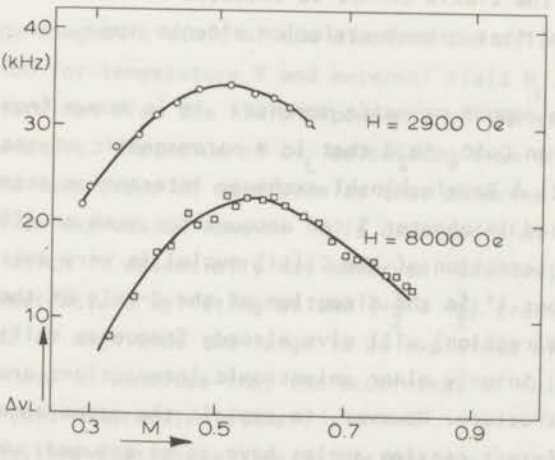

Fig. 37. Temperature dependence of $\Delta\nu_L$ in the Rb compound. Instead of the temperature, the reduced magnetization m has been used as variable.

applied field). In the ferromagnetic state in zero field no indication of these line splittings has been found, which is not in contradiction as dm/dH is about zero in that case.

Three possible mechanism which can be the origin of these finestructures remain.

a) *Magnetostriction.* From the experiments in the ferromagnetic state in zero field, which have been discussed in chapter 7.4, it has been concluded that the interaction parameters of those Cl(II) nuclei, for which the spontaneous magnetization is directed along the X-axis of the EFG tensor, are strongly influenced by spontaneous magnetostriction effects. Also the dependence of the rubidium quadrupole interaction on the direction of the external field (see section 6.6) points to the occurrence of magnetostriction. Therefore it may be possible that some minor magnetostriction effects appear which can lead to the observed line splittings. However, as little is known about the microscopic aspects of magnetostriction, it is very hard to say whether the shape and the temperature and field dependence of the observed finestructure can be explained in principal by such effects.
A magnetostrictive distortion will also influence the Cl(II) quadrupole interaction constants ν_q and η. We are however not able to determine these constants accurately in the ^{4}He temperature range as we can observe only two resonance lines with the external field along the X- and Y-axis of the EFG tensor, while the spectrum along the Z-axis cannot be detected at all. So it cannot be excluded on that ground that magnetostriction effects occur.

b) *Canting of the copper magnetic moments.* It is known from measurements by Wittehoek et al.[1] on $CuSO_4 \cdot 5H_2O$ that in a paramagnetic crystal a canted spin structure can exist. A Dzyaloshinski exchange interaction term of the form $D\vec{S}_1 \times \vec{S}_2$ as discussed in chapter 2 can account for such an effect. As the transferred hyperfine interaction of the Cl(II) nuclei is very anisotropic, a canting of the spins of about 1° in the direction of the Z-axis of the hyperfine interaction tensor (γ' direction) will give already frequency shifts of the right order of magnitude. So only minor anisotropic interactions are needed to cause the observed finestructure. However, to explain the appearance of a six-fold splitting, six different canting angles have to be assumed, which seems to be rather of belief.

c) *Indirect interaction between nuclear spins.* From NMR experiments in diamagnetic substances it is known that there exists an indirect interaction between nuclear spins of neighbouring atoms which leads to a finestructure of the resonance lines. This interaction takes place via the hyperfine couplings of the considered nuclei and those electrons which take part in the chemical

bonding of the molecule in question[2]. In the situation of the paramagnetic substance, however, this indirect interaction can take place via the time-averaged magnetic moment of the paramagnetic ions.

The resonance frequencies of the chlorine nuclei are strongly dependent on the time-averaged magnetic moment of the nearest paramagnetic copper ion with which they have a strong hyperfine interaction. Because the copper nuclear-magnetic moment can have four different orientations with respect to the total field at the nucleus, the time-averaged magnetic moments of the copper ions can have four only slightly different values due to the influence of the hyperfine interaction of the copper nucleus. This will result in four slightly different resonance spectra for the nearby chlorine ions because of the small differences in Larmor frequency.
Instead of a single $(+\frac{1}{2} \rightarrow -\frac{1}{2})$ transition for the Cl(II) nuclei, a four-fold splitting of this line will thus be observed. The difference in Larmor frequency between the outermost $(+\frac{1}{2} \rightarrow -\frac{1}{2})$ transitions for $\vec{H}_o \| \gamma$ will then be given by

$$\Delta\nu_L = \frac{4\pi F_{zz}(Cu)}{\gamma_e} F_{xx}(Cl) \frac{dm(T,H_o)}{dH_o}$$

where γ_e is the gyromagnetic ratio of the electron and $m(T,H_o)$ denotes the reduced magnetization for temperature T and external field H_o. The value of dm/dH_o can be determined from the field dependence of the reduced magnetization at constant temperature. The value of $\Delta\nu_L$ calculated from this expression is found to be of the same order of magnitude as that observed experimentally. From the above given expression however it is expected that $\Delta\nu_L$ will be proportional to dm/dH_o which is essentially not observed. Besides, the experiments show that the finestructure splitting of the $(+\frac{1}{2} \rightarrow +\frac{3}{2})$ transition for $\vec{H}_o \| c$ is at least one order of magnitude too large to be explained by this type of interaction. So we have to conclude that the occurrence of this finestructure cannot be due to this interaction either.
It seems to be possible that these line splittings are caused by the combined effect of some of the mentioned interactions. However, further experimental as well as theoretical work has to be performed to be able to determine the origins of this finestructure.

APPENDIX B

The influence of chlorine impurities on the bromine resonance spectra. The first bromine crystals that were used for the NMR experiments were grown from solutions containing approximately 2 °/oo chlorine ions. During the course of the experiments it became apparent that the concentration of these chlorine ions in the crystals was probably larger than in the solutions. The chlorine impurities occupy the Br(II) sites and probably the Br(I) sites too. They influence both the quadrupole and transferred hyperfine interaction of the nearby bromine nuclei, which results in a broadening of the Br resonance lines and even in extra bromine resonance spectra. After we noted the existence of these effects, crystals were grown from solutions containing less than 0.2 °/oo chlorine ions. These purer crystals were used for all the measurements discussed in this thesis. By comparing the spectra observed in the ferromagnetic state in the 2 °/oo Cl and 0.2 °/oo Cl crystals the following differences were detected.

Br(I) spectrum. In the 2 °/oo Cl crystals the width of the Br(I) resonance lines at T = 0.3 K in zero field is about 35 kHz, only the $+\frac{3}{2} \rightarrow -\frac{3}{2}$ transition has a linewidth of 20 kHz. The linewidth in the 0.2 °/oo Cl crystals is 20 kHz and 10 kHz for the $+\frac{3}{2} \rightarrow -\frac{3}{2}$ transition.

We think that this line broadening in the less pure crystals is caused mainly by the long-range influence of the impurities on the EFG tensor at the Br(I) nuclei. The influence of a spread in the magnetic interaction on the resonance linewidth will be less important as the magnetic interaction of the bromine nuclei is much smaller than the quadrupole interaction. Besides that, the influence of an impurity on the magnetic interaction will be very short-ranged.
These conclusions were confirmed by experiments on a 20 °/oo Cl crystal where the Br(I) α and β transitions could not be detected anymore, while the $+\frac{3}{2} \rightarrow -\frac{3}{2}$ transition was still observable.

In the purest crystals at least three extra sets of Br(I) β transitions, also with a linewidth of about 20 kHz, have been detected. The intensity of these extra resonance lines are unequal and are in the order of 10^{-3} of the normal β transitions. As the corresponding extra α transitions could not be detected at all because of a too weak signal intensity, it was not possible to calculate the magnetic and quadrupole interaction accurately for these extra

spectra. However, by comparing the resonance frequencies of the ^{79}Br and ^{81}Br extra resonance lines, it seems that the change in resonance frequency is caused by an increase of the PQR frequency of the order of a few hundred kHz, together with a decrease of the Larmor frequency of the order of 20 kHz.
In the 2 °/oo Cl crystals these extra transitions have not been observed, probably because of frequent overlap and larger width of these extra resonance lines.

Br(II) spectrum. The Br(II) resonance spectrum is much more influenced by the impurities than the Br(I) spectrum as all the interactions of the Br(II) nuclei are much stronger. The effects are clearly demonstrated by the shape of the $(+\frac{1}{2} \rightarrow -\frac{1}{2})$ transition. The enormous signal intensity of this transition allows us to observe in the 2 °/oo Cl crystals extra resonance lines, which have a linewidth of about 50 kHz, even if the total absorption rate of the transitions is of the order of 10^{-5} of that of the main resonance line.

At T = 1.2 K more than 20 extra transitions per isotope were observed from which about 80% at lower and 20% at higher frequency than the main transition. This entire extra spectrum in the NH_4 compound has a width of about 7 MHz. As the resonance frequencies of these $(+\frac{1}{2} \rightarrow -\frac{1}{2})$ transitions are in first order only determined by the magnetic interaction, these frequency shifts have to be due to changes in the transferred hyperfine interaction of the Br(II) nuclei in question, caused by the nearby Cl ions. This assumption has been verified by the comparison of the ^{79}Br and ^{81}Br extra spectra. The ratio of the frequency shifts of corresponding extra resonance lines of ^{79}Br and ^{81}Br with respect to the main transition was always exactly equal to the ratio of the γ values of the two isotopes. If these shifts were due to a change in the quadrupole interaction the ratio of these shifts would be equal to the ratio of the Q^2/γ values for the two isotopes, which differs largely from the ratio of the γ values.

The influence of the impurities on the Br(II) quadrupole interaction could not be measured as in these impure crystals the high-frequency transitions, from which the frequencies are mainly determined by the quadrupole interaction, have never been observed because they are strongly broadened by the spread in the quadrupole interaction. From the temperature independent linewidth of these transitions in the 0.2 °/oo Cl crystals, which is found to be about 1.5 MHz and which is not of magnetic origin, it can be concluded that already very small amounts of Cl impurities give rise to enormous broadening effects. So the influence of impurities on the quadrupole interaction has to be very large.

Apart from the appearance of the extra Br resonance lines also the $(+\frac{1}{2} \rightarrow -\frac{1}{2})$ transitions of the ^{35}Cl and ^{37}Cl nuclei situated at Br(II) sites could be

observed with a signal to noise ratio of about 10. The width of these Cl resonance lines is about 20 kHz. The corresponding Cl α transitions could not be detected, which can be calculated to be due to a too low signal intensity. If we assume for the chlorine nuclei equivalent principal axes for the T.H. interaction tensor and the EFG tensor as have been determined for the Br(II) sites, the local fields at the chlorine nuclei are calculated to be 20% smaller than the local fields at the corresponding bromine nuclei.

Conclusion. The chlorine impurities change the quadrupolar and transferred hyperfine interaction of the nearby Br(I) and Br(II) sites. This change in interactions is due to a change in the spatial charge distribution around the copper ion as the chlorine-copper interaction differs from the bromine-copper interaction. Because of the strong super exchange interactions between neighbouring copper ions, also the interactions at the next-nearest bromium sites will be influenced, which leads to the large number of extra Br(II) resonance lines.

The change in the local charge distribution surely will influence the local super exchange interaction between the copper ions. It has been observed indeed that the Curie temperature of the bromine compounds decreases with increasing concentration of the chlorine impurities.

The study of the bromine perturbation spectra can yield information about the interaction of the bromine nuclei with next-nearest copper ions. As this interaction is directly related to the super exchange interaction via the bromine ions, valuable extra information about the magnitude of the various super exchange interactions can be obtained.

References.

1) Wittekoek, S. and Poulis, N.J., Physica 32 (1966) 2051 (Commun. Kamerlingh Onnes Lab., Leiden, No. 352c).

2) Abragam, A., Principles of Nuclear Magnetism, Oxford University Press (London, 1962) p. 186.

Samenvatting.

Reeds meer dan tien jaar is het bekend dat de reeks isomorfe verbindingen $K_2CuCl_4 \cdot 2H_2O$, $(NH_4)_2CuCl_4 \cdot 2H_2O$, $Rb_2CuCl_4 \cdot 2H_2O$ en $(NH_4)_2CuBr_4 \cdot 2H_2O$ een ferromagnetische ordening vertonen bij een temperatuur van ongeveer 1 K. De soortelijke warmte-, susceptibiliteits-, en magnetisatie-metingen van Miedema et al.[1,2] en Wielinga[3] hebben aangetoond dat het magnetisch gedrag van deze vier verbindingen volledig met elkaar overeenstemt. Op een gereduceerde temperatuurschaal bleken alle soortelijke warmte kurven identiek te zijn. Het thermodynamisch en kritisch gedrag van deze verbindingen is verklaard met behulp van verschillende theoretische modellen voor de 3-dimensionale $S = \frac{1}{2}$ b.c.c. Heisenberg ferromagneet[4,5]. De naaste buren- en naast-naaste buren super exchange wisselwerkings constanten J_1 en J_2 konden berekend worden uit de experimentele waarden voor de Curie-Weiss temperatuur θ, de ordenings temperatuur T_c en uit de temperatuur afhankelijkheid van de soortelijke warmte.
Het belangrijkste doel van het werk dat in dit proefschrift beschreven wordt, is het uitbreiden van de kennis betreffende deze reeks isomorfe Heisenberg ferromagneten, met inbegrip van $Cs_2CuCl_4 \cdot 2H_2O$ en $Rb_2CuBr_4 \cdot 2H_2O$, door vanuit een microscopische gezichtshoek inzicht te verschaffen in de magnetische eigenschappen. Met dat doel zijn de magnetische en electrische hyperfijn interacties van alle kernen (behalve die van de zuurstof kernen) gemeten met behulp van kern resonantie technieken. Uit deze kern interacties kunnen we informatie verkrijgen m.b.t. de covalente binding van de buitenste electronen van zowel de diamagnetische als de magnetische ionen. Gebruik makende van een Molecular Orbital benadering kan de transfer van ongepaarde spin van het magnetische koper ion naar de verschillende diamagnetische liganden berekend worden. De verandering van de ongepaarde spin-dichtheids distributie door de substitutie van de halogeen en/of alkali ionen geeft informatie over de verschillende spin transfer mechanismen.
Er kan een verband gelegd worden tussen de spin transfer coefficienten en de grootte der super exchange interacties tussen de koper ionen. De genoemde experimenten leveren daarom ook een kwalitatieve schatting op van de sterkte der verschillende super exchange koppelingen in de zes verbindingen. Dit is te meer interessant daar er geen eenvoudige relatie gevonden wordt tussen de eenheids cel afmetingen en de grootte der exchange constanten.
De kern resonantie experimenten stellen ons ook in staat de richting van de spontane magnetisatie in de ferromagnetische toestand in nulveld te bepalen. Deze blijkt verschillend te zijn in de chloor en broom verbindingen. Het is

waargenomen dat de kern interactie parameters van één der chloorionen sterk verschillen in de paramagnetische en ferromagnetische toestand. Naar aanleiding hiervan geven we een mogelijke oorzaak aan voor het verschil in voorkeursrichting voor de chloor en broom verbindingen.
De temperatuur afhankelijkheid van de spontane magnetisatie in de buurt van het overgangspunt is ook gemeten. Door de gunstige omstandigheden, speciaal in de bromiden, kan de waarde van de kritische exponent β, die het exponentiele gedrag van de spontane magnetisatie dichtbij T_c beschrijft, veel nauwkeuriger bepaald worden dan mogelijk is m.b.v. macroscopische methoden.

In hoofdstuk 2 wordt een kort overzicht van de macroscopische magnetische eigenschappen van een 3-dimensionale b.c.c. Heisenberg ferromagneet gegeven. Speciaal het verband tussen de super exchange constanten J_1 en J_2 en de macroscopisch waarneembare grootheden wordt besproken. Daarbij wordt ook de invloed van anisotropie op deze grootheden bediscussieerd.
Het theoretische model, dat de vorming van covalente bindingen van een 3d overgangs metaal ion in een octaedrische omringing beschrijft, wordt in hoofstuk 3 uitgebreid behandeld. Een eenvoudige Molecular Orbital benadering wordt gebruikt om de betreffende electronen banen te beschrijven. De invloed van de spin transfer van het magnetisch ion naar de liganden, op de kristalveld splitsing en de spin-baan koppelings constante van het magnetisch ion wordt afgeleid. De uitdrukkingen voor de ligand hyperfijn interactie en het verband tussen spin transfer coefficienten en super exchange interactie worden bepaald.
In hoofdstuk 4 worden de eigenschappen van het Cu^{2+} ion in een kristalveld met tetragonale symmetrie en rhombische distorsie behandeld. De uitdrukkingen voor de g-tensor, de hyperfijn interactie tensor en de electrische veld gradient tensor worden afgeleid voor het geval van pure ionaire binding. Deze uitdrukkingen worden daarna gemodificeerd, overeenkomstig de M.O. benadering, om rekening te houden met een gedeeltelijk covalente binding.
In hoofdstuk 5 worden de verschillende bijdragen tot de kern spin Hamiltoniaan besproken. De analyse van de resonantie spectra voor $I = \frac{3}{2}$, het meest voorkomende geval in deze verbindingen, wordt uitgebreid behandeld. Afgezien van storings theorie uitdrukkingen voor de resonantie frekwenties, die niet in alle voorkomende situaties toepasbaar zijn, zal ook aan de analyse volgens de methode van Brown en Parker aandacht besteed worden. Na een beschrijving van de experimentele opstelling, wordt de kristalstructuur behandeld. Uitgaande van de lokale symmetrie van de ion posities kan het aantal te verwachten kern resonantie spectra bepaald worden. Ter vergemakkelijking van de beschrijving van de hoofdasrichtingen der kern interactie tensoren worden lokale richtingen binnen een

koper octaeder vastgelegd. Ook wordt een eenduidige notatie voor de nulveld spectra in de ferromagnetische toestand gegeven. Aan het eind van dit hoofdstuk worden enkele specifieke aspecten van de kern resonantie in ferromagnetische verbindingen aan de orde gesteld.
De resultaten van de experimenten in de paramagnetische toestand worden weergegeven in hoofdstuk 6. Achtereenvolgens zullen we behandelen de bepaling van de kristalveld splitsingen, g-tensor en de waarde van de Curie-Weiss temperatuur θ. Daarna wordt de bepaling van de richting der hoofdassen van de frekwentie shift-en de electrische veld gradient tensoren, en de waarden van hun componenten voor alle kernen, besproken.
De kern resonantie spectra die waargenomen zijn in de ferromagnetische toestand, en de informatie die van deze spectra verkregen wordt, zijn beschreven in hoofdstuk 7. Ook de temperatuur afhankelijkheid van de spontane magnetisatie net onder het overgangspunt wordt hier besproken.
Uiteindelijk zullen in hoofdstuk 8 alle experimentele resultaten geanalyseerd worden in termen van spin transfer coefficienten voor de verschillende diamagnetische ionen. De consistentie van het toegepaste theoretische model zal getoetst worden en de tekortkomingen aangeduid. De waargenomen verschillen in de waarde van de spin transfer coefficienten voor overeenkomstige ionen in de verschillende verbindingen zullen informatie verschaffen over de transfer mechanismen en de kwalitatieve veranderingen van de exchange interactie.

Het grootste deel van het experimentele werk hetgeen in de hoofdstukken 6 en 7 beschreven wordt, is reeds gepubliceerd in Physica[6,7,8]. Daarenboven zijn twee korte berichten over een deel der experimenten verschenen in de verslagen van internationale conferenties[9,10].

Referenties.

1) Miedema, A.R., Van Kempen, H. and Huiskamp, W.J., Physica 29 (1963) 1266 (Commun. Kamerlingh Onnes Lab., Leiden, No. 336a).
2) Miedema, A.R., Wielinga, R.F. and Huiskamp, W.J., Physica 31 (1965) 1585 (Commun. Kamerlingh Onnes Lab., Leiden, No. 345a).
3) Wielinga, R.F., Thesis, Leiden (1968).
4) Dalton, N.W. and Wood, D.W., Phys. Rev. 138 (1965) 779.
5) Wood, D.W. and Dalton, N.W., Proc. Phys. Soc. 87 (1966) 755.
6) Klaassen, T.O., Gevers, A. and Poulis, N.J., Physica 61 (1972) 95 (Commun. Kamerlingh Onnes Lab., Leiden, No. 393a).

7) Klaassen, T.O., Gevers, A., Looyestijn, W.J. and Poulis, N.J., Physica 64 (1973) 149 (Commun. Kamerlingh Onnes Lab., Leiden, No. 398c).
8) Klaassen, T.O., Looyestijn, W.J. and Poulis, N.J., to be published in Physica.
9) Klaassen, T.O. and Poulis, N.J., Proc. 7th Intern. Conf. Magnetism, Grenoble (1970) 1157.
10) Klaassen, T.O. and Poulis, N.J., Proc. 17th Congress Ampere, Turku (1972), to be published.

Ten einde te voldoen aan de wens van de faculteit der Wiskunde en Natuurwetenschappen volgt hier een overzicht van mijn studie.

Na een HBS-b opleiding aan het Dalton Lyceum te 's-Gravenhage begon ik in 1960 mijn studie aan de Rijksuniversiteit te Leiden. Het kandidaatsexamen met de hoofdvakken natuurkunde en wiskunde en bijvak sterrekunde werd in 1964 afgelegd. Sindsdien ben ik verbonden aan de werkgroep vaste stof fysica VS-L 1 van de stichting FOM, waarvan Prof. Dr. N.J. Poulis de leiding heeft. In de tijd tussen kandidaats- en doctoraalexamen assisteerde ik Dr. S. Wittekoek, die mij, tijdens zijn onderzoek aan antiferromagnetische lineaire ketens de beginselen van de kern resonantie techniek bijbracht.

Begin 1967 kwam ik als wetenschappelijk assistent, en na mijn doctoraalexamen dat ik eind 1967 aflegde, als wetenschappelijk medewerker, in dienst bij de stichting FOM.

Sinds 1966 vervulde ik diverse functies bij het natuurkunde practicum.

Het tot stand komen van dit proefschrift is mogelijk geworden dankzij de bijdrage van vele medewerkers uit het Kamerlingh Onnes Laboratorium, en met name uit de werkgroep. De discussies met Prof. Dr. N.J. Poulis, Dr. W.Th. Wenckebach en Dr. M.W. van Tol waren zeer waardevol. De gesprekken met Dr. H.W. Capel met betrekking tot theoretische aspecten van het magnetisme, en met Prof. Dr. N. Bloembergen, betreffende de oorsprong van de fijnstructuur der chloor resonantie lijnen, heb ik zeer op prijs gesteld. Ik ben veel dank verschuldigd aan Drs. J.J. van Klink, Drs. A. Gevers, Drs. J. Heyn en de heer W.J. Looyestijn voor de assistentie die zij verleenden bij de uitvoering der experimenten.
Drs. J.A. van Santen en medewerkers verrichten de e.s.r. metingen en Dr. J. Reedijk bepaalde de kristalveld splitsingen.
De heren D. de Jong, W.F. Elbers en J. Hoogwerf verleenden technische assistentie, terwijl de heren C.J. van Klink en L. van As de glasapparatuur verzorgden. Mevr. M.A. Otten-Scholten groeide een deel der kristallen en adviseerde bij problemen van chemische aard. De tekeningen voor dit proefschrift werden vervaardigd door de heer W.F. Tegelaar. Het manuscript werd getypt door mevrouw E. de Haas-Walraven.